

Conceptual Design of Supercritical O₂-Based PC Boiler

Final Report

**Andrew Seltzer
Zhen Fan
Archie Robertson**

November 2006

DE-FC26-04NT42207

**Foster Wheeler Power Group, Inc.
12 Peach Tree Hill Road
Livingston, New Jersey 07039**

DISCLAIMER

This report was prepared as an account of work sponsored by an agency of the United States Government. Neither the United States Government nor any agency thereof, nor any of their employees, makes any warranty, express or implied, or assumes any legal liability or responsibility for the accuracy, completeness, or usefulness of any information, apparatus, product, or process disclosed, or represents that its use would not infringe privately owned rights. Reference herein to any specific commercial product, process, or service by trade name, trademark, manufacturer, or otherwise does not necessarily constitute or imply its endorsement, recommendation, or favoring by the United States Government or any agency thereof. The views and opinions of authors expressed herein do not necessarily state or reflect those of the United States Government or any agency thereof.

ABSTRACT

The objective of the system design and analysis task of the Conceptual Design of Oxygen-Based Supercritical PC Boiler study is to evaluate the effects of oxygen firing on supercritical PC boiler design, operation and system performance. Simulations of the oxygen-fired plant with CO₂ sequestration were conducted using Aspen Plus and were compared to a reference air-fired 460 MWe plant. Flue gas recycle is used to control the flame temperature and resultant wall temperature in the O₂-fired PC. Parametric trade-off studies were made to determine the effect of flame temperature on system efficiency. The degree of improvement in system performance of various modifications was investigated.

The objective of the advanced oxygen separation system integration task of the study is to evaluate the benefits, effects, and limitations of the integration of advanced oxygen separation technologies into a supercritical O₂-fired PC. Simulations of the power generation unit, oxygen separation unit, and CO₂ sequestration system were conducted using the Aspen Plus software. The improvement of the O₂-fired PC system performance incorporating the Oxygen Ion Transport Membrane (OITM) and Ceramic Auto-thermal Recovery (CAR) were investigated. A parametric study was conducted to determine the sensitivity of the design and performance to various variables. Compared to the other CO₂ removal and sequestration technologies, the oxygen-fired PC integrated with OITM shows substantially less CO₂ removal penalty. The CO₂ removal penalty of the oxygen-fired PC integrated with CAR is between cryogenic air separation and OITM.

The objective of the furnace and heat recovery area design and analysis task of the study is to optimize the location and design of the furnace, burners, over-fire gas ports, and internal radiant surfaces. The furnace and heat recovery area were designed and analyzed using the FW-FIRE, Siemens, and HEATEX computer programs. The furnace is designed with opposed wall-firing burners and over-fire air ports. Water is circulated in the furnace by forced circulation to the waterwalls at the periphery and divisional wall panels within the furnace.

Compared to the air-fired furnace, the oxygen-fired furnace requires only 65% of the surface area and 45% of the volume. Two oxygen-fired designs were simulated: 1) with a cryogenic air separation unit (ASU) and 2) with an oxygen ion transport membrane (OITM).

The maximum wall heat flux in the oxygen-fired furnace is more than double that of the air-fired furnace due to the higher flame temperature and higher H₂O and CO₂ concentrations. The coal burnout for the oxygen-fired case is 100% due to a 500°F higher furnace temperature and higher concentration of O₂. Because of the higher furnace wall temperature of the oxygen-fired case compared to the air-fired case, furnace water wall material was upgraded from T2 to T92.

Compared to the air-fired heat recovery area (HRA), the oxygen-fired HRA total heat transfer surface is 35% less for the cryogenic design and 13% less for the

OITM design due to more heat being absorbed in the oxygen-fired furnace and the greater molecular weight of the oxygen-fired flue gas. The HRA tube materials and wall thicknesses are nearly the same for the air-fired and oxygen-fired designs since the flue gas and water/steam temperature profiles encountered by the heat transfer banks are similar.

The capital and operating costs of the pulverized coal-fired boilers required by the three different plants (air-fired, O₂-fired with cryogenic ASU and O₂-fired with OITM) were estimated by Foster Wheeler and the balance of plant costs were budget priced using published data together with vendor supplied quotations. The cost of electricity produced by each of the plants was determined and oxygen-based plant CO₂ mitigation costs were calculated and compared to each other as well as to values published for some alternative CO₂ capture technologies. Compared to other CO₂ sequestration technologies, the O₂-fired PC is substantially more cost effective than both natural gas combined cycles and post CO₂ removal PCs and it is superior, especially when a supercritical steam cycle is applied, to integrated gasification combined cycles.

Table of Contents

ABSTRACT	3
1.0 INTRODUCTION	9
2.0 EXECUTIVE SUMMARY	11
3.0 EXPERIMENTAL	17
4.0 RESULTS AND DISCUSSION	18
4.1 SYSTEM DESIGN AND ANALYSIS	18
4.1.1 <i>Reference Site and Conditions</i>	18
4.1.2 <i>Air-Fired Reference Case (case-1)</i>	19
4.1.3 <i>Oxygen-Based PC Plant – Base Case</i>	22
4.1.4 <i>Parametric Cases</i>	28
4.1.5 <i>Part Load</i>	40
4.1.6 <i>Comparison With Post Combustion CO₂ Capture</i>	42
4.1.7 <i>Furnace Waterwall Temperature</i>	42
4.2 ADVANCED O₂ SEPARATION SYSTEM INTEGRATION	43
4.2.1 <i>O₂-Fired PC Integrated with Cryogenic ASU (case-6)</i>	43
4.2.2 <i>O₂-Fired PC Integrated with OITM</i>	45
4.2.3 <i>O₂-Fired PC Integrated with CAR</i>	61
4.2.4 <i>Comparisons</i>	67
4.3 FURNACE AND HEAT RECOVERY AREA DESIGN AND ANALYSIS	69
4.3.1 <i>Furnace Design and Analysis</i>	69
4.3.2 <i>Boundary Conditions</i>	71
4.3.3 <i>Furnace Waterwall and Division Wall Design</i>	115
4.3.4 <i>Furnace Waterwall Corrosion</i>	123
4.3.5 <i>Heat Recovery Area Design and Analysis</i>	125
4.4 ECONOMIC ANALYSIS	131
4.4.1 <i>Main Assumptions</i>	131
4.4.2 <i>Plant Cost Basis</i>	134
4.4.3 <i>Total Plant Investment (TPI)</i>	142
4.4.4 <i>Total Capital Requirement (TCR)</i>	142
4.4.5 <i>Operating Costs And Expenses</i>	143
4.4.6 <i>Cost Of Electricity (COE)</i>	144
4.4.7 <i>Tube Weld Overlay</i>	145
4.4.8 <i>Reduced Pipeline Pressure</i>	146
4.4.9 <i>Comparison with Other Technologies</i>	155
5.0 CONCLUSION	157
6.0 REFERENCES	161
7.0 BIBLIOGRAPHY	163
8.0 LIST OF ACRONYMS AND ABBREVIATIONS	164

List of Figures

Figure 4.1.1 - Reference Case of Air-fired Supercritical PC.....	21
Figure 4.1.2 – Oxygen purity effect on ASU specific power	23
Figure 4.1.3 - Carbon burnout vs. O ₂ concentration to boiler	25
Figure 4.1.4 - Base case of O ₂ -fired supercritical PC.....	27
Figure 4.1.5 - O ₂ -fired supercritical PC with liquid CO ₂ pump (Case-3)	31
Figure 4.1.6 - Temperature-Quality diagram for wet-end heat exchangers.....	32
Figure 4.1.7 – Equilibrium and adiabatic temperatures vs. O ₂ concentration.....	33
Figure 4.1.8 - Boiler design with HRA series pass	38
Figure 4.1.9 - Boiler design with HRA series pass (56% Flue Gas Recycle)	39
Figure 4.1.10 - Flue gas recycle flow vs. part load operation	41
Figure 4.1.11 Efficiency at part load operation.....	41
Figure 4.2.1 - Base case of O ₂ -fired supercritical PC with Cryogenic ASU	44
Figure 4.2.2 - A Typical Oxygen Ion Transport Membrane Schematic [4].....	47
Figure 4.2.3 – Integration of Oxygen Ion Transport Membrane into O ₂ -PC.....	48
Figure 4.2.4 - O ₂ -PC with OITM	51
Figure 4.2.5 – Effect of OITM O ₂ Recovery Efficiency on Efficiency	54
Figure 4.2.6 – Effect of Sweep Gas Pressure on LMPD	55
Figure 4.2.7 – Effect of OITM Pressure on System Efficiency and LMPD: Variable O ₂ Recovery	57
Figure 4.2.8 – Effect of O ₂ Recovery on System Efficiency	57
Figure 4.2.9 – Effect of OITM Pressure on System Efficiency and LMPD: Constant and Variable O ₂ Recovery	58
Figure 4.2.10 - O ₂ -PC with OITM with 58% Recycle Flow.....	60
Figure 4.2.11 - CAR Process Schematic	61
Figure 4.2.12 – Integration of CAR Process into O ₂ -PC.....	65
Figure 4.2.13 - O ₂ -PC with CAR.....	66
Figure 4.3.1 – Computational Model of Air-Fired Furnace (with right side wall removed)	76
Figure 4.3.2 – Computational Model of Oxygen-Fired Furnace With OFA.....	77
Figure 4.3.3 – Air-Fired Boundary Conditions	78
Figure 4.3.4 – Oxygen-Fired Boundary Conditions (Cryogenic ASU)	79
Figure 4.3.5 – Oxygen-Fired Boundary Conditions (OITM).....	80
Figure 4.3.6 – Air-Fired Boiler Design.....	81
Figure 4.3.7 – Summary of FW-FIRE Furnace Modeling Results	82
Figure 4.3.8 – Gas Velocity for Air-Fired Case	83
Figure 4.3.9 – Gas Temperature for Air-Fired Case.....	84
Figure 4.3.10 – O ₂ Mole Fraction for Air-Fired Case.....	85
Figure 4.3.11 – Wall Heat Flux for Air-Fired Case	86
Figure 4.3.12 – Wall Temperature for Air-Fired Case	87
Figure 4.3.13 – Wall CO for Air-Fired Case	88
Figure 4.3.14 – Char Mass Fraction (72 microns) for Air-Fired Case.....	89
Figure 4.3.15 – Char Mass Fraction (176 microns) for Air-Fired Case.....	90
Figure 4.3.16 – Air-Fired and Oxygen-Fired Boiler Outlines	91
Figure 4.3.17 – Oxygen-Fired Boiler Design (Cryogenic ASU)	92
Figure 4.3.18 – Oxygen-Fired Boiler Design (OITM).....	93
Figure 4.3.19 – Gas Velocity for O ₂ -Fired Case.....	94

Figure 4.3.20 – Gas Temperature for O ₂ -Fired Case	95
Figure 4.3.21 – O ₂ Mole Fraction for O ₂ -Fired Case	96
Figure 4.3.22 – Wall Heat Flux for O ₂ -Fired Case.....	97
Figure 4.3.23 – Wall Temperature for O ₂ -Fired Case	98
Figure 4.3.24 – Wall CO for O ₂ -Fired Case.....	99
Figure 4.3.25 – Char Mass Fraction (69 micron) for O ₂ -Fired Case.....	100
Figure 4.3.26 – Char Mass Fraction (169 micron) for O ₂ -Fired Case.....	101
Figure 4.3.27 - Flue gas recycle flow vs. part load operation	102
Figure 4.3.28 – Summary of O ₂ -Fired Part Load Results, Cryogenic ASU	103
Figure 4.3.29 – Gas Temperature for O ₂ -Fired Part Load, Cryogenic ASU	104
Figure 4.3.30 – Wall Heat Flux for O ₂ -Fired Part Load, Cryogenic ASU	105
Figure 4.3.31 – Average and Peak Heat Flux in Waterwalls	106
Figure 4.3.32 – Gas Velocity for O ₂ -Fired with OITM.....	107
Figure 4.3.33 – Gas Temperature for O ₂ -Fired Case With OITM.....	108
Figure 4.3.34 – O ₂ Mole Fraction for O ₂ -Fired Case With OITM	109
Figure 4.3.35 – Wall Heat Flux for O ₂ -Fired Case With OITM.....	110
Figure 4.3.36 – Wall Temperature for O ₂ -Fired Case With OITM	111
Figure 4.3.37 – Wall CO for O ₂ -Fired Case With OITM	112
Figure 4.3.38 – Char Mass Fraction (69 micron) for O ₂ -Fired Case, OITM.....	113
Figure 4.3.39 – Char Mass Fraction (169 micron) for O ₂ -Fired Case, OITM.....	114
Figure 4.3.40 – Advantage of Low Mass Flux Design.....	117
Figure 4.3.41 – Tube Wall Temperature with Smooth, Standard Rifled, and Optimized Rifled Tubes	118
Figure 4.3.42 – Rifled Tube Design	119
Figure 4.3.43 – Outside Tube Wall Temperature with Peak Heat Flux	120
Figure 4.3.44 – Tube Inlet Mass Flow With a 10% Heat Flux Step Increase (No Pressure Equalization Header)	121
Figure 4.3.45 – Tube Inlet Mass Flow With a 10% Heat Flux Step Increase (With Pressure Equalization Header at 80')	122
Figure 4.3.46 – Predicted Wall Corrosion (mil/yr) in Air-Fired and O ₂ -Fired Furnaces.....	124
Figure 4.3.47 – HRA Tube Bank Design.....	128
Figure 4.3.48 – HRA Tube Bank Performance	130
Figure 4.4.1 – Increase in COE of O ₂ Plant Above Air-Fired Reference Plant..	152
Figure 4.4.2 – COE Breakdown	153
Figure 4.4.3 - Comparison of Levelized Cost of Electricity Among Alternative Technologies	156
Figure 4.4.4 - Comparison of Mitigation Costs Among Alternative Technologies	156

List of Tables

Table 4.1.1 - Summary of Plant Performance and Economics	15
Table 4.1.1 - Site Conditions.....	18
Table 4.1.2 - Setup and Assumptions.....	19
Table 4.1.3 - Case Summary	29
Table 4.1.4 - Flame adiabatic temperature effect on performance	34
Table 4.1.5 – Flame adiabatic temperature effect on boiler flue gas flow	34
Table 4.2.1 – Comparison of O ₂ PC with Cryogenic and OITM ASU	50
Table 4.2.2 – Parametric Case Summary	52
Table 4.2.3 - Effect of OITM O ₂ Recovery Efficiency on LMPD	54
Table 4.2.4 – Effect of Flame Temperature on Performance	59
Table 4.2.5 - Comparison for CAR with Cryogenic ASU	62
Table 4.2.6 – Comparison for CAR Using Different Sweep Gases	63
Table 4.2.7 – O ₂ PC Efficiency with Different O ₂ Separation Techniques	64
Table 4.2.8 - Gains from OITM and CAR Compared to Cryogenic ASU	67
Table 4.2.9 – Comparison of CO ₂ Removal Technologies	68
Table 4.4.1 - Coal Properties	132
Table 4.4.2 - CO ₂ Effluent Purity Design Conditions.....	132
Table 4.4.3 – Economic Study Assumptions.....	133
Table 4.4.4 - Cost of 430.2 MWe Air-Fired Supercritical PC Plant (\$1000 Yr 2006)	138
Table 4.4.5 - Cost of 347.0 MWe ASU Based Supercritical PC Plant (\$1000 Yr 2006)	139
Table 4.4.6 - Cost of 463.3 MWe OITM Based Supercritical PC Plant (\$1000 Yr 2006)	140
Table 4.4.7 - Comparison of Total Plant Costs (\$1000 Yr 2006)	141
Table 4.4.8 - Air Fired PC Plant Capital Investment & Revenue Requirement .	147
Table 4.4.9 - ASU Based PC Plant Capital Investment & Revenue Requirement	148
Table 4.4.10 - OITM Based PC Plant Capital Investment & Revenue Requirement	149
Table 4.4.11 - Summary of Plant Economics and CO ₂ Mitigation Costs.....	150
Table 4.4.12 - Plant Daily Consumable Requirements	151
Table 4.4.13 – COE and CO ₂ MC with Weld Overlay and 2200 psi Pressure ..	154

1.0 Introduction

The objective of the Conceptual Design of Oxygen-Based supercritical PC Boiler study is to develop a conceptual pulverized coal (PC)-fired power plant, which facilitates the practical capture of carbon dioxide capture for subsequent sequestration. The system design and analysis task, which was performed using the Aspen Plus computer program, is aimed at optimizing the PC boiler plant operating parameters to minimize the overall power plant heat rate. The flow rates and other properties of individual streams of the power plant were calculated as the results of the Aspen Plus simulations. The required performance characteristics of such operating components as pulverized coal-fired furnace, heat recovery area, flue gas recuperator, and economizer were determined.

Two plant configurations were simulated: 1) a conventional air-fired PC power plant and 2) the proposed oxygen-based supercritical PC plant. In order to compare the performance of the oxygen-based plant with that of the conventional plant, the main steam generation rate in the both plants was kept constant.

The objective of the advanced oxygen separation system integration task is to identify promising, low cost advanced options of oxygen separation, which can be integrated into the O₂-fired PC power plant. Currently, a number of new oxygen separation technologies are in development. They are categorized as high temperature ion membranes, such as oxygen ion transport membrane (OITM), and high temperature sorption, such as ceramic auto-thermal recovery (CAR). The former relies on oxygen transport through a ceramic membrane, and the latter on oxygen storage in perovskite type materials. Integration of these advanced oxygen separations into the O₂-fired PC has the potential to substantially reduce the cost of CO₂ removal. This task deals with the system-level evaluation of the O₂-fired PC integrated with these advanced oxygen separation methods.

The advanced oxygen separation system integration task, which was performed using the Aspen Plus computer program, is aimed at a system level optimization to minimize the overall heat rate and maximize system performance. Two types of advanced oxygen separation systems and related configurations were simulated: 1) high temperature membrane technology (OITM) and 2) high temperature oxygen sorbent technology (CAR). Determined are the required performance characteristics of the operating components such as the boiler (with air heater for OITM), GT expander, wet-end economizer for low-grade heat recovery, and air separation equipment.

The furnace and heat recovery area design and analysis task, which was performed using the FW-FIRE, Siemens and HEATEX computer programs, is aimed at optimizing the location and design of the furnace, burners, over-fire gas ports, and internal radiant surfaces. Three furnace and HRA designs were developed: 1) a conventional air-fired PC power plant and 2) an oxygen-based

PC plant with cryogenic ASU and 3) an oxygen-based PC plant with oxygen ion transport membrane.

The objective of the economic analysis is to prepare a budgetary estimate of the capital and operating costs of the O₂-fired PC power plants to permit comparison to an equivalent, conventional, air-fired power plant (e.g. the reference plant) as well as other CO₂ capture technologies.

2.0 Executive Summary

The objective of the Conceptual Design of Oxygen-Based supercritical PC Boiler study is to develop and design a conceptual pulverized coal-fired power plant, which facilitates the practical capture of carbon dioxide capture for subsequent sequestration.

The reference plant employs a supercritical steam turbine with conditions, 4035psia/1076°F/1112°F/2.0”Hg, fires high-volatile bituminous Illinois 6 coal, and produces 460 MWe at the generator. A conventional air-fired case was simulated as the comparison basis. The air-fired plant has a boiler efficiency of 88.2% and a net plant efficiency of 39.5%.

The system design and analysis task (Task 1), which was performed using the Aspen Plus computer program, is aimed at optimizing the PC boiler plant operating parameters to minimize the overall power plant heat rate. The oxygen-based plant model contains all the components in the conventional plant model (with the exception of the FGD and SCR) plus the addition of an air separation unit and a flue gas cooler. Flue gas is recycled to control the flame temperature inside the PC boiler to minimize NO_x formation, to minimize ash slagging in the furnace combustion zone, and to avoid the application of exotic materials. Equipment to compress and liquefy the CO₂ effluent to 3000 psia and to reduce the moisture to 50 ppm (to avoid transport pipe corrosion) was included in the O₂-PC system model. Compression to 3000 psia is conservative compared to the pressure of 2200 psia specified in Reference 14.

The supercritical O₂-PC power plant simulated with the same flame temperature as the air-fired PC, shows a plant net efficiency drop from 39.5 to 30.8%, and a power reduction from 430 to 332 MWe. The flue gas flowing through the boiler changes from 3555 to 3363 klb/hr (179 to 125 Mcf/hr, a 30% reduction in volumetric flow). As the result of the air separation unit (ASU) power and CO₂ compressions, the specific power penalty for CO₂ removal is 129 kWh/klb_{CO2}.

Parametric trade-off runs were made by varying the amount of recycled flue gas (which directly affects the flame temperature) while maintaining the same boiler outlet O₂ concentration (3%, vol.) as the air-fired case, and by varying the temperature of the recycled flue gas. The results show that by reducing the recycled flue gas flow rate by 38% (by volume), and by raising the temperature of the recycled flue gas from 95°F to 260°F, the equilibrium temperature increases from 3480°F to 4160°F, the system efficiency increases from 30.8% to 32.9%, and the specific penalty for CO₂ removal reduces from 129 to 99 kWh/klb_{CO2}.

The objective of Task 2 is to develop a system design of a conceptual pulverized coal-fired oxygen combustion power plant, integrated with advanced oxygen separation technology. The baseline oxygen-based PC boiler incorporates cryogenic O₂ separation, which can produce oxygen with high purity; but it requires substantial capital and operating costs. Membrane separation of O₂ has

been demonstrated at small scale employing very thin membrane fibers, which preferentially allow O₂ to permeate, but not N₂. Membrane separation has the potential to use less power at a lower capital cost.

The advanced oxygen separation system integration task (Task 2), which was performed using the Aspen Plus computer program, is aimed at a system level optimization to minimize the overall heat rate and maximize system performance. Two types of advanced oxygen separation systems and related configurations were simulated: 1) high temperature membrane technology (OITM) and 2) high temperature oxygen sorbent technology (CAR).

Oxygen separation by oxygen ion transport membrane is driven by the difference in oxygen partial pressure across a membrane. To produce this pressure difference, the air is pressurized by a compressor and heated to a high temperature. The hot pressurized air is fed to an oxygen ion transport membrane (OITM), where about 85% of its O₂ is separated through membrane, and the remaining O₂ is carried by hot vitiated air to a gas expander. Power generated from the expander is used to drive the air compressor. The OITM does not consume electrical power; instead, it absorbs heat, generates power, as it separates O₂ from air.

The O₂-fired reference plant with cryogenic ASU has a net plant efficiency of 31.9%, a net power generation of 338 MWe, and a CO₂ removal penalty of 114 kWh/klbCO₂. The O₂-fired reference plant with OITM has a net plant efficiency of 36.1%, a net power generation of 463 MWe, and a CO₂ removal penalty of 42 kWh/klbCO₂.

Parametric trade-off runs were conducted by varying the O₂ recovery efficiency, the pressure difference across the membrane, the OITM operating pressure, the compressor discharge temperature, and the furnace flame temperature. OITM faces significant challenges with respect to the manufacture and stability of membranes, and scale up and design of large plants.

The ceramic auto-thermal recovery (CAR) process is based on sorption and storage of oxygen in a fixed bed containing ionic and electronic conductor materials. For the CAR process utilizing extracted steam as the sweep gas, net system efficiency is increased by only by 0.7% point compared to the cryogenic ASU process. But if the CAR process uses recycled flue gas as the sweep gas, system efficiency can be increased by 2.6% points, compared to the gain of 3.2% points of the OITM process. At the same equilibrium temperature (4160°F), the efficiency reduction of the O₂-PC compared to the air-fired PC is 6.5% points with cryogenic air separation, 3.3% points with OITM, and 4.3% points with CAR.

The furnace and heat recovery area design and analysis task (Task 3), which was performed using the FW-FIRE, Siemens, and HEATEX computer programs, is aimed at optimizing the location and design of the furnace, burners, over-fire gas ports, and internal radiant surfaces.

A simulation was made for both the reference air-fired case and for the oxygen-fired case. Two oxygen-fired models were constructed: one for the cryogenic ASU design (with radiant superheater partial division walls) and the second for the OITM design with a furnace wall radiant superheater and a high temperature air heater. Boundary conditions are based on ASPEN simulations of the power plant.

The furnace is designed with opposed wall-firing burners and over-fire air ports located at one burner pitch above the top burner row. The O₂-PC supercritical boiler incorporates the BENSON vertical technology, which uses low fluid mass flow rates in combination with optimized rifled tubing. Water is circulated in the furnace by forced circulation to the waterwalls at the periphery and divisional wall panels within the furnace.

For the air-fired furnace simulation, the maximum flue gas temperature is approximately 3350°F. The maximum heat flux is approximately 70,000 Btu/hr-ft² and is located on the side wall at the top of the burner zone. The total heat absorbed by the furnace walls before the furnace exit is 1770 MM Btu/hr. The maximum temperature of the waterwalls is approximately 870°F and of the division walls is approximately 1000°F. Total burnout of all particle sizes is 99.6%. Average NO_x concentration at the furnace outlet is 276 ppmvw (0.38 lb/MMBtu).

Compared to the air-fired furnace, the oxygen furnace requires only 65% of the surface area and 45% of the volume. Two oxygen-fired designs were simulated: 1) with cryogenic ASU and 2) with OITM. The mixed primary/secondary gas O₂ content (before combustion) is approximately 40%.

In the oxygen-fired furnace, the maximum flue gas temperature is approximately 3900°F for cryogenic ASU and 3850°F for OITM. The maximum heat flux is 171,000 Btu/hr-ft² for cryogenic ASU and 180,000 Btu/hr-ft² for OITM. The maximum wall heat flux in the oxygen-fired furnace is more than double that of the air-fired furnace due to the higher flame temperature and higher H₂O and CO₂ concentrations. The total heat absorbed by the furnace walls before the furnace exit is approximately 2287 (cryogenic) and 2029 (OITM) MM Btu/hr. The coal burnout for the oxygen-fired case is 100% due to the high furnace temperature and high concentration of O₂. NO_x is 261 ppmvw (0.18 lb/MMBtu).

The maximum temperature of the oxygen-fired furnace is approximately 1060°F for the waterwalls, 1065°F for the division walls, and 1100°F for OITM radiant superheater walls. Because of the higher temperature of the oxygen-fired case compared to the air-fired case, furnace tube material was upgraded from T2 to T92.

Since the boiler is a supercritical once-through sliding pressure unit, part load cases (72%, 50%, and 25%) were run and evaluated with thermal/hydraulic and structural criteria. A pressure equalization header is included at an elevation of 80' to ensure stable operation at low loads.

To reduce the corrosion in the O₂-PC, tube weld overlays with high Nickel and Chromium contents (e.g. alloy 622) are applied to the waterwalls. This reduces the predicted maximum corrosion from 45 mil/yr to 10 mil/yr.

HEATEX was used to determine the heat recovery area (HRA) design of the convective tube banks between the furnace exit and the SCR/air heater. These tube banks include the finishing superheater, finishing reheater, primary superheater, primary reheater, upper economizer, and lower economizer.

For the air-fired design, total surface area of all convective banks is 335,025 ft². The total heat transferred to the water/steam is 1431 MM Btu/hr as 3.59 MM lb/hr of flue gas is cooled from 2185°F to 720°F.

For the cryogenic ASU oxygen-fired design, convective bank total surface area is 218,693 ft² and the total heat transferred to the water/steam is 1151 MM Btu/hr as 2.12 MM lb/hr of flue gas is cooled from 2450°F to 695°F. For the OITM oxygen-fired design, convective bank total surface area is 274,466 ft² and the total heat transferred to the water/steam is 1185 MM Btu/hr and to the air is 990 MM Btu/hr as 2.68 MM lb/hr of flue gas is cooled from 2950°F to 695°F. The total heat transfer surface required in the oxygen-fired HRA is less than the air-fired HRA due to more heat being absorbed in the oxygen-fired furnace and the greater molecular weight of the oxygen-fired flue gas.

The HRA tube materials and wall thicknesses are nearly the same for the air-fired and oxygen-fired designs since the flue gas and water/steam temperature profiles encountered by the heat transfer banks are similar.

A tubular convective air heater is included in the OITM O₂-PC to provide the necessary air heating for the membrane separation process. The furnace air heater is an Incoloy MA956 three-pass tubular design situated above the furnace nose.

The objective of the economic analysis task (Task 4) is to prepare a budgetary estimate of the capital and operating costs of the O₂-fired PC power plants to permit comparison to an equivalent, conventional, air-fired power plant (e.g. the reference plant) as well as other CO₂ capture technologies. The economic analyses of the plants were carried out based on the EPRI Technical Assessment Guide (TAG) methodology. Plant capital costs were compiled under the Code of Accounts developed by EPRI. The estimate basis is year 2006 dollars, a 20-year life, and an 85 per cent capacity factor. Table 4.1.1 summarizes the performance and economics of the plants.

Table 4.1.1 - Summary of Plant Performance and Economics

	Reference Air-Fired Plant	ASU Based Plant	OITM Based Plant
Net Power Output, MWe	430.2	347.0	463.3
Efficiency, % (HHV)	39.5	33.0	36.1
Coal Flow, Klb/hr	319.0	308.0	375.4
Total Plant Cost			
Millions of Dollars	633.0	723.3	953.0
\$/kW	1,471	2,084	2,057
Levelized COE, \$/MWhr	50.41	66.17	63.48
CO2 Mitigation Cost, \$/tonne		20.23	16.77

Total plant costs are \$633 million (1471 \$/kW) for the air-fired reference plant, \$723 (2084 \$/kW) million for the cryogenic ASU O₂-PC, and \$953 (2057 \$/kW) million for the OITM O₂-PC. Even though the OITM O₂-PC has a total plant cost that was 32 per cent higher than the ASU O₂-PC, its higher power output results in a slightly lower \$/kW cost of \$2,057/kW versus \$2,084/kW.

The levelized cost of electricity (COE) was calculated for each of the plants assuming an 85 per cent capacity factor. The COE value is made up of contributions from capital cost, operating and maintenance costs, consumables, and fuel costs. The levelized COE was calculated to be \$50.41/MWhr for the reference plant, \$66.17/MWhr for the cryogenic ASU O₂-PC, and \$63.48/MWhr for the OITM O₂-PC. Again, because of its higher output, the OITM O₂-PC has a lower levelized cost of electricity (\$63.48/MWhr versus \$66.17/MWhr) and a lower CO₂ mitigation cost (MC) (\$16.77/tonne versus \$20.23/tonne) than the ASU O₂-PC.

The addition of weld overlay increases the COE approximately 0.75%, but reducing the pipeline pressure from 3000 psia to 2200 psia (specified in Ref. 14) reduces the COE by 0.3%. Thus, the combined effect of these two adjustments on the COE is relatively small (+0.4% for cryogenic O₂-PC and +0.1% for the OITM O₂-PC).

Compared to the COE of the supercritical cryogenic O₂ PC, the COE for the other technologies is 52% higher for Air PC, 35% higher for NGCC, 15% higher for IGCC, and 5% higher for the subcritical O₂PC, and 4% lower for the supercritical O₂PC with OITM. Compared to the MC of the supercritical cryogenic O₂ PC, the

MC for the other technologies is 238% higher for NGCC, 192% higher for Air PC, 25% higher for IGCC, 5% higher for the subcritical O₂PC, and 17% lower for the supercritical O₂PC with OITM.

3.0 Experimental

This work performed for this report was performed utilizing computer program simulations. No experimental equipment was used.

4.0 Results and Discussion

4.1 System Design and Analysis

4.1.1 Reference Site and Conditions

In December 2000, Parsons published a study of the cost of electricity of several case studies of CO₂ sequestration from a PC boiler by post-combustion capture (Ref. 1). In September 2005, Foster Wheeler released a report of conceptual design of O₂-fired PC boiler (Ref. 3). To provide a consistent comparison with the cases analyzed in the previous reports, the same site conditions (59°F, 14.7 psia, 60% RH) and the same fuel (Illinois #6) were used. Site Conditions and fuel properties are presented in Table 4.1.1. Fuel HHV and LHV were estimated by a DuLong's method and the stoichiometric air ratio of 867 lb_{air}/lb_{coal} was calculated based on the fuel ultimate analysis.

Table 4.1.1 - Site Conditions

Standard site:		air, %v	dry	wet	coal, Ill#6	%w	sorb	%w
elevation, ft	0	N2	78.085	77.297	C	63.75	CaCO3	100
amb p, psia	14.70	O2	20.947	20.735	H	4.5		
amb T, F	59	Ar	0.935	0.926	O	6.88		
amb T, wet, F	51.5	CO2	0.033	0.033	N	1.25		
RH, %	60	H2O	0.000	1.010	S	2.51		
P-H2O, psia	0.247	sum	100.000	100.000	A	9.99		
Y-H2O, %v	1.010				M	11.12		
condenser P, "Hg	2.00				V	34.99		
					F	44.19		
					sum	100.0		
					fuel HHV	btu/lb		
					given	11666		
					aspen	11631		

The CO₂ fluid produced from the oxygen-based PC power plant is not chemically pure, but can be readily sequestered in geologic formations (depleted oil and gas reservoirs, unmineable coal seams, saline formations, and shale formations) or in oceans. The liquid CO₂ exits the plant at over 2000 psia. The CO₂ fluid inside pipeline under this pressure is in a liquid or a supercritical state. The other gases in the delivered CO₂ are limited to H₂O < 50 ppm (to avoid acid corrosion), and Ar+N₂ < 3% (to avoid phase separation). The excess gases in CO₂ stream either have to be purged or recycled. However, since SO₂, as an acid gas, similar to CO₂, it can be sent to pipeline directly under moisture free condition, and as mentioned in literature, it does not need to be separated out from CO₂ product. Furthermore it is also not necessary to remove the small concentration of NO_x in the CO₂ effluent since it can be sequestered along with the CO₂.

4.1.2 Air-Fired Reference Case (case-1)

To study the effects of CO₂ removal on the performance of the power plant, an air-fired supercritical PC boiler was been simulated in detail as a reference case. This model was used as the base, which was then extended to include the air separation unit (ASU) and CO₂ compression unit for O₂-fired PC cases.

The reference plant employs a supercritical steam turbine with conditions, 4035psia/1076°F/1112°F/2.0”Hg, fires high-volatile bituminous coal, and produces 460 MWe at the generator. It employs eight feed water heaters to raise the final feed water temperature to 569°F. It uses an auxiliary steam turbine to directly drive the high-pressure feed water pump.

Case 1 is the reference air-fired supercritical PC boiler case, and the model and results shown in Figure 4.1.1 and Table 4.1.2.

Table 4.1.2 - Setup and Assumptions

Setup and Result							
ST		Result		Aux power	MWe	dP-air	"H2O
main P, psia	4035	net power, MWe	430	condensed water pump	0.6	AAHX	4.0
main T, F	1076	net eff, %	39.5	HP feed water pump	17.5	duct	6.0
RH P, psia	823	gross @ST, MW	477	FGD pump	0.8	nozzle	10.0
RH T, F	1112	aux power, MW	46.0	CT pump	3.4	sum	20.0
FWHs	8	as %	9.7	PA Fan	1.1		
end wet, %	9.5	HHV in, mmbtu	3721	SA Fan	2.0	dp-gas	"H2O
end P, "Hg	2.0	Q to st, mmbtu	3281	ID Fan	5.4	FSH	0.5
		Q, cond, mmbtu	1696	FGD Fan	4.1	FRH	0.5
FWH	F	boiler eff, %	88.2	cooling tower Fan	1.9	RH	1.0
TD	5	ST cycle eff, %	47.7	coal handling	2.0	PSH	0.7
DC	10	Generator eff, %	98.3	sorb handling	0.8	UECO	0.3
FW T	569			ash handling + ESP	1.8	ECO	2.0
		Flow		others (=1%)	4.6	AAHX	1.6
DeSuperheat		air, klb	3270	total	46.0	Damper	4.3
SH, %	5	coal, klb	319			BHG	5.5
water T, F	569	sorb, klb	26	FGD & SCR		FGD	12.0
		flue gas, klb	3556	L/G	10	sum	28.4
Boiler		O ₂ , %	3.0	Ca/S	1.05		
PA, %	20	H ₂ O, %	8.6	Excess air, %	85	dP-Fan	"H2O
UBC, %	1.0	CO, ppmv	14	NH ₃ /NO _x	1.0	PAFan	60
radiation/margin, %	0.59	NO _x , ppmv	22	DeSO _x , %	98	IDFan	28
EXA, %	17.9	SO _x , ppmv	1979	DeNO _x , %	90	SAFan	20
flame T, F	3685	after FGD	37				
stack T, F	289	Ash, klb	33			eff	%
blowdown, %	0	C, %	6.0			FDfan	75
milller exit T, F	219	main st, klb	2950			IDFan	70
		RH st, klb	2406			CWPump	80
		end st, klb	1573			BFPump	80
						Motor/mech	95

The Aspen Plus model includes coal mills, flue gas heater, pulverized coal-fired furnace, steam generator, superheater, reheater, economizer, ash-removal unit, nitrogen oxides (NO_x) selective catalytic reactor (SCR), flue gas de-sulfurization reactor (FGD), air blower, induced draft (ID) fan, feed water pump, cooling water

pump, feed water heaters, and a single reheat steam turbine. A coal drying function has been modeled and added into mill module to produce the correct mill exit gas temperature. The furnace was simulated by a zero dimensional model for heat and mass balances. However, all key tube banks of the heat recovery area (HRA) were individually modeled. The furnace roof heat absorption was also simulated. The high-pressure steam temperature is controlled by water spray for de-superheat. The simulation also included heat losses from the boiler and HRA enclosure, as well as from the steam pipes. Some user-defined models were included to perform emission calculations. User built-in calculations have been added to determine boiler efficiency, system net efficiency, and net power. The heat carried by exhaust streams was automatically calculated by the program.

For a given steam turbine output and a fuel, Aspen Plus iterates to determine the feed rates of air, coal, etc., based on specified temperature approaches and excess air requirement.

The system configuration, detailed setup parameters and summary of results for the case 1 reference case are shown in Figure 4.1.1 and Table 4.1.2. The system has a steam turbine cycle efficiency (generator power divided by heat transferred to the steam cycle) of 47.6%, a boiler efficiency (heat to steam cycle divided by heat input from fuel to boiler) of 88.2%, an unburned carbon loss (UBC) of 1.0%, and a net plant efficiency of 39.46% (net plant heat rate of 8647 Btu/kWh). It has a gross power of 460 MWe at the generator, 18 MWe from auxiliary steam expander, an auxiliary power of 46 MWe, and a net power of 430 MWe. Total heat input from the fuel is 3720 MM Btu/hr.

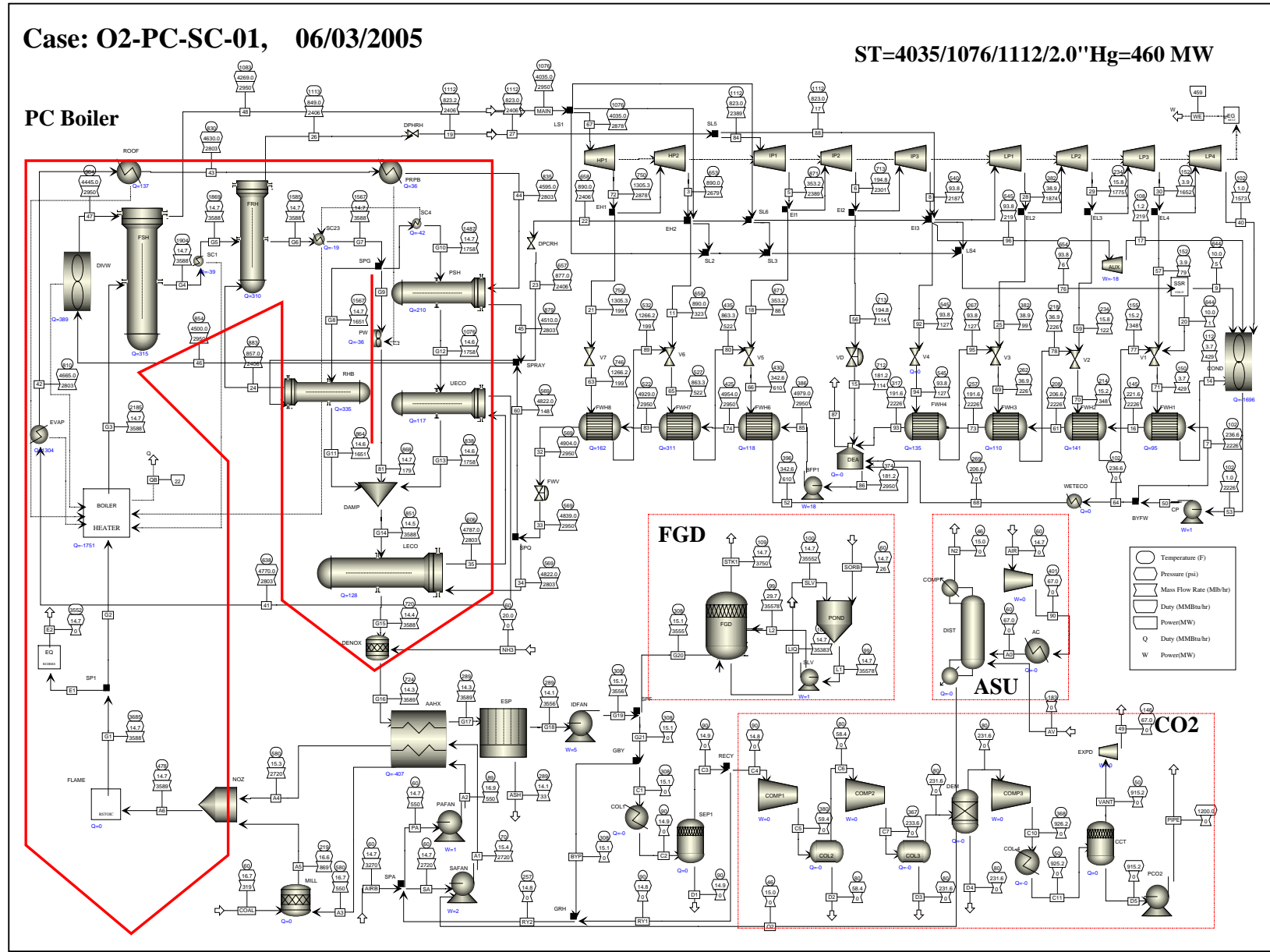
The temperature of the flue gas exhausted to the stack is 289°F. The flue gas exiting the boiler contains 3.0%, vol., wet O₂ (18% excess air) and contains 739 klb/hr (1.72 lb/kWh) of CO₂. This 3.0% O₂ level is kept constant for all of the O₂-fired cases. A SCR is applied to control NO_x with NH₃/NO_x=1.0, and an FGD is used to control SO_x by lime solution with Ca/S=1.05, L/G=10, and 85% excess air for aeration.

The breakdown of auxiliary power for case 1 is listed in Table 4.1.2. Most of these power consumptions were simulated directly by the Aspen module. Some required user Fortran for those processes lacking Aspen modules, such as solids handling. The power consumption was based on stream flows and design data.

Fan power consumption was simulated based on the pressure drops from both air side and gas side. The total auxiliary power consumption, including FGD, for case 1 is approximately 9.7% of the gross power, while it was about 9.2% for a subcritical case.

Because of high temperature and high CO₂ concentration, the CO concentration is high, producing a flame temperature, which is lower than the adiabatic combustion temperature. To represent this effect on boiler design, an estimation of the equilibrium flame temperature was modeled.

Figure 4.1.1 - Reference Case of Air-fired Supercritical PC



4.1.3 Oxygen-Based PC Plant – Base Case

4.1.3.1 Boiler Plant Modifications

The oxygen-based (or oxygen-fired) plant model contains essentially all the components in the conventional plant model. In addition, it also includes an air separation unit (ASU) and a flue gas cooler. In the O₂-fired plant, the FGD is not needed because the SO₂ is acid gas similar to CO₂ and can thus be sent to pipeline together with the CO₂. A substantial portion of the SO_x will be removed as the flue gas is cooled down in the CO₂ cooling and compression equipment.

The steam side components remain very similar to the air-fired case with only some changes in heat bundle duties in the heat recover area (HRA).

In O₂-fired cases, flue gas is recycled to control the flame temperature inside the PC-fired boiler to minimize NO_x formation, minimize ash slagging in the furnace combustion zone, and avoid the application of exotic materials.

Before the flue gas is separated into a recycled and effluent stream (to the pipeline), it is cooled to 90°F. Since this is below the acid/moisture dew point, a heat exchanger containing acid-resistant materials must be used. The recycled gas is then reheated, before the forced draft (FD) fan, by mixing it with a bypassed hot gas to avoid reaching the dew point. After the O₂ from ASU plant is mixed with recycled flue gas, it is heated by the flue gas exiting the boiler in a gas-gas heat exchanger, which acts as a recuperator to improve cycle efficiency and reduce fan power requirements.

It is assumed in this study that there is no tramp air ingress through the sealed boiler.

4.1.3.2 Air Separation Unit

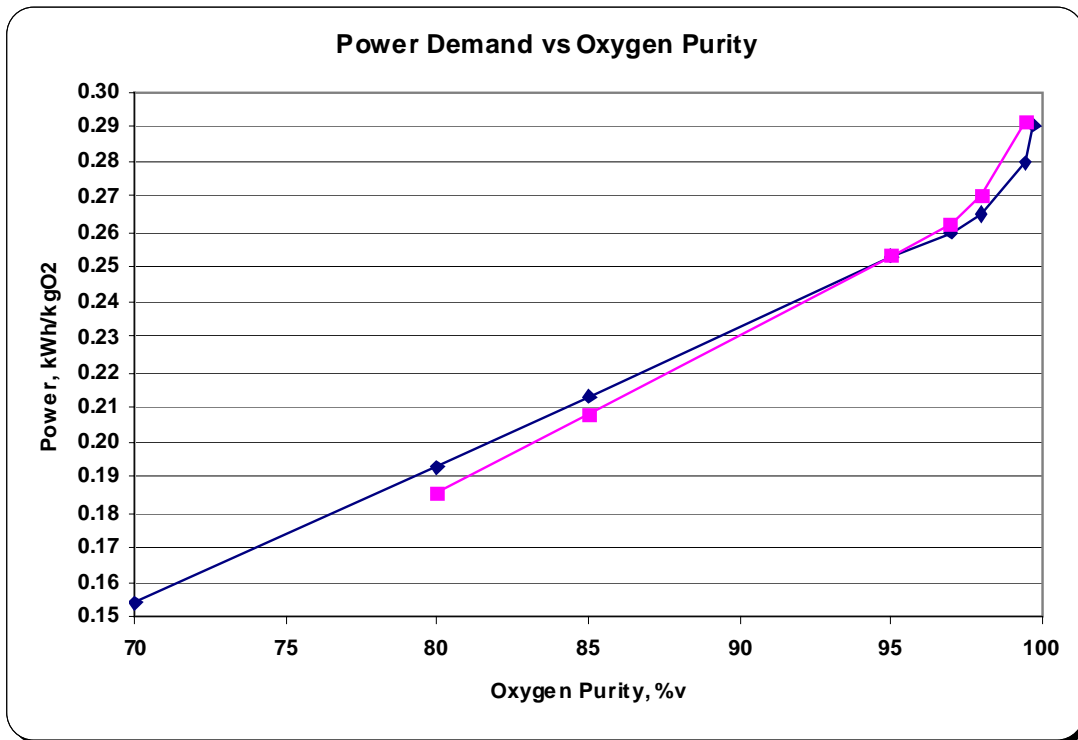
For an O₂-fired PC, O₂ purity is a key parameter for system performance and economics. A high purity O₂ will produce a high purity of product CO₂ gas, which will reduce CO₂ purification and compression power. However, producing high purity O₂ requires high ASU plant operational and equipment costs. Furthermore, too high O₂ purity is not necessary because the fuel combustion itself will generate some gases, such as N₂ and some excess O₂ is required for complete combustion, in addition to CO₂ as flue gas. Therefore there is a balance point to give an optimum.

The method of air separation chosen for this study is the commercially available large-scale cryogenic air separation technique. A traditional cryogenic ASU plant was simplified in the simulation to include the power consumption, but without details of distillation columns and cold heat exchangers. The Aspen model does not include the air purifier, which removes moisture, hydrocarbons, CO₂, and NO_x in an adsorber and is located between the cold box and air compressor.

Although the separated N₂/Ar gases could potentially be sold as byproducts, no economic credit for this is taken in this study. No heat recovery from the ASU air compressor inter-stage coolers is included, because recovery of this low grade heat is inefficient.

Power consumption for different O₂ purity is plotted in Figure 4.1.2. For the O₂ purity of 99.5% used in this study, a power consumption of 24.5 kWh/klb_{air} is applied. For a 460 MWe steam turbine generation, the ASU plant consumes about 70 MWe, or 15% of generated power, which is a large penalty for CO₂ removal.

Figure 4.1.2 – Oxygen purity effect on ASU specific power



Advanced air separation methods such as high temperature membrane method will be incorporated into the cycle in task 2 (Section 4.2) to reduce both operation and capital costs.

4.1.3.3 CO₂ Compression Unit

The flue gas effluent stream (mainly CO₂) has to be compressed to the high pipeline pressure of 1200 to 3000 psia depending upon end user specification. The CO₂ sequestration equipment is added to the system and the effluent is conservatively compressed to 3000 psia. The dominant moisture in flue gas is condensed out first during flue gas cooling before the first stage compression. The condensed water contains acid gases and has to be treated before recycle or discharge.

The flue gas composition after cooling but before the first stage CO₂ compressor from this base case (case-2) is:

CO ₂	O ₂	N ₂ +Ar	SO _x	H ₂ O
90.4	3.3	1.3	1.1	3.6

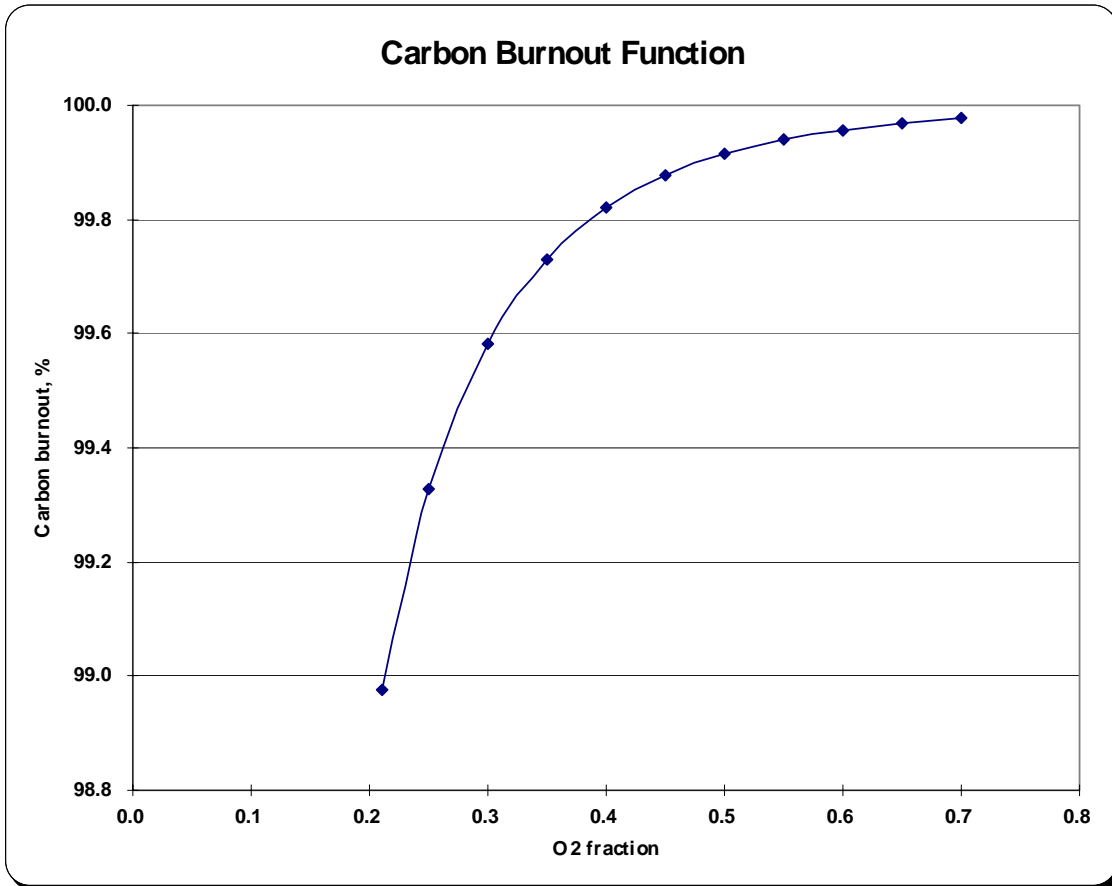
In literature, residual O₂ as low as 1.3% was used. Reducing O₂ content, such as from 3.0% to 2.0% by reducing excess air, is helpful in reducing CO₂ compression power, but it is judged that an oxygen content of approximately 3.0% is required for good combustion efficiency. Both CO₂ and SO_x are acid gases. They combine with moisture to form acid, which causes a corrosion problem along CO₂ pipeline. Therefore, after the 2nd stage, a chemical method of active dehydration with TEG (Triethyleneglycol) is applied to remove the rest of moisture to a very low level of less than 50 ppm, where the TEG can be regenerated by heating. In the model, the TEG dehydration was simulated, but the TEG itself was not simulated.

A four-stage compression with inter-stage cooling was applied. To reduce power, an equal compression pressure ratio of approximately 4.0 was applied.

4.1.3.4 O₂-fired PC: Base Case (case-2)

Figure 4.1.4 presents the base case system model. The key parameter for the base case is that the adiabatic temperature in the boiler was kept the same as the reference air case (at about 3690°F) by adjusting the recycle gas flow. Both fuel and air feed rates were iterated to match the heat duty and 3.0%v exit O₂ level. Compared to reference air-fired case, the case 2 air flow rate is reduced by 13.4% (from 3270 klb/hr to 2832 klb/hr), O₂ concentration to the boiler is 28.3% (compared to 20.7% for the air-fired case) yielding an increased combustion efficiency and a lower UBC (unburned carbon). The relation of UBC and O₂% has been included in modeling as shown by Figure 4.1.3 (based on FW-FIRE modeling results).

Figure 4.1.3 - Carbon burnout vs. O₂ concentration to boiler

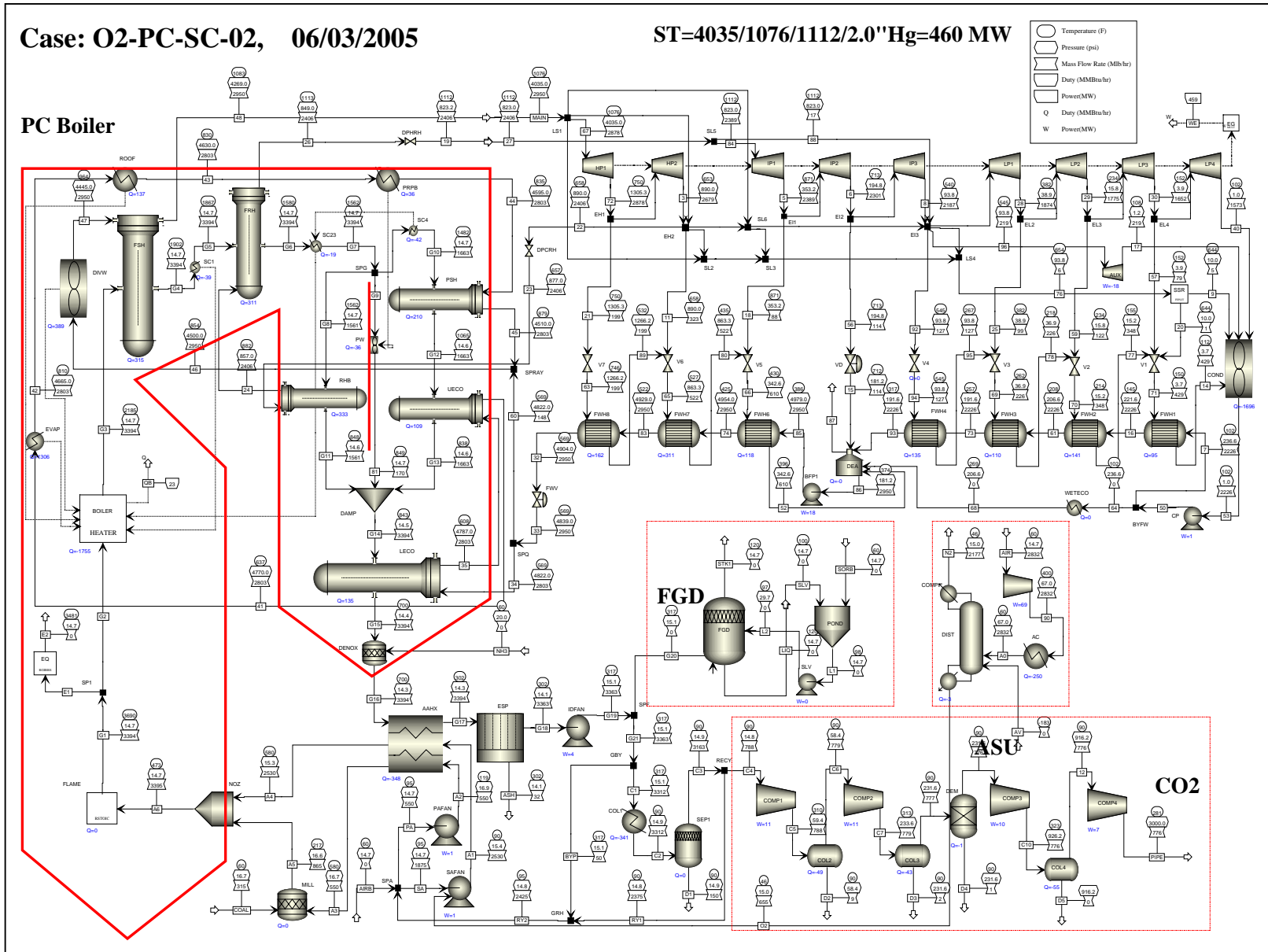


The oxidant from the ASU was 99.5% O₂ purity. ASU and CO₂ plant power consumptions were 68.7 and 38.4 MWe respectively. This resulted in a total auxiliary power of 144.5 MWe, or about 30.4% of gross power. All CO₂ generated from fuel combustion was 100% removed with a final CO₂ purity of 93.8%v. The efficiency penalty for CO₂ removal was 8.7% in points with efficiency drop from 39.46 to 30.81%, and the related electric power penalty was 129 kWh/klb_{CO₂}. The extra cooling duties for the CO₂ stream were added into cooling tower calculation for auxiliary power.

The volumetric flow in the O₂-fired PC case was reduced from 179 to 125 MMft³/hr, or to 70%, due to a high gas molecular weight of CO₂ instead of N₂. The gas mass flow was reduced from 3555 to 3363 klb/hr, or 95% in comparison to the air-fired case. The recycled gas flow was 2425 klb/hr, at a temperature of 95°F, which has been heated 5°F by a bypass flue gas stream as shown in Figure 4.1.4. It is noted that compared to the air-fired case, the coal feed rate was reduced from 319 to 315 klb/hr as the result of low UBC, and low excess air.

Because of high CO_2 content in flue gas at high flame temperature, part of CO_2 dissociated and more CO slipped, the equilibrium flame temperature differed from adiabatic temperature.

Figure 4.1.4 - Base case of O₂-fired supercritical PC



4.1.4 Parametric Cases

Various cases were simulated to evaluate the effects on O₂-PC performance of different designs and operating conditions, as shown by Table 4.1.3, in which the red highlight shows the key parameter changed in comparing with previous cases. All these cases, including part load cases (100% to 25%), will be explained and discussed in details in the following sections.

In Table 4.1.3, the efficiency drop was directly calculated from the difference between cases with and without CO₂ removal. But in general, the specific power penalty for the CO₂ removal cannot be calculated by difference directly, because extra power may be produced by firing more when integrated with different O₂ separation techniques. In some cases, the extra power by added firing may be greater than the power required for CO₂ removal. Therefore a new definition, here, is introduced as

$$\text{kWh/lb}_{\text{CO}_2} = (\text{eff drop}) * (\text{power/efficiency})_{\text{air}} / \text{lb}_{\text{CO}_2} \quad (1)$$

Equation (1) is the way to compare penalty for CO₂ removal for different systems without cost estimation, especially for a complex system such as O₂-PC integrated with a high temperature oxygen separation membrane method, where even more net power is produced from with CO₂ removal than without.

Table 4.1.3 - Case Summary

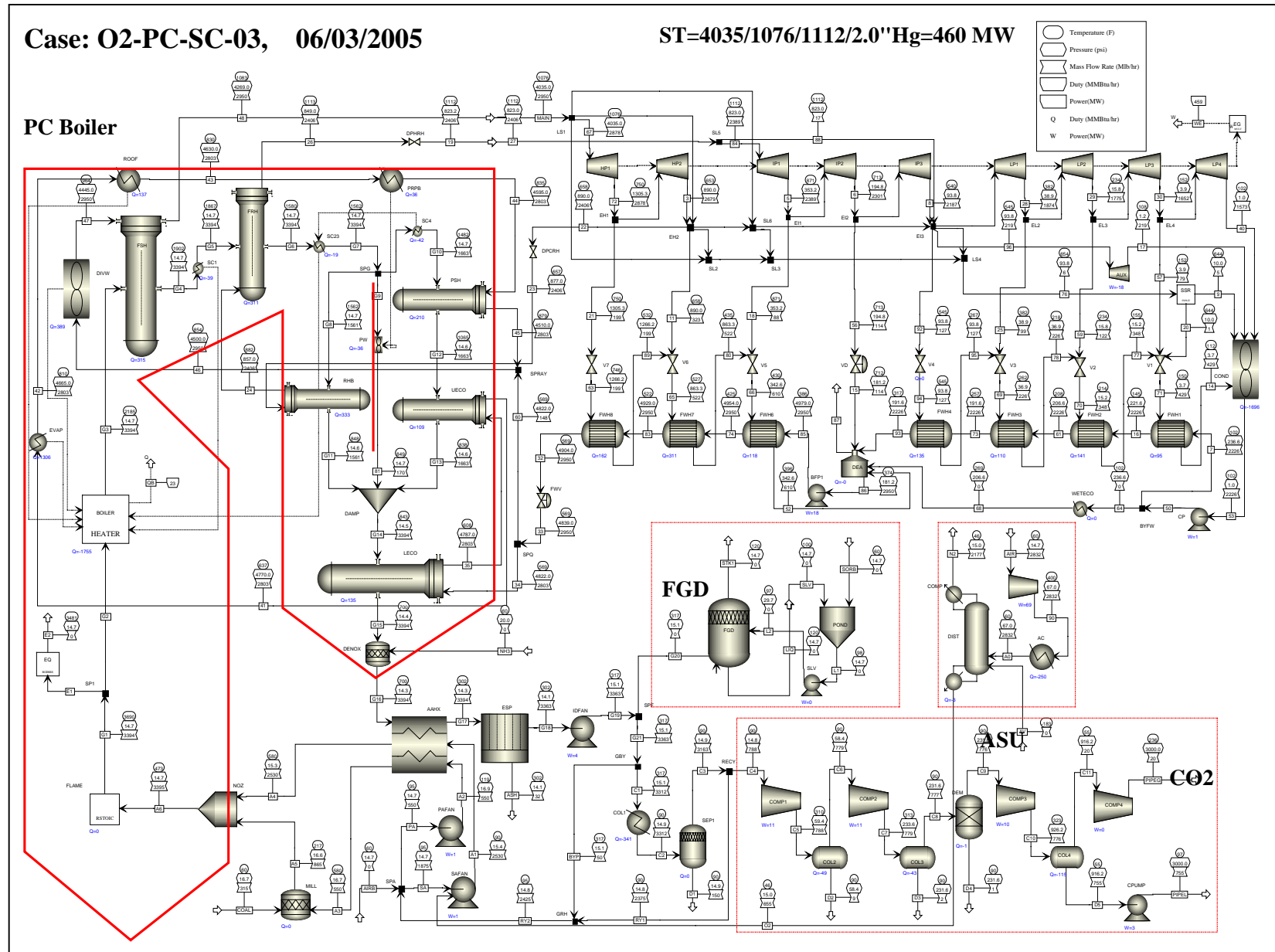
case		01	02	03	04	05	06	07	08	09	10	p100	p72	p50	p25	6A	6B	9A	9B
Waste heat economizer		no	yes	yes	yes	yes	yes	yes	yes	no	no	yes	yes						
HRA Arrangement		parallel	series																
CO2 Condensation		-	no	yes	yes	yes	yes	yes	yes	yes	yes	yes							
Vent Gas Recycle		-	-	-	no	no	no	no	no	no	no	no	no						
Coal flow	klb/hr	319.0	315.0	315.0	312.0	310.7	309.4	308.0	308.0	308.0	308.0	308.0	229.4	168.0	98.4	309.4	309.4	308.0	308.0
Oxidant flow	klb/hr	3270	655	655	649	647	645	644	644	644	644	644	480	350	206	645	645	644	644
Air flow	klb/hr	3270	2832	2832	2806	2798	2790	2784	2784	2784	2784	2784	2074	1513	889	2790	2790	2784	2784
O2 purity	%	-	99.5	99.5	99.5	99.5	99.5	99.5	99.5	99.5	99.5	99.5	99.5	99.5	99.5	99.5	99.5	99.5	99.5
Recycle gas flow	klb/hr	0	2425	2425	2429	2046	1751	1162	1162	1166	1166	1166	1151	1072	697	1751	1751	1166	1166
	%	0.0	72.1	72.1	72.4	68.8	65.5	55.8	55.8	55.9	55.9	55.9	62.7	68.2	70.3	65.5	65.5	55.9	55.9
Recycle gas temperature	F	-	95	95	138	142	146	163	163	260	260	259	225	205	206	146	146	260	259
Boiler Inlet O2	%, v	20.7	28.3	28.3	27.8	30.8	33.8	42.2	42.2	41.1	41.1	41.1	35.5	30.9	29.1	33.8	33.8	41.1	41.1
Boiler Outlet O2	%, v	3.0	3.0	3.0	3.0	3.0	3.0	3.0	3.0	3.0	3.0	3.0	3.0	3.0	3.0	3.0	3.0	3.0	3.0
Boiler outlet flue gas flow	MM cf/hr	179	125	125	126	109	96	75	75	77	77	75	61	49	26	96	96	77	75
	klb/hr	3555	3363	3363	3357	2972	2675	2083	2083	2087	2087	2087	1837	1572	991	2675	2675	2087	2087
Adiabatic Temperature	F	3685	3690	3690	3678	4010	4321	5178	5178	5104	5104	5104	4509	4001	3723	4321	4321	5104	5104
Equilibrium Temperature	F	3552	3481	3481	3474	3669	3830	4182	4182	4161	4161	4161	3919	3672	3514	3830	3830	4161	4161
Gas Temp. to FSH	F	2185	2185	2185	2185	2185	2185	2185	2185	2185	2185	2450	2146	1918	1458	2450	2185	2450	2450
Water temp. to evap.	F	638	638	638	638	615	597	592	592	596	596	593	574	553	495	666	603	591	594
UBC	%	1.00	0.49	0.49	0.51	0.39	0.30	0.15	0.15	0.16	0.16	0.16	0.27	0.37	0.43	0.30	0.30	0.16	0.16
Boiler Efficiency	%	88.16	89.28	89.28	90.14	90.52	90.90	91.31	91.31	91.31	91.31	91.31	-	-	-	90.90	90.90	91.31	91.31
Pipeline pressure	psia	0	3000	3000	3000	3000	3000	3000	3000	3000	2000	3000	3000	3000	3000	3000	3000	3000	3000
Generated CO2 flow	klb/hr	739	732	732	725	723	720	718	718	718	718	718	535	391	230	720	720	718	718
CO2 purity	%,v wet	14.0	81.3	81.3	80.0	78.7	77.5	74.2	74.2	71.3	74.2	71.3	73.9	76.2	77	77.5	77.5	71.3	71.3
Removed CO2 flow	klb/hr	0	732	732	725	723	720	718	718	718	718	718	535	391	230	720	720	718	718
CO2 removal efficiency	%	0	100	100	100	100	100	100	100	100	100	100	100	100	100	100	100	100	100
CO2 purity	%	-	93.8	93.8	93.8	93.7	93.7	93.6	93.6	93.6	93.6	93.6	93.5	93.7	93.6	93.7	93.7	93.6	93.6
Gross Power	MW	476.2	476.2	476.2	476.2	476.2	476.2	476.2	483.1	486.4	486.4	486.5	349.0	239.2	119.3	476.2	476.2	486.4	486.5
Auxiliary Power	MW	46.0	37.4	37.6	37.6	37.1	36.6	36.9	37.5	38.1	38.1	37.7	26.1	16.5	7.2	36.6	36.6	38.1	37.7
ASU power	MW	0.0	68.7	68.7	68.1	67.9	67.7	67.6	67.6	67.6	67.6	67.6	50.3	36.7	21.6	67.7	67.7	67.6	67.6
CO2 compression power	MW	0.0	38.4	34.7	34.4	34.3	34.2	34.2	34.2	34.2	34.2	34.2	25.5	18.6	10.9	34.2	34.2	34.2	34.2
Net Power	MW	430.2	331.7	335.2	336.1	336.9	337.7	337.5	343.9	346.6	347.9	347.0	247.1	167.4	79.6	337.7	337.7	346.6	347.0
Net Efficiency	%	39.46	30.81	31.14	31.53	31.73	31.94	32.07	32.67	32.93	33.05	32.97	31.52	29.16	23.67	31.94	31.94	32.93	32.97
Efficiency Drop	% pts.	-	8.7	8.3	7.9	7.7	7.5	7.4	6.8	6.5	6.4	6.5	7.9	10.3	15.8	7.5	7.5	6.5	6.5
CO2 removal energy	kWh/klbCO2	-	129	124	119	117	114	112	103	99	97	99	0	0	0	114	114	99	99

4.1.4.1 O₂-fired PC with Liquid CO₂ Pump (case-3)

Case-3, as shown in Figure 4.1.5, was formed from case-2 by adding the CO₂ condensing process into CO₂ plant. The CO₂ gas is compressed first by a three-stage compressor to over 900 psia, and then is cooled down by cooling water to its dew point. Most of the CO₂ is condensed out as liquid, some of the CO₂ stays in gas by equilibrium partial pressure, where the gas dew point reduces from 76 to 55°F during condensation. Both the gas stream and the liquid stream from the condenser are boosted to the pipeline pressure by a small gas compressor and a liquid pump, respectively. Thus a potentially large gas compressor is replaced by a small compressor and a liquid pump. The gas stream is cooled down to nearly same temperature as the liquid, and then mixed with the liquid CO₂ stream. The final CO₂ stream therefore consists of the same liquid compositions as that of the case-2.

In this way, the last stage of compression is accomplished by liquid pumping. The power saving is about 3.7 MWe, or 1.1% to the net power, while the efficiency increases from 30.81 to 31.14%. The electric power penalty is reduced from 129 in case-2 to 124 kWh/klb_{CO₂} in case-3. Because of this power saving, this option will be applied to most of CO₂ compression processes for the other cases.

Figure 4.1.5 - O₂-fired supercritical PC with liquid CO₂ pump (Case-3)



4.1.4.2 O₂-fired PC with Hot Gas Recycle (case-4)

A case with hot gas recycle (case 4) was run to evaluate its effect on the system performance. A hot gas recycle brings more energy back into boiler, reduces fuel and O₂ feed rates, and reduces ASU duty, but it requires more power to the fan because of the increased recycle gas volumetric flow.

As result, increasing the recycle gas temperature from 95°F to 138°F increases the boiler efficiency from 89.3% to 90.1% and net efficiency from 31.14% to 31.53%. The resultant fuel saving is approximately 3.0 klb/hr or 1.0%. The size of the gas-gas heat exchanger increases due to the reduction in LMTD (fluid temperature difference is reduced from 212°F to 166°F for the hot end, and from 120°F to 78°F for the cold end).

There is a limit to increasing the recycle gas temperature without increasing the stack gas temperature, which will reduce efficiency and increase cooling duty. One option mentioned in literature is to raise both stack gas and recycle gas temperatures, and then recover heat from stack gas to replace part of the feedwater heaters.

Figure 4.1.6 - Temperature-Quality diagram for wet-end heat exchangers

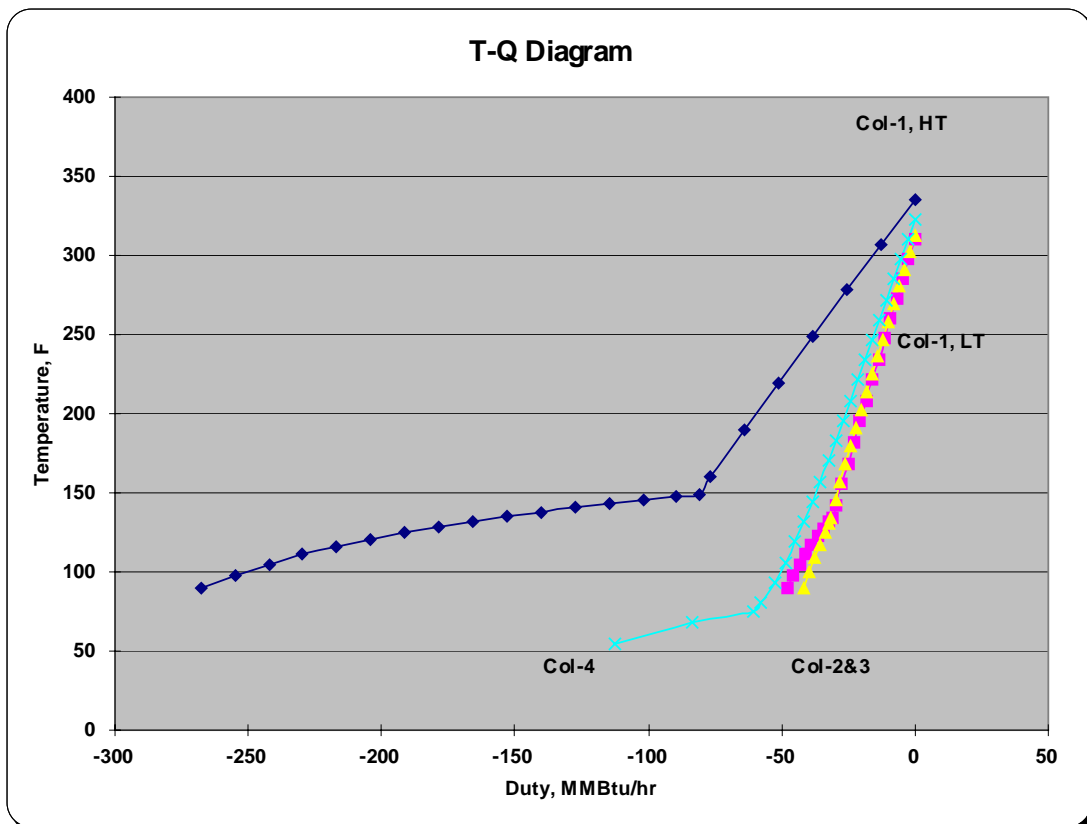
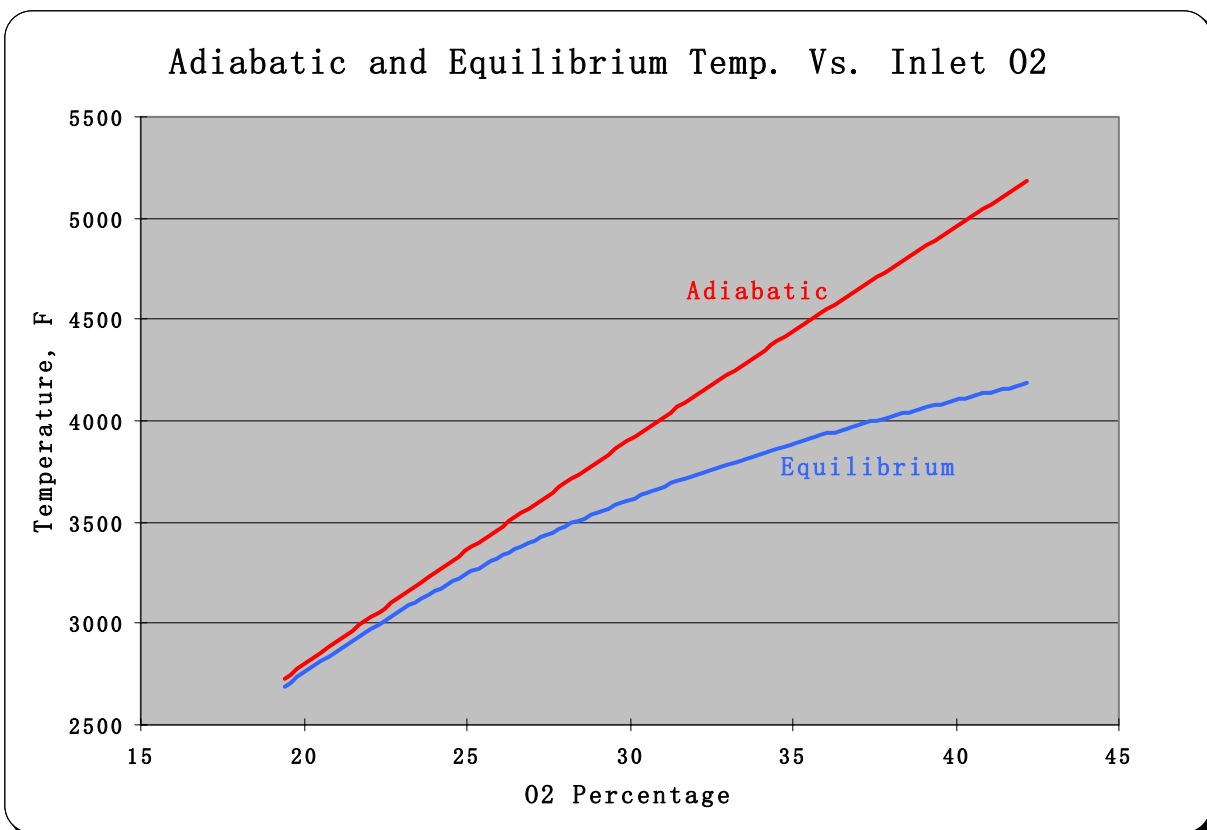


Figure 4.1.6 shows the cooling curves for flue gas cooling before each stage of CO₂ compressor. Part of the heat can be recovered to preheat the condensate. If 90 MMBtu/hr of heat is recovered (exit temperature = 142°F), the steam saved from extraction generates an additional 2.2 MWe, or an efficiency increase of 0.2% point. If a total 150 MMBtu/hr of heat is recovered, the steam saved from extraction generates an additional 3.4 MWe, or an efficiency increase of 0.3% points.

4.1.4.3 O₂-fired PC with High Flame Temperature (case 4 to 7)

In cases of 4 to 7 the amount of flue gas recycle was reduced, to increase the O₂% level to the boiler. This increase in boiler O₂% creates a higher adiabatic temperature and less flue gas flow, which reduces the size of the furnace and increases the boiler and overall cycle efficiency. The adiabatic temperature is the maximum theoretical temperature that can be reached by the combustion with no loss of heat and no dissociation. Actual flame temperature is lower than the adiabatic temperature especially at adiabatic temperatures greater than 3600°F due to flue gas dissociation of CO₂ to CO and O₂ (Figure 4.1.7).

Figure 4.1.7 – Equilibrium and adiabatic temperatures vs. O₂ concentration



The effect of adiabatic temperature on cycle efficiency is shown by Table 4.1.4, where case-4 has nearly the same adiabatic temperature as air-fired reference case, while cases 5 to 7 have higher adiabatic temperatures. Although there is little change in gas exhaust flow to CO₂ compressor among cases 4 to 7, the decreasing recycle gas flow results in reduced auxiliary power consumption for both the FD and ID fans. It is noted that both the total power and the auxiliary power are relatively insensitive to the adiabatic temperature when it is greater than 4320°F. However the efficiency related indices such as net efficiency, coal flow rate, and CO₂ removal penalty improve with increased flame temperature even when it is beyond 4320°F.

Table 4.1.4 - Flame adiabatic temperature effect on performance

case		01	04	05	06	07
Adiabatic Temperature	F	3685	3678	4010	4321	5178
Boiler Inlet O ₂	%, v	20.7	27.8	30.8	33.8	42.2
Coal flow	klb/hr	319.0	312.0	310.7	309.4	308.0
Boiler Efficiency	%	88.16	90.14	90.52	90.9	91.31
Total Aux Power, MW	MW	46.0	140.1	139.3	138.5	138.7
Net Power	MW	430.2	336.1	336.9	337.7	337.5
Net Efficiency	%	39.46	31.53	31.73	31.94	32.07
Generated CO ₂ flow	klb/hr	739	725	722.7	720	718
Efficiency Drop	% pts.	-	7.9	7.7	7.5	7.4
CO ₂ removal energy	kWh/klbCO ₂	-	119	117	114	112

Table 4.1.5 shows the relationship of flue gas flow both in mass and in volume to boiler adiabatic temperature. The air-fired data is shown for comparison. It can be observed that the O₂-fired PC has a lower volumetric flow rate than does the air-fired PC due to the higher molecular weight of the flue gas (i.e. CO₂ versus N₂).

Table 4.1.5 – Flame adiabatic temperature effect on boiler flue gas flow

case		01	04	05	06	07
Boiler outlet flue gas flow	MM cf/hr	179	126	109	96	75
	klb/hr	3555	3357	2972	2675	2083
Adiabatic Temperature	F	3685	3678	4010	4321	5178
Equilibrium Temperature	F	3552	3474	3669	3830	4182

From case 4 to case 7 the ratio of the O₂-fired PC volumetric flow rate to the air-fired PC volumetric flow rate drops from 70% to 42%, which means for a constant flue gas velocity, boiler size is reduced.

Another advantage of decreasing the quantity of recycle gas is the increase in O₂ content in the boiler (from 27% to 42% by vol. from case 4 to case 7), which improves the fuel combustion and reduces the required height of the furnace. This credit from the reduction of UBC has been approximated in this system study, while a more thorough treatment will be modeled in the 3-D CFD boiler simulation study (Section 4.3).

4.1.4.4 O₂-fired PC with Wet-End Economizer (case-8, 9)

One option to increase system efficiency is to use an economizer to recover low-grade heat from compressor inter-stage coolers, and from the flue gas cooler before the CO₂ plant. Case-8 is such a case for integration of low grade heat recovery (based on case-7), where the heat recovered was used for low pressure feed water heating. A method of condensate split stream was applied. The steam extractions from ST at different LP ports were adjusted to match the duties. This option incurs no cost increase because all these heat exchangers were already installed to cool the flue gas for the CO₂ plant. The only difference is in that the cold side cooling water was replaced by condensate from the ST. In this way, the cooling water duty was reduced too.

The temperature-quality diagrams for these low-grade heat coolers are plotted in Figure 4.1.6, where 150°F, just above the flue gas dew point, was used as hot exhaust temperature for heat recovery. This leads to a temperature approach at the hot side of about 50°F, which is sufficient for economizer design and sizing. Because the tube wall temperature is below the flue gas temperature, part of the moisture is condensed out on the wall. A wet-end heat exchanger design therefore has to be considered for this application.

Additional cooling is required to reduce gas temperature from 150 to 90°F by cooling water before gas compression, and the condensate from gas moisture needs to be drained out before the compressor.

The dominant change of this option is to produce more power from the generator as the result of less steam extraction. The total power generated increased substantially from 476 to 483 MWe, or 2% increase in net power. This leads to better system performance as the electrical power penalty is reduced from 112 to 103 kWh/klb_{CO₂}, an 8% drop. The efficiency drop changed from 7.4% to 6.8% in points. The net efficiency increased from 32.07% to as 32.67%, a net 0.6% point increase.

The application of the wet-end heat exchanger to recover low-grade heat brings the benefit that the temperature of the hot recycle gas can be further boosted. This will cause a high gas exit temperature from gas-gas heat exchanger to ID fan. The heat from this high temperature exit stream can be recovered by an economizer, which means more steam condensate will be extracted and sent to economizer to pick up more low-grade heat. Because of temperature approach limitation at cold side of gas-gas heat exchanger, this option will not bring any

more energy back to the boiler. Instead, it will discharge more heat to the economizer and to the feed water. Therefore both the system efficiency and total power will be increased.

Since this option does not bring more energy to boiler, the fuel feed rate, and the boiler efficiency were not changed. The main change is power generation, from 483 to 486 MWe in total as compared with case-8. As a result, the power penalty reduced to 99 kWh/klb_{CO2}, and the efficiency drop to 6.5% in points. The net system efficiency changed to 32.93%.

This hot gas recycle brings back more moisture to the boiler, as 15%v, and flue gas moisture went up to 23.8%v. This moisture slightly changes the boiler performance, such as recycle gas mass and volumetric flows, adiabatic temperature, and O₂%v to boiler. The high moisture content in gas tends to reduce the difference between equilibrium and adiabatic flame temperatures, which is similar to water-gas shift equilibrium, where CO is shifted by water vapor to as H₂, and the generated H₂ is much easier to be burned than the CO.

4.1.4.5 O₂-fired PC with Reduced Pipeline pressure (case-10)

This pressure change only affects the CO₂ plant power. When this pressure changed from 3000 to 2000 psia, the CO₂ compression power changed from 34.2 to 32.9 MWe with liquid CO₂ pumping as the last stage. While the power for the last stage compression, if only gas compressor is used without CO₂ liquid pumping, would change from 6.5 to 3.9 MWe. Therefore even without the requirement of CO₂ purification, the CO₂ condensation before last stage is important in power saving, especially for the high pipeline pressure. At the Ref. 14 specified pressure of 2200 psia, overall cycle efficiency is increased by 0.1% points versus a pressure of 3000 psia.

4.1.4.6 O₂-fired PC with HRA Series Pass (case-6A/6B, 9A/9B)

Because of the reduced flue gas flow and lower HRA duty for high O₂ concentration operating cases, designing the HRA in series instead of parallel will produce a more compact design. The modified HRA arrangement will not affect the heat balance, but will affect the mechanical design and the heat duty arrangement. Due to less heat picked up by the pre-superheater, the water spraying for steam superheat temperature control was setup before the finishing superheater.

Case-6B (Figure 4.1.8) applies nearly the same HRA inlet temperature (1451 vs. 1460°F), as the case-6, while the case-6A applies a higher HRA inlet temperature, 1732°F, to increase the energy discharge to HRA to maintain a better temperature profile. In case-6a, part of heat duty was shifted from boiler to HRA, which was absorbed by a larger economizer resulting in a higher feed water temperature (666 vs. 603°F), while the furnace water wall heat duty was reduced from 1441 to 1198 MMBtu/hr.

Because of less flue gas recycle required for the higher adiabatic temperature of case-9, there was not enough heat to maintain the same HRA temperature profile. Consequently, either the economizer water temperature can be reduced or the HRA inlet temperature can be increased. A high HRA inlet temperature was applied for case-9A to keep the water temperature from economizer at about 590°F. The higher HRA inlet temperature also helped to shift heat duty from division wall to the finish superheater.

The exit steam temperature from the division wall was about 1021°F in case-9A, which could require expensive high-grade materials to be used. In order to reduce this temperature, a different approach was used in case-9B, where the PSH (primary superheater) was removed and its heat duty was shifted to the finishing superheater. Kept constant were the flue gas temperature to the economizer, the water temperature to the evaporator, and the LMTD of lower reheater. Consequently, the finishing superheater size increased since its duty changed from 289 to 416 MMBtu/hr.

Case-9B (Figure 4.1.9) has a modification, where the heat picked up by roof was reduced from 134 to 50 MMBtu/hr, and the difference was shifted to water wall, which leads to an increased steam exit temperature from water wall. This does not affect the heat and material balances, but only the design.

Figure 4.1.8 - Boiler design with HRA series pass

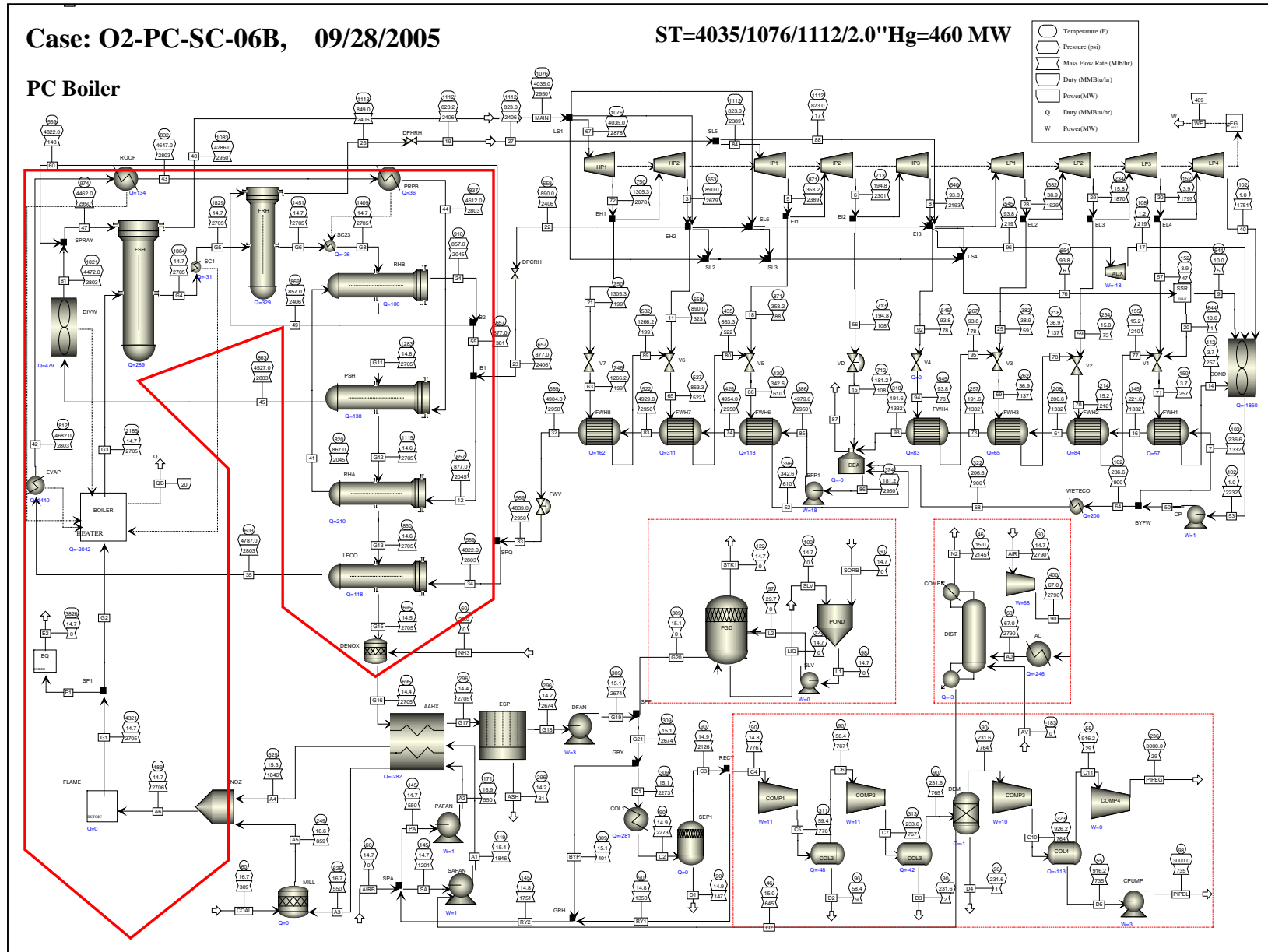
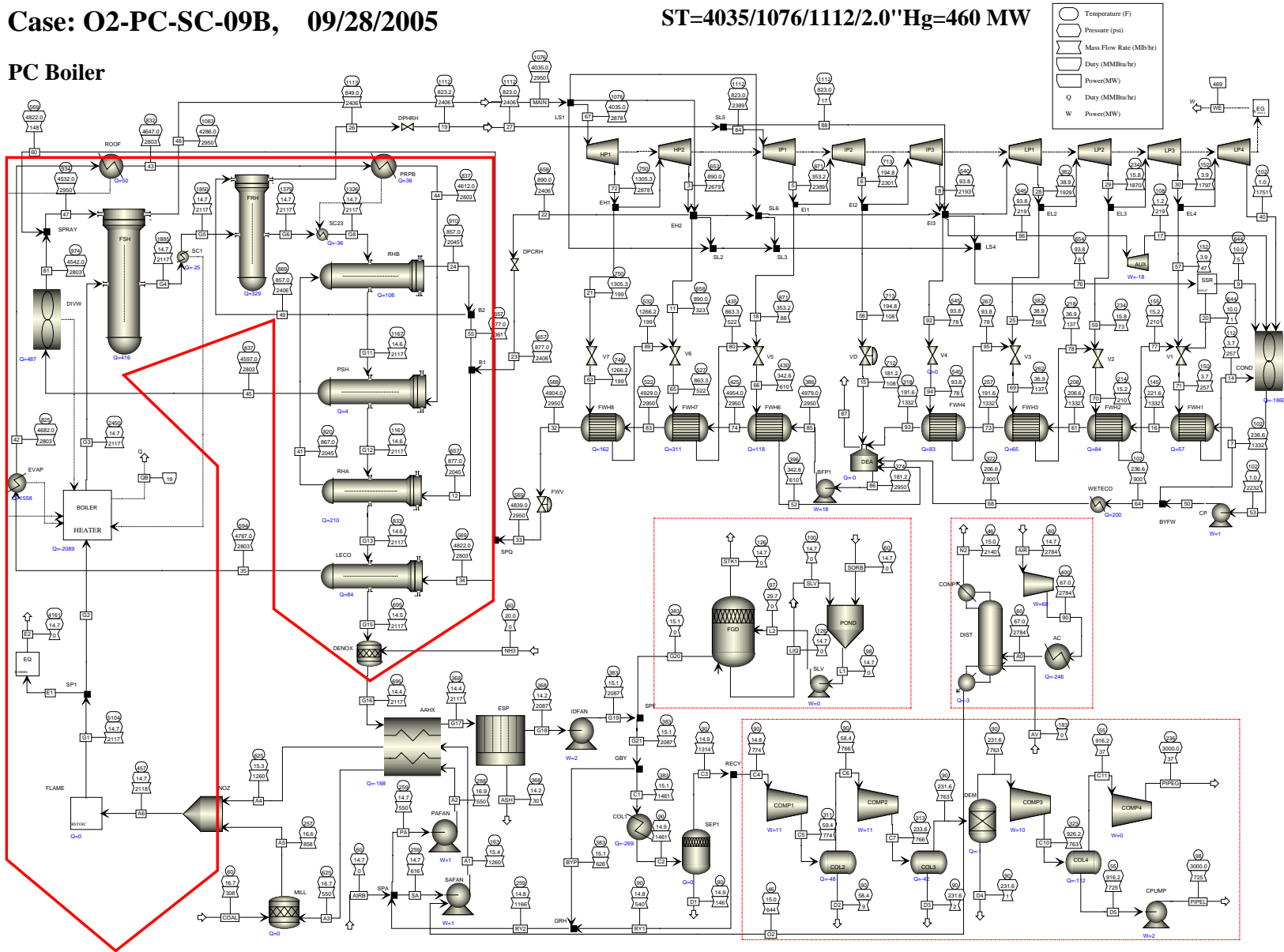


Figure 4.1.9 - Boiler design with HRA series pass (56% Flue Gas Recycle)

Case: O2-PC-SC-09B, 09/28/2005

ST=4035/1076/1112/2.0"Hg=460 MW

PC Boiler



4.1.5 Part Load

For a sliding pressure supercritical system design, part load performance has to be considered and evaluated. For this purpose, the Aspen model can be used by converting its design model to a simulation model, where all of the equipment sizes are fixed from the design case. Based on the 100% load condition, the heat transfer coefficients are functions of operating conditions, such as temperatures and Reynolds number. At full load, the heat transfer coefficients vary from 14.4 for the finishing superheater to 9.7 Btu/ft²-hr-F for economizer. In order to simulate the air-air heat exchanger, the original lumped module was replaced by two modules for both the primary air and the secondary air. The steam turbine was also converted in the simulation model such that the turbine exit parameters are floated as loading changes. The model for feedwater heaters was adjusted so that the extraction pressures were automatically calculated.

The water wall absorption of boiler is difficult to be simulated by the zero dimensional Aspen model. Therefore its performance such as the gas exit temperature was calculated separately using the 3-D FW-FIRE model and iterated with Aspen.

Note that in conventional air fired PC boiler, the excess air has to be increased during part load to maintain steam exit temperatures. Increasing excess air is not necessary for the oxygen-fired boiler since the quantity of flue recycle can be increased at part load to maintain steam temperatures. Increasing flue gas recycle flow rather than excess air has less adverse effect on plant performance and emissions.

The 72% part load (72% generator power) is shown as Case p72 in Table 4.1.3. The amount of flue gas recycled is adjusted to produce sufficient SH and RH steam temperatures. The water spray to SH was adjusted from 5% to 4% to boost SH steam temperature. In this way, the efficiency loss is kept at a minimum when boiler is operated in part load.

The loading is further reduced to 50% as shown by p50 in Table 4.1.3. At this load, the main steam pressure is 2125 psia. At this pressure, the steam turbine can be operated at a reasonably high temperature to keep the system efficiency high. Therefore the boiler was adjusted to maintain both the SH and RH steam conditions as near as possible to those at 100% load. Note that the flue gas recycle flow changes only slightly as the loading changes from 100% to 50%.

The lowest part load case for this study was 25% as shown by p25. In corresponding to a sliding pressure, both SH and RH steam temperatures were adjusted through the combination of firing rate and gas circulation rate to make sure the end steam exhausted from the steam turbine at right conditions. Because of lower steam conditions, the system efficiency reduced substantially.

Figure 4.1.10 and Figure 4.1.11 are plots, which show the effect of part load on performance. At some loadings, the flue gas absolute recycling flow does not change much, but its ratio to boiler flow changes because of less total boiler gas flow as shown by Figure 4.1.10. Figure 4.1.11 shows the relation between part load and system efficiency.

Figure 4.1.10 - Flue gas recycle flow vs. part load operation

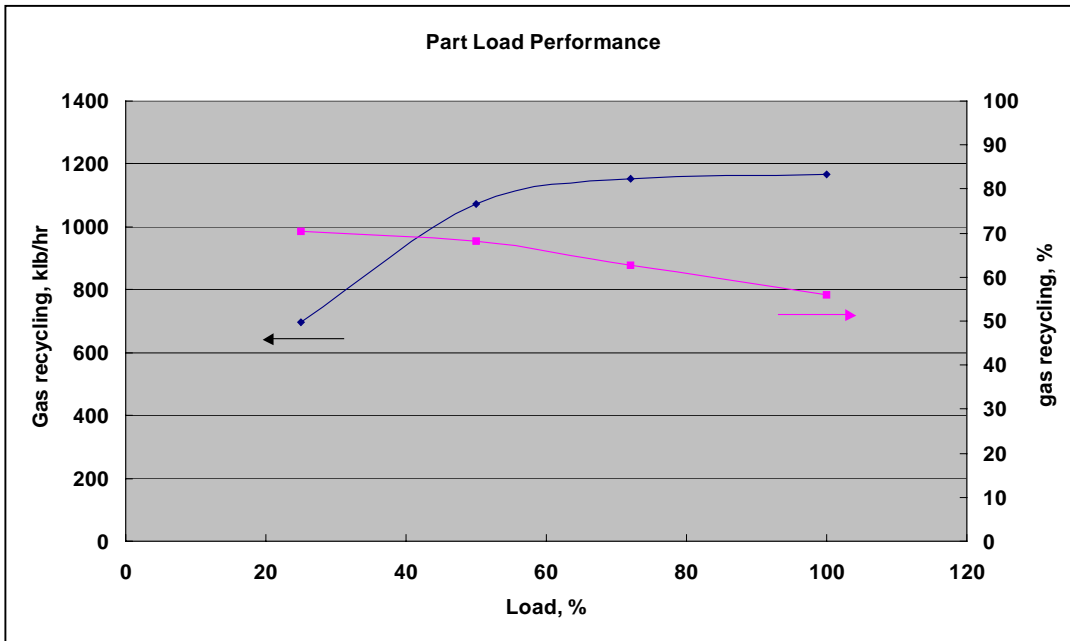
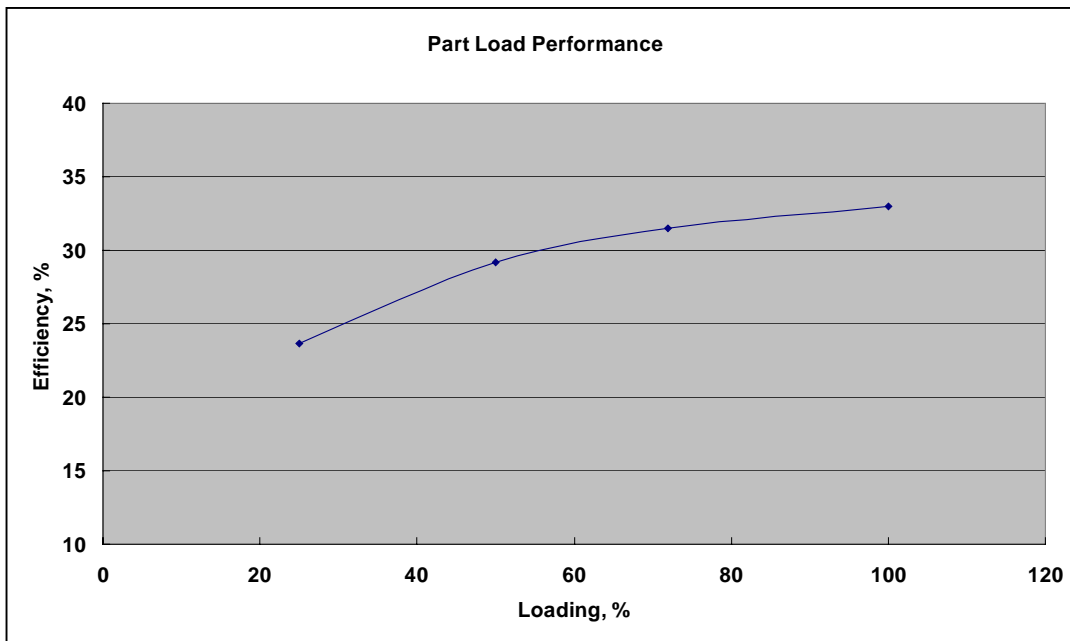


Figure 4.1.11 Efficiency at part load operation



4.1.6 Comparison With Post Combustion CO₂ Capture

CO₂ cannot be captured and sequestered without reducing both the plant power and efficiency because of the potential energy stored in the pressurized liquid CO₂. A minimum of 40 kw/klb_{CO2} additional auxiliary power is required for CO₂ compression. The difference between technologies lies in the difference in power requirements of the different CO₂ or O₂ separation techniques.

Parsons (Ref. 1) performed studies on CO₂ removal by a post capture method for a conventional PC boiler. In their study for post combustion CO₂ removal, the plant efficiency drops from 40.5% to 28.9% for a supercritical (3500 psia/1050°F/1050°F/1050°F/2.0"Hg) boiler, and from 42.7% to 31.0% for an ultra supercritical (5000 psia/1200°F/1200°F/1200°F /2.0"Hg) boiler. In the study presented herein, the CO₂ removal using an O₂-fired PC is used, which relies on an ASU. At a pipeline pressure of 2000 psia (as applied in the Parsons study) the efficiency drops from 36.7% to 30.4% for the subcritical (2415psia/1000°F/1000°F/2.5"Hg) boiler [3], and from 39.5% to 33.1% for the supercritical (4035psia/1076°F/1112°F/2.0"Hg) boiler. The net efficiency drops for these cases are

- 11.7% points for supercritical, post combustion CO₂ removal
- 11.7% points for ultra supercritical, post combustion CO₂ removal
- 6.3% points for subcritical, O₂ fired
- 6.4% points for supercritical, O₂ fired

Another comparison basis is the kWh per klb CO₂ removal, where the kW is power generation difference between cases with and without CO₂ removal. Comparing the post CO₂ capture to the O₂-fired case yields:

- 187 kWh/lbCO₂ for supercritical, 90% post combustion removal
- 188 kWh/lbCO₂ for ultra supercritical, 90% post combustion removal
- 99 kWh/lbCO₂ for subcritical, O₂ fired 100% removal
- 97 kWh/lbCO₂ for supercritical, O₂ fired 100% removal

Thus the efficiency drop and change in power penalty for CO₂ removal appears independent of steam cycle. From the above data, it is clear that the O₂-PC has significant advantages over the post combustion CO₂ capture.

4.1.7 Furnace Waterwall Temperature

The level of radiation in the O₂-fired boiler is significantly higher than an air-fired boiler due to greater concentrations of radiating gas species (CO₂ and H₂O) and higher flame temperature. Consequently, it is important to select the proper amount of recycled flue gas to limit the water wall temperature such that a reasonable waterwall material can be used. The maximum waterwall temperature and furnace heat flux is determined in Section 4.3.

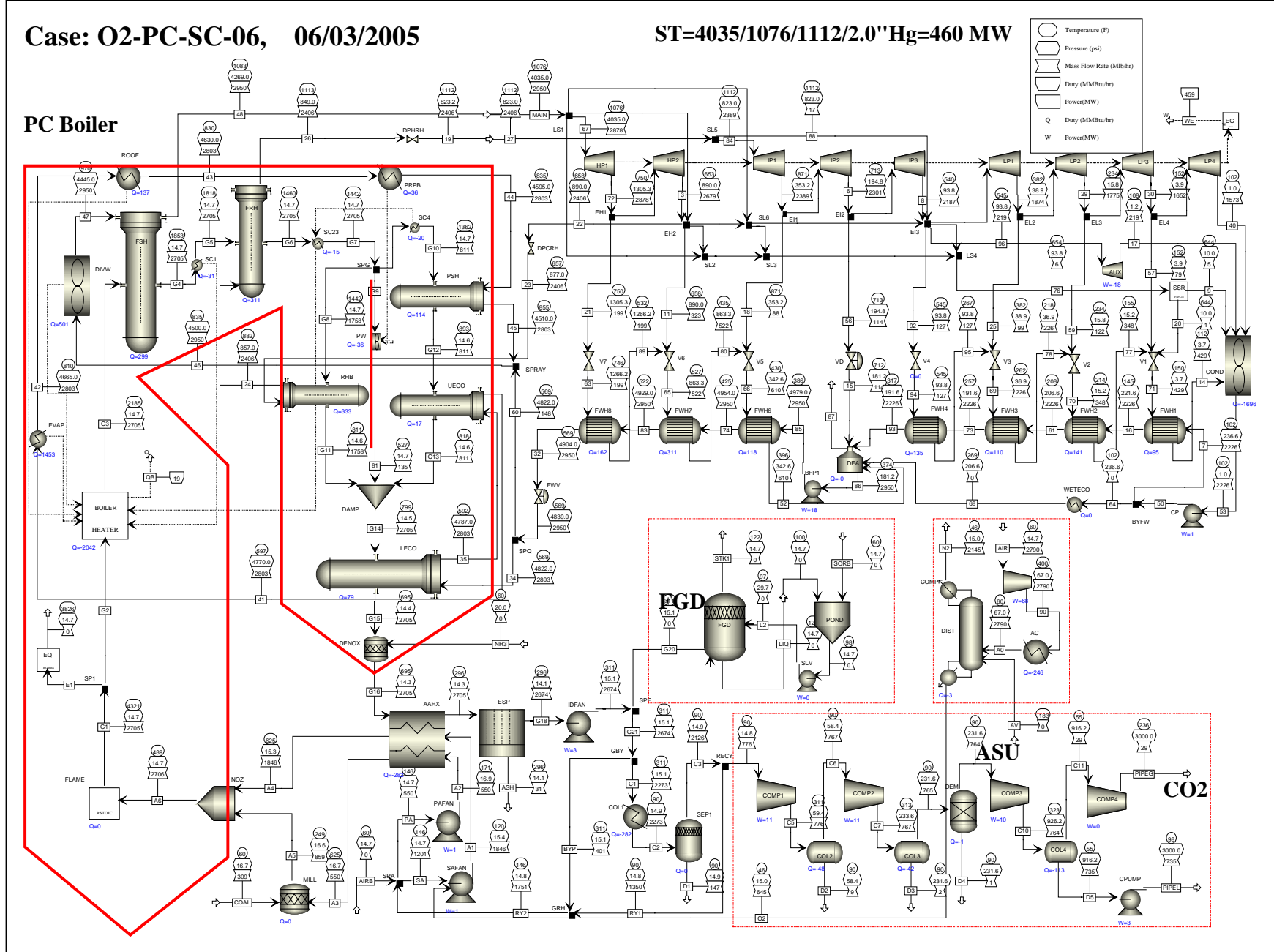
4.2 Advanced O₂ Separation System Integration

4.2.1 O₂-Fired PC Integrated with Cryogenic ASU (case-6)

The model of the oxygen-fired plant with cryogenic ASU was described in Section 4.1.3.

Figure 4.2.1 presents the cryogenic ASU base case system model (case-6). Flue gas recycle flow rate is 65.5% resulting in a boiler equilibrium temperature of 3830°F and an overall cycle efficiency of 31.94%. The oxidant from the ASU is 99.5% O₂ pure. ASU and CO₂ plant power consumptions is 67.7 and 34.2 MWe, respectively, resulting in a total auxiliary power of 138.5 MWe, or about 29.1% of gross power. The efficiency drop compared to the air-fired case is 7.5% in points (39.46% to 31.94%), and the associated power penalty is 114 kWh/klb_{CO₂}.

Figure 4.2.1 - Base case of O₂-fired supercritical PC with Cryogenic ASU



4.2.2 O₂-Fired PC Integrated with OITM

Advanced oxygen separation through high temperature membranes such as OITM is currently under development [2, 4, 5, 7]. Oxygen ion transport membranes have the potential to provide a major reduction in oxygen separation capital and energy consumption.

Oxygen ion transport is driven by the difference in oxygen partial pressure across a membrane. Oxygen atoms adsorb on the cathode (high oxygen partial pressure side of the membrane) and dissociate into ions as they pick electrons. These ions travel from cathode to anode (the low oxygen partial pressure) by jumping through lattice sites and vacancies until they reach the anode side of the membrane. On the anode side, the oxygen ions yield their electrons to become atoms/molecules, which are then desorbed into the gas phase. Electrons from the anode side are carried through the membrane to the cathode side to complete the circuit. The rate of oxygen transport through such membranes is temperature sensitive, and can be very fast at high temperatures. These membranes have infinite selectivity for oxygen over other gases, because only oxygen ions can occupy the lattice positions. A typical schematic of the oxygen ion transport membrane process is presented in Figure 4.2.2.

The OITM process and design data are based on Reference 7. A schematic of the OITM process incorporated within the O₂-PC plant is shown in Figure 4.2.3. To integrate the OITM into the O₂-fired PC, air is pressurized by a compressor, and then heated to a high temperature. High pressure air provides a high oxygen partial pressure on the airside of the OITM to reduce the size and cost of the OITM. Air enters the compressor at 60°F and 14.7 psia and is compressed at 85% efficiency to 215 psia and 743°F. The compressed air is heated to 1652°F by a tubular air heater inside the PC furnace. This hot pressurized air is fed to the OITM, where about 85% of its O₂ is separated through the membrane to an exit pressure of 16 psia, and the rest of the vitiated air or O₂-depleted air is sent to a gas expander to generate power at 86% turbine efficiency. Power generated from the expander is used to drive the air compressor. Since the power generated in the gas expander is greater than the air compressor power the OITM system produces a net power output.

The separated O₂ from the membrane is carried by a heated sweep gas. The use of a sweep gas reduces the oxygen partial pressure on the low-pressure side of the membrane and consequently reduces the size and cost of the OITM. A recuperator is applied between inlet and outlet sweep gas flows to reduce the heat requirement. Heat transfer from the sweep gas to the membrane to the air is neglected as it is expected to be relatively small (it was also neglected in Reference 7). The mixture of sweep gas and O₂ is then injected into the furnace. In this design, the OITM does not consume electrical power; instead, it absorbs heat, generates power, and separates O₂ from air. Therefore it is expected to reduce ASU operating and capital costs.

From a heat and mass balance point of view, if there is no heat transfer between the air and sweep gas, the model can be simplified by directly mixing the separated O₂ with the sweep gas. Thus, to simplify the model, the recuperator and OITM are combined into a single module in the Aspen model. The operational details of the OITM, such as the O₂ flux through the membrane as a function of OITM temperature and pressure, were not included in the Aspen model. These details are necessary only for OITM size and cost estimations. Moreover, the Aspen model does not directly model the recuperator, but the recuperator design and configuration is required for the economic analysis.

Without performing a detailed economic study, it is difficult to determine the optimum OITM operating pressure. However, Reference 8 specifies that for an economic design, the ratio of oxygen partial pressures of the feed gas (air) to the permeate stream (sweep gas) should be approximately 7. The base case OITM design has an oxygen partial pressure ratio of 4.9 at the air inlet and 10.2 at the air outlet, yielding an approximate average ratio of 7.5. Reference 8 specifies that an 85% O₂ recovery and an operating temperature of 1652°F is within the operating range of the OITM. The effect of O₂ recovery and OITM operating pressure on system performance and OITM design is examined in Section 4.2.2.3.1 and Section 4.2.2.3.2, respectively.

Several cases incorporating an OITM ASU into the O₂-PC have been simulated to evaluate the effect of different conceptual designs and operating conditions on power plant performance.

Figure 4.2.2 - A Typical Oxygen Ion Transport Membrane Schematic [4]

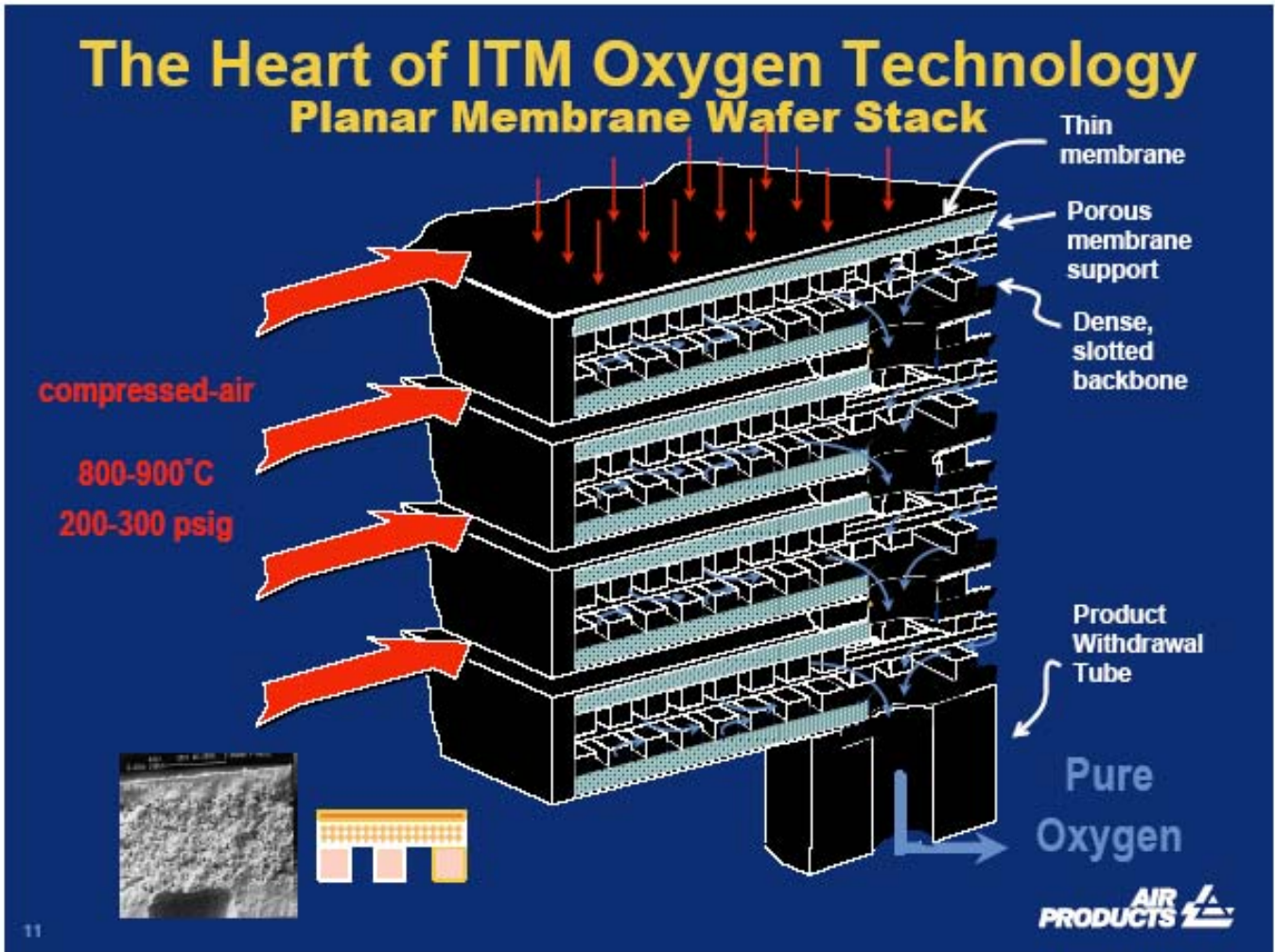
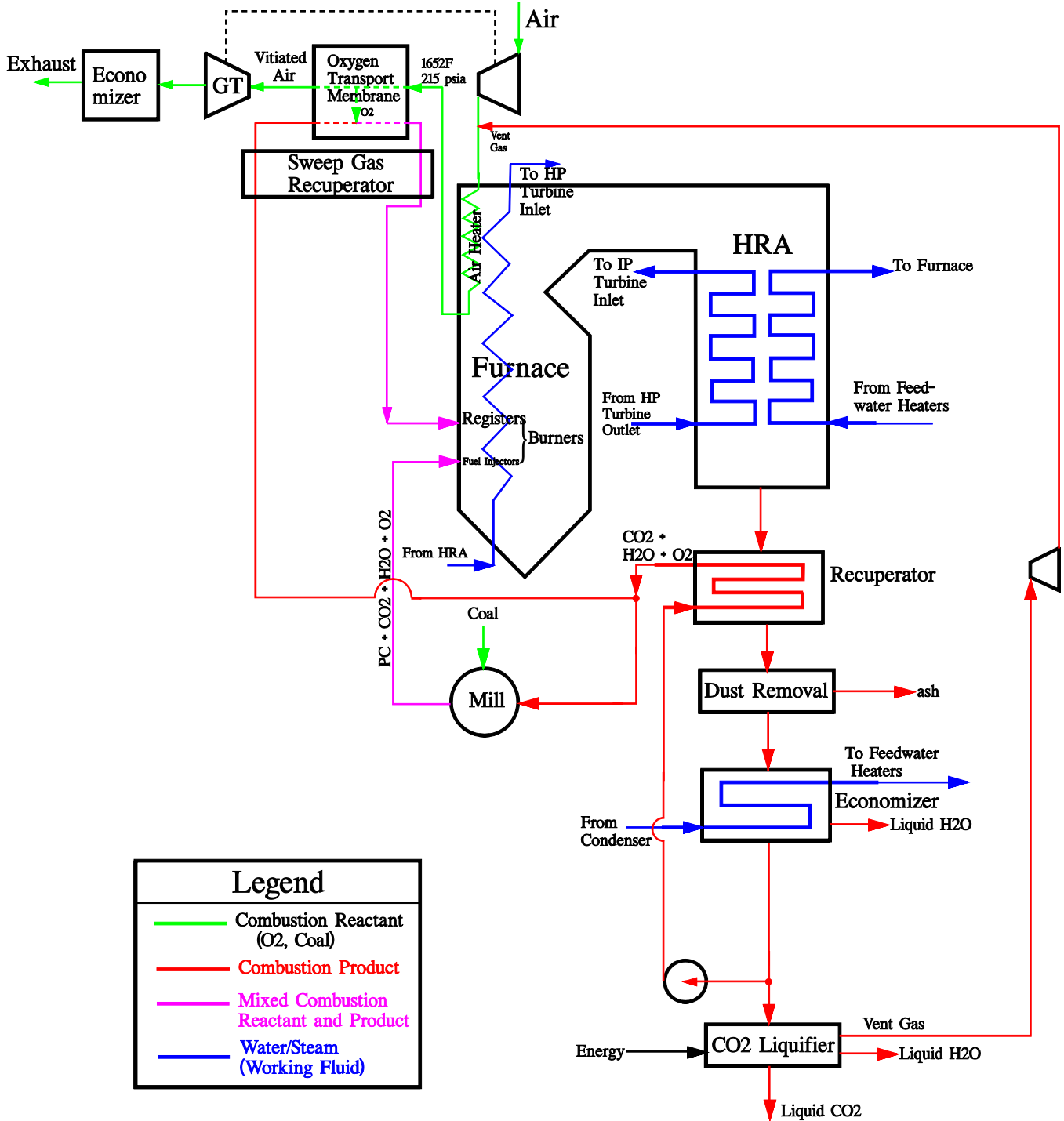


Figure 4.2.3 – Integration of Oxygen Ion Transport Membrane into O2-PC



4.2.2.1 Process Gains

The inclusion of a gas turbine expander in the O₂-PC power plant utilizing the OITM increases the overall system efficiency by allowing work to be done in the gas turbine at a higher temperature than can be achieved by the steam from the boiler. This principle has been applied by FW in its 1st generation Pressurized Fluidized Bed Combustor (PFBC) design. A further enhancement is the 2nd generation PFBC design (similar to IGCC) in which the turbine entrance temperature is increased by syngas combustion. This concept was also applied in the FW High Performance Power System (HIPPS) design, which includes an in-furnace high temperature air heater similar to the one required for the O₂-PC OITM concept.

4.2.2.2 Base Case (case-11)

Figure 4.2.3 shows a schematic of the OITM ASU integrated with the O₂-fired PC power plant. The OITM system includes a sweep gas system, and an air supply system. The pressurized vent gas from the CO₂ plant is recycled back to the air separation unit, where it is mixed with the compressed air. In this way the rich O₂ in the vent gas can be recovered, and the air to compressor can be reduced. Therefore this vent gas recycling increases system efficiency and reduces the operating cost.

Figure 4.2.4 (case-11) is a process flow diagram generated by Aspen Plus for the OITM ASU integration. Air is compressed to about 200 psia by a compressor, and then heated within the boiler to about 1650°F. This hot pressurized air is fed to OITM, where about 85% of its O₂ is separated through a membrane, and the rest of vitiated air is sent to an expander. The separated O₂ from the membrane is carried by a heated recycled flue gas after gas-to-gas heat exchange. A recuperator is applied between inlet and exit sweep gas flows (not shown in Figure 4.2.4 since it lumped inside the OITM module). The mixture of sweep gas and O₂ is fed directly to the boiler. The exhaust gas from the expander passes through an economizer to release its heat for feedwater heating. Power generated from the expander is used to drive the air compressor.

The O₂ obtained from the OITM is swept with recycled flue gas. Since the compressed air is heated to 1650°F inside the boiler, a special heat exchanger and boiler design has to be used for the OITM application (Sections 4.3.2.2.3 and 4.3.5.4). The boiler air heater duty is 974 MMBtu/hr. The coal feed rate is 377 klb/hr as compared with 319 klb/hr for the air-fired case-1, and 309 klb/hr for the O₂-fired (cryogenic ASU) case-6. The corresponding flue gas flow increased to 3497 klb/hr, nearly approaching the air-fired flow of 3552 klb/hr. The boiler O₂ concentration is 31%v, which is nearly the same as case-6.

Because of increased flue gas flow created by greater coal-firing, more heat is carried to the boiler HRA in case-11 than in case-6. As result, distribution of heat

duty shifts: the heat duty of the division wall reduces from 501 MMBtu/hr in case-6 to 396 MMBtu/hr in case-11, while the sum of the primary superheater and upper economizer duties increases from 131 MMBtu/hr in case-6 to 411 MMBtu/hr in case-11. Consequently, the inlet furnace feedwater temperature increases from 597°F in case-6 to 666°F in case-11. The total furnace duty for case-11 increases because of the 974 MMBtu/hr air heater duty, although the heat to waterwalls is reduced from 2042 to 1583 MMBtu/hr.

Because more low-grade heat is released from the gas turbine (GT) exhaust and from boiler, all low-pressure feedwater heaters are shut off. The low-pressure feedwater heating is provided in parallel by the GT economizer and a HRA flue gas exhaust economizer (in parallel to flue gas heat recuperator), as well as by part of the compressor inter-stage coolers.

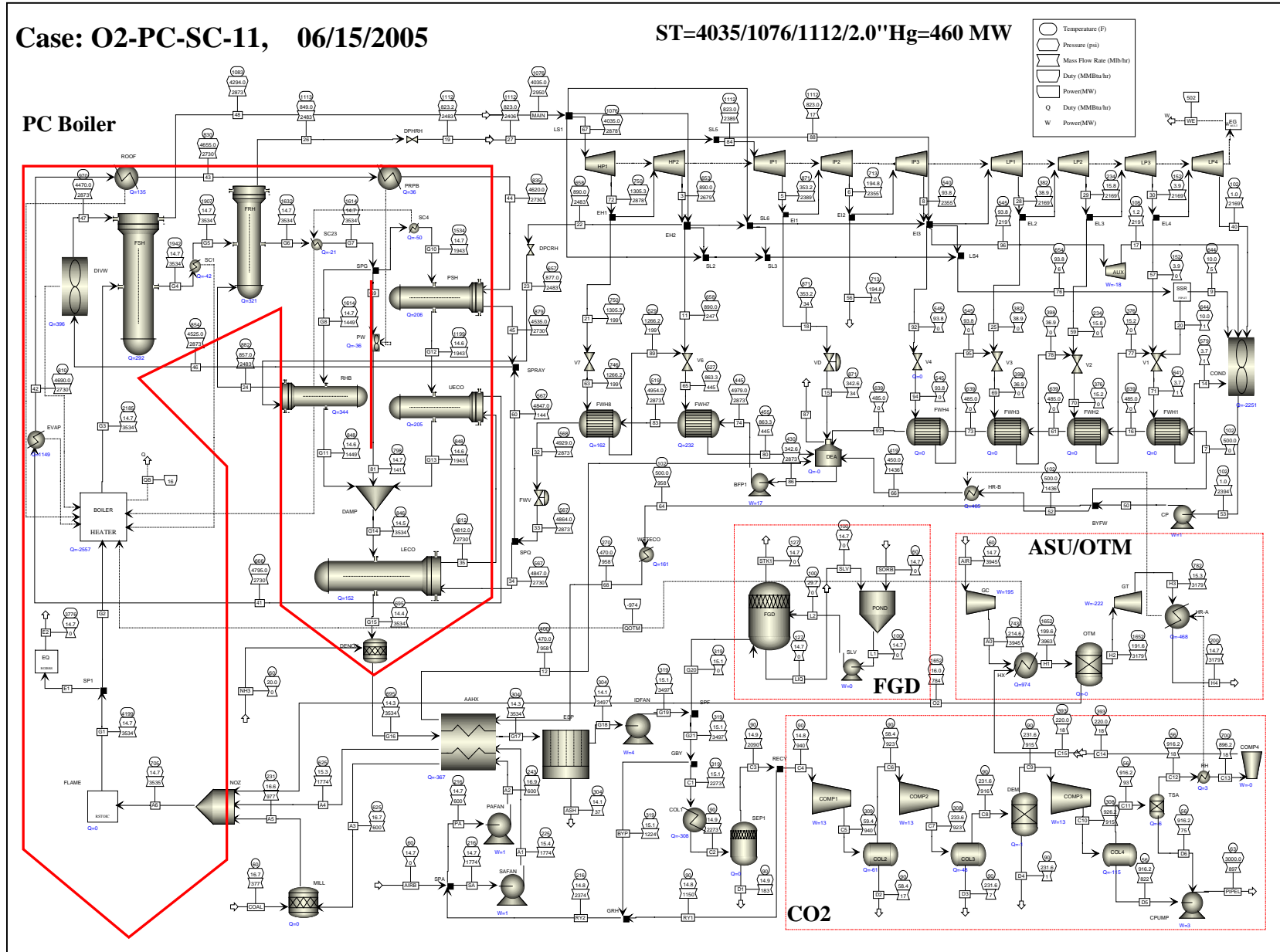
The OITM O₂-PC incorporates the recycling of vent gas from the CO₂ compression system back to the OITM. The high-pressure vent gas from the CO₂ plant is heated with GT exhaust gas before it is expanded for power recovery. After the expansion to the OITM operation pressure, the O₂-rich vent gas is mixed with compressed air and sent to the OITM. Consequently, the compressor air flow and power is reduced. The emission control equipment treats the vent gas prior to the OITM requiring smaller equipment sizes due to the high pressure of the vent gas.

The replacement of the cryogenic ASU with the OITM greatly reduces the efficiency loss penalty. This is caused by lower equivalent ASU power, better system integration, increased power from the OITM GT, and more low-grade heat recovery from cooling. As shown in Table 4.2.1 the OITM reduces the efficiency drop by 52% and the CO₂ removal power penalty by 61%.

Table 4.2.1 – Comparison of O2PC with Cryogenic and OITM ASU

	Air-fired	O2-fired	O2-fired
ASU	-	cryogenic	OITM
Main steam flow, klb/hr	2950	2950	2950
Coal flow, klb/hr	319	309.4	377
Net power, MW	430	338	462
Net efficiency, %	39.5	31.9	35.8
ASU Power, MW	0	67.7	-26.7
CO2 Compression Power, MW	0	34.2	41.3
CO2 removal flow, klb/hr	0	720	874
Efficiency penalty, % points	0	7.5	3.6
CO2 removal penalty, kWh/klbCO2	0	114	45

Figure 4.2.4 - O2-PC with OITM



4.2.2.3 OITM Parametric Studies

Several OITM parametric cases were run as described in the following sections. The results are summarized in Table 4.2.2.

Table 4.2.2 – Parametric Case Summary

case		01	06	09	10	11	12	13	14	15	16	17	18	19
Air separation method		None	Cryo	Cryo	Cryo	OITM	CAR							
Waste heat economizer		no	no	yes	yes									
HRA Arrangement		parallel	series											
CO2 Condensation		-	yes	yes										
Vent Gas Recycle		-	no	no	no	yes	no							
Coal flow	klb/hr	319.0	309.4	308.0	308.0	377.7	376.0	403.8	377.7	377.7	377.7	389.4	375.4	307.7
Natural Gas Flow	klb/hr													4.0
Oxidant flow	klb/hr	3270	645	644	644	784	780	838	784	784	784	808	781	1849
Air flow	klb/hr	3270	2790	2784	2784	3945	3685	4945	4284	3810	3875	4067	3930	3165
O2 purity	%	-	99.5	99.5	99.5	100	100	100	100	100	100	100	100	43.2
Recycle gas flow	klb/hr	0	1751	1166	1166	2374	2356	2523	2374	2374	2374	2392	1525	1190
	%	0.0	65.5	55.9	55.9	67.9	67.8	67.8	67.9	67.9	67.9	67.4	57.7	56.0
Recycle gas temperature	F	-	146	260	260	216	217	223	214	217	216	220	249	150
Boiler Inlet O2	%, v	20.7	33.8	41.1	41.1	31	31.1	31.1	31	31	31	31.4	39.3	41.8
Boiler Outlet O2	%, v	3.0	3.0	3.0	3.0	3.0	3.0	3.0	3.0	3.0	3.0	3.0	3.0	3.0
Boiler outlet flue gas flow	MM cf/hr	179	96	77	77	139	138	150	139	139	139	142	100	81
	klb/hr	3555	2675	2087	2087	3497	3474	3723	3497	3497	3497	3550	2644	2126
Adiabatic Temperature	F	3685	4321	5104	5104	4196	4202	4208	4196	4196	4196	4243	5120	5120
Equilibrium Temperature	F	3552	3830	4161	4161	3770	3773	3775	3770	3771	3771	3792	4169	4155
Gas Temp. to FSH	F	2185	2185	2185	2185	2185	2185	2185	2185	2185	2185	2185	2185	2450
Water temp. to evap.	F	638	597	596	596	666	664	690	666	666	666	672	599	591
UBC	%	1.00	0.30	0.16	0.16	0.38	0.38	0.38	0.38	0.38	0.38	0.38	0.16	0.15
Boiler Efficiency	%	88.16	90.90	91.31	91.31	-	-	-	-	-	-	-	-	-
Pipeline pressure	psia	0	3000	3000	2000	3000	3000	3000	3000	3000	3000	3000	3000	3000
Generated CO2 flow	klb/hr	739	720	718	718	874	869	934	874	874	874	900	866	729
CO2 purity	%,v wet	14.0	77.5	71.3	74.2	75	74.9	74.9	75	75	75	74.8	70.8	76.5
Removed CO2 flow	klb/hr	0	720	718	718	874	869	934	874	874	874	900	866	729
CO2 removal efficiency	%	0	100	100	100	100	100	100	100	100	100	100	100	100
CO2 purity	%	-	93.7	93.6	93.6	96.9	96.9	96.9	96.9	96.9	96.9	96.9	96.9	94.2
Gross Power	MW	476.2	476.2	486.4	486.4	519.7	515.8	520.3	519.3	520.0	519.8	521.8	519.5	488.7
Auxiliary Power	MW	46.0	36.6	38.1	38.1	43.0	42.8	44.0	43.1	43.0	43.0	43.4	41.6	42.5
ASU power	MW	0.0	67.7	67.6	67.6	-26.7	-22.0	-42.2	-24.3	-27.3	-27.1	-35.9	-26.6	32.0
CO2 compression power	MW	0.0	34.2	34.2	32.9	41.3	41.1	44.1	41.3	41.4	41.4	42.6	41.2	34.3
Net Power	MW	430.2	337.7	346.6	347.9	462.1	453.9	474.4	459.2	462.9	462.5	471.7	463.3	379.9
Net Efficiency	%	39.46	31.94	32.93	33.05	35.80	35.33	34.38	35.58	35.87	35.83	35.45	36.11	35.19
Efficiency Drop	% pts.	-	7.5	6.5	6.4	3.7	4.1	5.1	3.9	3.6	3.6	4.0	3.3	4.3
CO2 removal energy	kWh/klbCO2	-	114	99	97	46	52	59	48	45	45	49	42	64

4.2.2.3.1 Effect of O₂ Recovery Efficiency (case 11 to 13)

As described in Section 4.2.2.1, shifting more duty to the GT will increase system efficiency. Increasing OITM O₂ recovery efficiency reduces the required air flow rate and decreases the GT mass flow and power generated.

In Case-12 the O₂ recovery is increased from 85% to 90.5%. As a result of high O₂ recovery, less air is required to be fed to the system, and so less power is generated in the GT. This leads to a reduction of system efficiency from 35.8% to 35.3%.

In Case-11 and Case-12 the low-grade heat released from GT exhaust, flue gas cooling before CO₂ compression, and CO₂ compressor inter-stage cooling is recovered to heat the low-pressure feedwater. In Case-13, when the O₂ recovery is reduced from 85% to 73%, more air has to be fed to OITM (4945 vs. 3945 klb/hr) and so more heat is required by the OITM. The system fires more coal (404 vs. 378 klb/hr) and as result, the system generates more low-grade heat than can be recovered, which results in an increase of GT exhaust temperature from 200°F to 330°F. This reduces the system efficiency even with increased extra power from the GT.

It is clear that the two opposing effects, more GT power and more low grade heat from increased air flow, form a system with an optimum performance for a given air side pressure as shown by Figure 4.2.5, where the system efficiency is maximum when the O₂ recovery is approximately 85%. Note that recovering additional low-grade heat as through the use of a high-pressure economizer will shift the optimum O₂ recovery efficiency. As more of the low grade heat is recovered by the use of more complex heat integration schemes or by co-generation heat export, then the optimum O₂ recovery efficiency is reduced and the maximum system efficiency is increased. Such a reduction in O₂ recovery efficiency reduces the size of the OITM because of increased logarithm mean pressure difference (LMPD).

Table 4.2.3 shows a comparison of different cases under the same airside pressure, including a case published by Alstom [7]. It is obvious that the higher is the O₂ recovery efficiency, the lower is the LMPD, and the larger is the OITM size.

Figure 4.2.5 – Effect of OITM O₂ Recovery Efficiency on Efficiency

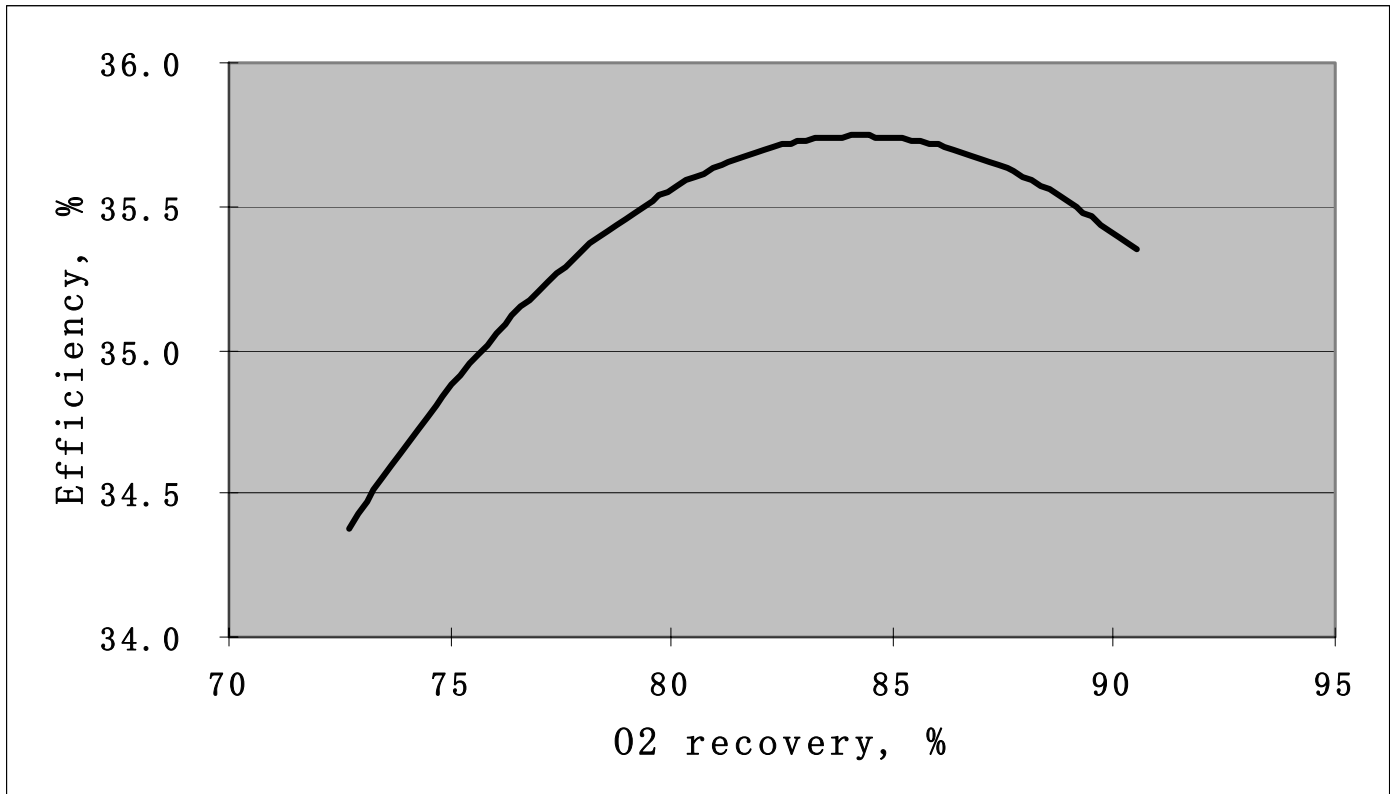


Table 4.2.3 - Effect of OITM O₂ Recovery Efficiency on LMPD

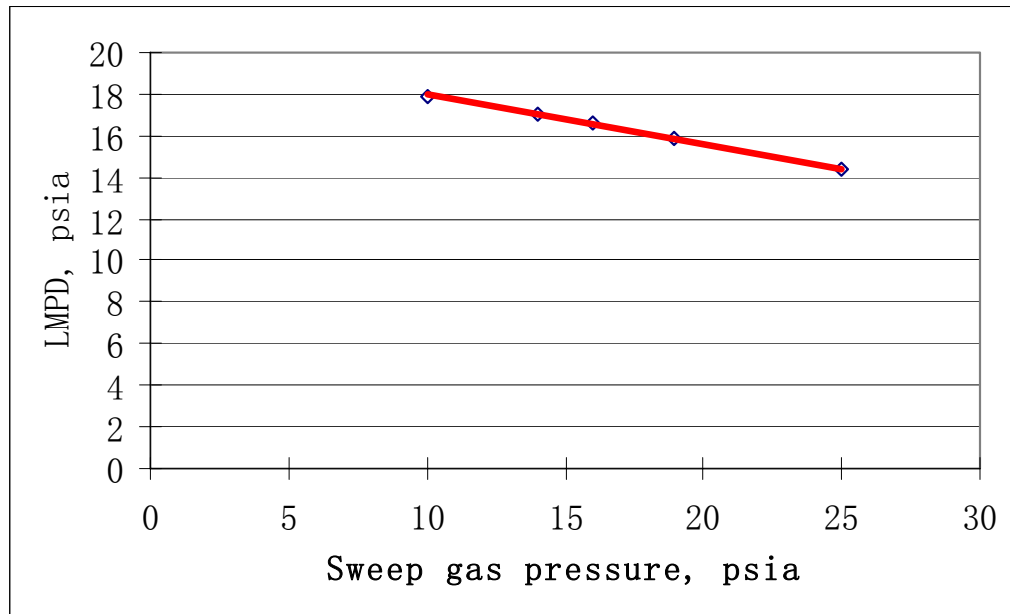
Case	Al st om	Case- 11	Case- 12	Case- 13
O ₂ recovery, %	85	85	90	73
O ₂ to boiler, %	70	31	31	31
LMPD	14.7	16.5	13.9	20.9

4.2.2.3.2 Effect of LMPD Across the Membrane (cases 14-16)

The performance of the OITM relies on the O₂ partial pressure difference across the OITM membrane. Similar to the LMTD used in a heat transfer process, a LMPD is a key design parameter for a mass transfer process. The LMPD can be used to compare the design size of different options.

An increase in the O₂ level to the boiler increases the sweep gas outlet O₂ partial pressure resulting in a reduced LMPD as shown in Table 4.2.3 (compare Alstom to case-11). Similarly an increase in sweep gas total pressure reduces the LMPD as shown in Figure 4.2.6. The effect is fairly small because of the limited operating pressure variation of the sweep gas.

Figure 4.2.6 – Effect of Sweep Gas Pressure on LMPD



The air side pressure directly affects the OITM performance. Increasing the air side pressure (OITM operating pressure) will:

- (1) Increase LMPD, and so reduce OITM size
- (2) Increase compressor discharge temperature (CDT), and require less heat from the boiler
- (3) Reduce turbine exhaust temperature (TET), and so release less low grade heat and reduce the optimum O₂ recovery efficiency
- (4) Increase equipment thickness

In Case-14 the OITM operating pressure is raised from 200 psia to 250 psia with constant coal feed rate and furnace air heater duty. This 250 psia OITM pressure requires the compressor discharge pressure to be increased from 214 to 265 psia, which raises the compressor discharge temperature. Thus, for the same operating temperature the OITM needs less heat per unit mass of air, and so the air to the OITM is increased to balance the heat released from the boiler. Because the amount of the O₂ required is fixed, the O₂ recovery is adjusted for the increased air flow through the OITM. Figure 4.2.7 shows that raising the air side pressure from 200 psia to 250 psia results in a small reduction in system efficiency (from 35.8 to 35.6%) and an attendant small increase in the CO₂ removal specific power penalty (from 46 to 48 kWh/klb_{CO2}). The system efficiency decreases with increased OITM pressure because of less heat being carried to the OITM per unit air. However, due to the increased air flow to the OITM, the LMPD is increased from 16.5 to 24.9 psia, which results in a decrease in OITM size of 34%.

Opposite to the case-14, cases 15 and 16 were run with reduced OITM pressures of 180 psia and 190 psia, respectively. As shown in Figure 4.2.7, lower OITM operating pressure (for a given operation temperature) increases system efficiency because more heat is transferred from the boiler to the OITM cycle per unit mass of air. However, as the OITM pressure is reduced the LMPD decreases requiring a larger OITM size. In this scenario, the oxygen recovery is adjusted to changes on the airside pressure, which results in an indirect relationship between system efficiency and the O₂ recovery as shown in Figure 4.2.8. Figure 4.2.8 presents a linear correlation for which each percent change in O₂ recovery causes a 0.03 percent point change in efficiency.

Figure 4.2.9 shows the effect of OITM pressure on LMPD when the O₂ recovery efficiency is constant and O₂ flow rate is variable (as in Figure 4.2.7). This is compared in Figure 4.2.9 with the effect of OITM on LMPD when the O₂ flow rate is constant and the O₂ recovery efficiency is variable (as in Figure 4.2.7).

The selection of the OITM operating pressure is a trade-off between the cost of OITM and the system efficiency. If the OITM cost is not too high in future commercial application, the optimum OITM operating pressure will be relatively low. Furthermore, a higher OITM operation temperature will be better for the system efficiency. However, the magnitude of this temperature is constrained by material limitations.

**Figure 4.2.7 – Effect of OITM Pressure on System Efficiency and LMPD:
Variable O2 Recovery**

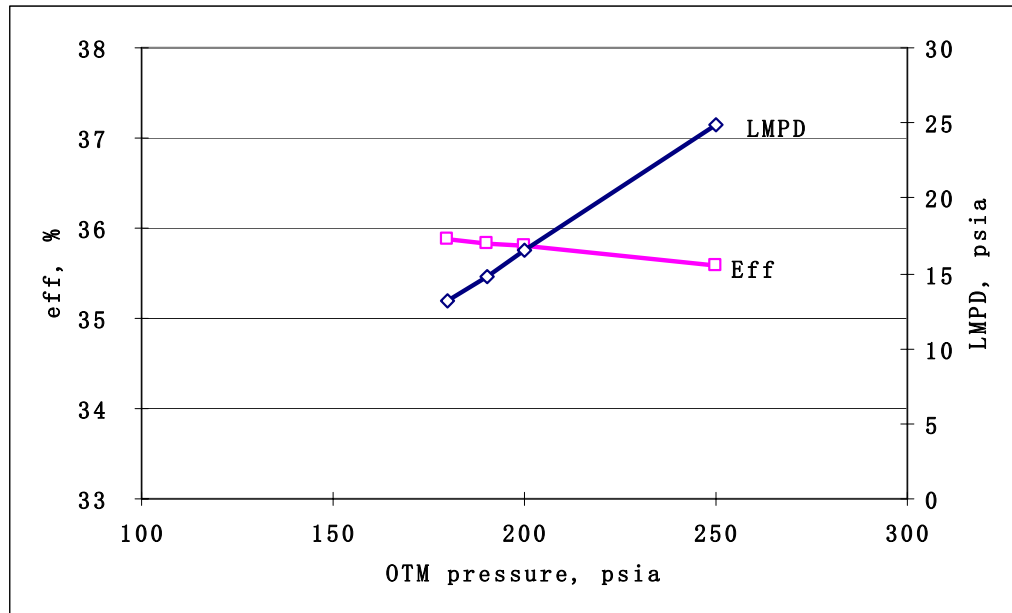


Figure 4.2.8 – Effect of O₂ Recovery on System Efficiency

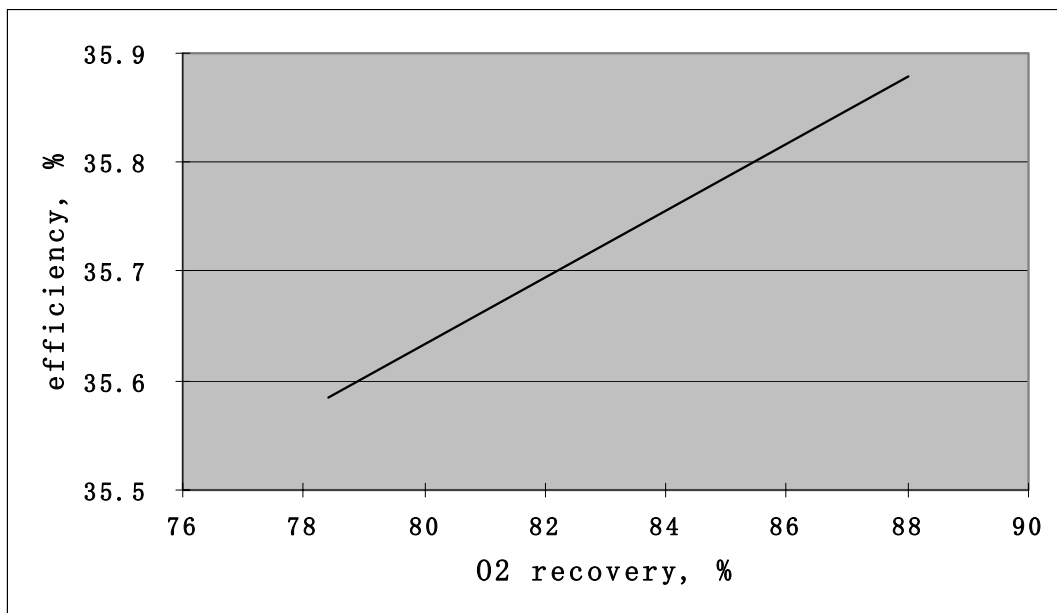
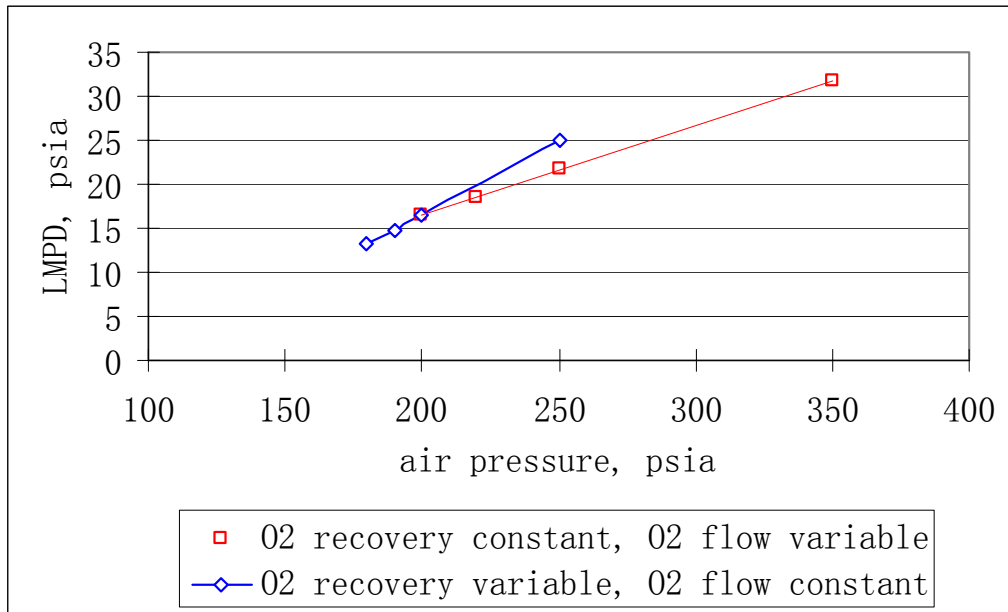


Figure 4.2.9 – Effect of OITM Pressure on System Efficiency and LMPD: Constant and Variable O2 Recovery



4.2.2.3.3 Effect Of Compressor Discharge Temperature (case 17)

Another way to boost the system efficiency is to transfer more heat to the gas turbine by increasing the temperature difference between the compressor discharge temperature (CDT) and the turbine inlet temperature (TIT). Increasing the TIT results in an increase in OITM operating temperature, which may be restricted due to material limitations. Without increasing the pressure, the increase of TIT will increase turbine exhaust temperature, which results in more low-grade heat that can be recovered in the HRSG. Another approach is to reduce CDT by the use of a compressor with inter-stage cooling. This will reduce compressor power, and let more heat be transferred from the boiler to the turbine, but it releases more low-grade heat from inter-stage cooling. If this heat cannot be recovered, system efficiency would be reduced. As discussed before, for the present configuration and integration, there was no margin to recover more low-grade heat. Therefore the inter-stage cooler will be applicable only for co-generation of heat and power, where low-grade heat could be recovered by low-pressure steam export.

Case-17 employs an alternative method to reduce compressor power by inter-stage water quench to avoid the need for low-grade heat recovery. This quench (20 klb/hr of water) reduced the CDT from 743 to 698°F, and therefore more heat flowed from the boiler to the gas turbine. As a result, the coal to boiler increased from 377.7 to 389.4 klb/hr, and the corresponding air to the OITM increased from 3945 to 4067 klb/hr (for the same OITM O₂ recovery efficiency). The power from

the GT increased from 26.7 to 35.9 MWe, and the net power increased from 462 to 472 MWe. However, the system net efficiency was reduced from 35.80 to 35.45%, and the corresponding net penalty for CO₂ removal increased from 46 to 49 kWh/klb_{CO2} because of efficiency loss. The great benefit from this option was the 10 MWe net power gain. Note also that the furnace air heat duty increased from 974 to 1060 MMBtu/hr.

4.2.2.3.4 Effect of Furnace Flame Temperature (case 18)

Increased furnace flame temperature increases heat transfer, especially for radiant transfer, and so it will reduce the furnace size for both for the waterwalls and air heater. Similar to the effect of excess air in the boiler, higher flame temperature slightly increases system efficiency because of less flue gas flow out of the system.

Higher flame temperature cases have been evaluated for the cryogenic ASU O₂-PC, as reported in Section 4.1.4.3. For the cryogenic ASU O₂-PC raising the equilibrium temperature from 3830°F (case 6) to 4182°F (case 7) increased system efficiency about 0.15% in point, and reduced specific power penalty for CO₂ removal from 114 to 112 kWh/klb_{CO2} as shown in Table 4.2.4.

Case 18 (Figure 4.2.10) was generated from case 11 by raising the equilibrium temperature to nearly the same equilibrium temperature as case 7. Table 4.2.4 shows that for the OITM ASU O₂-PC raising the equilibrium temperature to 4169°F increases system efficiency by about 0.3% in point, and reduces the CO₂ removal specific power penalty from 46 to 42 kWh/klb_{CO2}. It is clear that increased flame temperature can reduce equipment size and slightly improve system efficiency, but could be limited by material cost in the furnace.

Table 4.2.4 – Effect of Flame Temperature on Performance

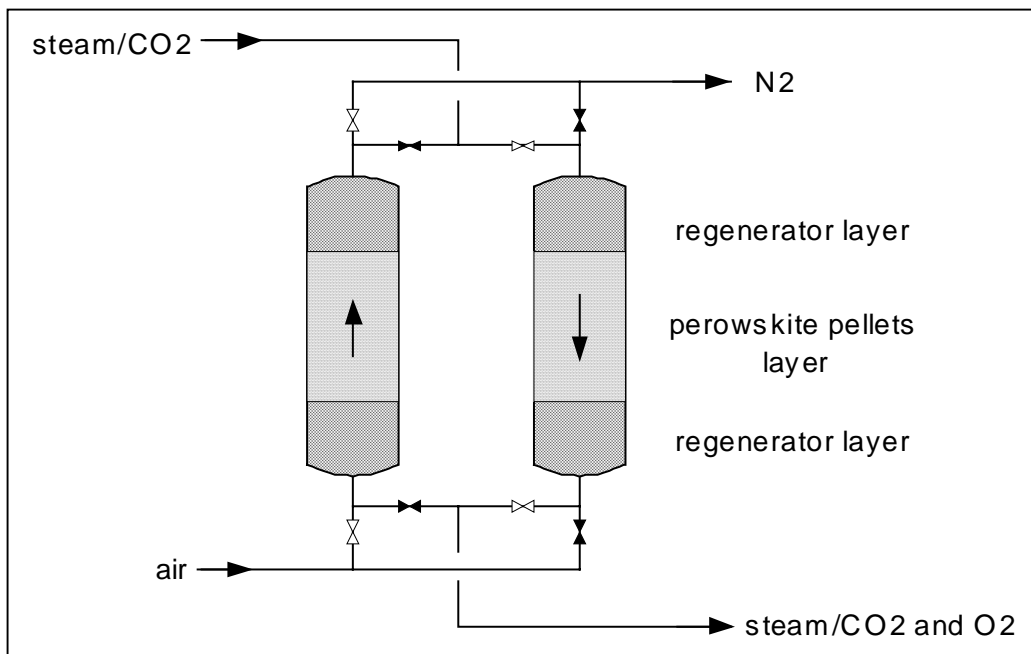
Case	6	7	11	18
Adiabatic Flame T, F	4321	5178	4196	5120
Equilibrium flame T, F	3830	4182	3770	4169
Recycle flue gas T, F	146	163	216	249
system eff, %	31.94	32.07	35.80	36.11
kWh/klbCO2	114	112	46	42

4.2.3 O₂-Fired PC Integrated with CAR

4.2.3.1 Overview

The ceramic auto-thermal recovery (CAR) process [5, 6] is based on sorption and storage of oxygen in a fixed bed containing ionic and electronic conductor materials operated at high temperature and increased pressure. The stored oxygen is then released by pressure reduction using sweeping gas, such as recycled flue gas, or steam extracted from low-pressure section of steam turbine as shown in Figure 4.2.11. The continuous operation is obtained by employing multiple beds in a cyclic way, which is similar to the Pressure Swing Absorption (PSA) process. A large vessel is provided to provide a five second buffer time to smooth out any fluctuations in either flow and/or composition caused by a batch adsorption-desorption operation cycle. An important feature of the CAR process is in that it can be tailored to produce low-pressure oxygen at the concentration required for O₂-fired combustion by using recycled cleaned flue gas as a sweep gas. The CAR process is based on conventional sorbent bed adsorption that is easy to fabricate and readily available. The scaling up for such a process is similar to the PSA process, and has fewer challenges than the OITM technology.

Figure 4.2.11 - CAR Process Schematic



In general during adsorption, heat is released and system temperature is raised. The CAR adsorption process has to be operated at high temperature, therefore the air is preheated to a certain temperature before being fed to the adsorption bed. The heat generated during adsorption can be recuperated to heat up the

fresh air to reduce heat loading. For this purpose, a recuperator is employed to transfer heat between exhaust oxygen depleted air and the fresh air, where the heat generation during adsorption raises the exhaust air temperature. As result, the fresh air needs less preheating (i.e. 1020°F) for the CAR process, compared to 1650°F for the OITM process. On the other hand, the desorption process is associated with heat absorption, where heat has to be transferred to the bed during oxygen release. This is done by direct injection of natural gas into bed to combust with oxygen and by pre-stored heat in the sorbent bed during adsorption. The CAR process is so designed that it also stores the energy in the bed during the heat release in the adsorption cycle and releases this heat during the stripping cycle, by means of installation of inert layers on both ends of sorbent bed for heat storage. In this so called “auto-thermal recovery”, more heat is stored in bed, less heat is carried out by oxygen-depleted air, and less heat is required from fuel combustion to strip oxygen.

High oxygen concentration can be obtained by steam stripping providing that the steam is condensed out downstream. Oxygen concentration is limited to about 30-40% if the flue gas is applied as a sweep gas. As reported in the BOC study [5] with steam as sweeping gas, the air-to-steam molar ratio is about 2.66 with O₂ recovery over 90%, which leads to an oxygen concentration in the sweeping gas of about 33-36%v before steam condensing.

Simulated integration of the CAR process to the O₂-PC has been reported by BOC to determine the technical and economical feasibility [5]. The air-fired reference plant is an existing ultra-supercritical lignite-fired 865 MWe Lippendorf power plant near Leipzig, Germany. A simulation of an oxyfuel power plant with cryogenic air separation was employed for comparison. The same plant was then applied for integration study with CAR process, where low-pressure steam extracted from steam turbine was applied as a sweep gas. Table 4.2.5 summarizes the key results.

Table 4.2.5 - Comparison for CAR with Cryogenic ASU

Case	Air	ASU	CAR
Net Power, MWe	865	687	726
Net efficiency, %(LHV)	42.6	33.3	34.0
Efficiency drop, % point	-	9.3	8.6

Comparing the CAR to the cryogenic process, the efficiency drop reduced from 9.3 to 8.6% points, and the net power increased from 687 to 726 MWe. As reported, it is clear from the results of study that the steam consumption is a critical variable for this option. The steam extraction required for oxygen stripping is about 200 kg/s in comparison with the main steam flow as 692 kg/s.

The reason recycled flue gas was not used as sweep gas was that the flue gas has to be cleaned up to avoid any contaminates to the sorbent bed, and the

effects of contaminants have not yet been studied in detail. In general, to be economic, recycle gas clean up should be avoided because the clean gas will be sent back to boiler, where it mixes with combustion gases to become dirty gas again. Optimally, the gas clean up process should be applied to the flue gas exiting from system and flowing to the CO₂ plant. Moreover, this stream has much less flow to be treated than does the recycled flue gas.

Since the CAR process is based on swings in the partial pressure of oxygen, it will be affected by pressure, and LMPD (logarithmic mean pressure difference). Increased adsorption pressure will enhance oxygen adsorption from air, and a low desorption pressure will favor adsorbed oxygen release. However too high a pressure will require more power for air compression. If steam is used as a sweep gas, heat carried by the sweep gas can be recovered through feedwater heating during steam cooling and condensing. If flue gas is used as a sweep gas, hot sweep gas can be directly fed to boiler.

In order to explore the advantage of integration with CAR process for O₂-fired combustion, an Aspen simulation has been made for the CAR process operated with recycled flue gas sweep gas. The difference in principle between steam and flue gas sweep gases is their pressure ratios, where steam extracted at 1.6 bar could continuously expand to a pressure as low as 0.038 bar to generate more power with a pressure ratio of 1.6/0.038, while the flue gas has to be compressed from about 1.0 bar to 1.6 bar to consume power with pressure ratio as 1.6/1.0. Thus, the substitution of flue gas by extracted steam reduces power because the low pressure ratio of the flue gas is replaced by the high pressure ratio of steam for the same amount of gas volumetric flow. The reduced power can be calculated by difference between power from steam expansion and power for recycle gas compression, without including the changes in auxiliary power and low grade heat integration. The net result is shown by Table 4.2.6.

Table 4.2.6 – Comparison for CAR Using Different Sweep Gases

Oxidant	Air		O ₂	
Air Separation Method	-	Cryo	CAR	CAR
Sweep Gas	-	-	steam	flue gas
Net Power, MWe	865	687	726	767
Net Efficiency, % (LHV)	42.6	33.3	34.0	35.9
Efficiency Drop, % point	-	9.3	8.6	6.7

As can be seen in Table 4.2.6, the system efficiency increases about 1.9% points when steam is replaced by recycled flue gas as the sweep gas. As compared with the cryogenic ASU, the CAR process with gas recycle sweep gas has an increased system efficiency of 2.6% in points, which is close to 3.2% points achieved by the OITM. It is obvious from the standpoint of system efficiency that the future of the CAR process is to use recycle flue gas as a sweep gas.

Note that in the CAR process, natural gas is fired to provide a portion of the heat for stripping out the adsorbed oxygen from sorbent bed, which is similar to the gas absorption-regeneration cycle. Because of auto-thermal recovery process, the ratio of energy input from the natural gas to coal is only about 3.2%, which is much less than the heat requirement by the OITM process.

4.2.3.2 Optimized Integration of CAR in O₂-PC

Advanced oxygen separation CAR process has been integrated into the oxygen fired PC as shown in the Figure 4.2.12 schematic. A multi-bed adsorption-desorption batch operation cycle is simulated by a quasi-continuous operation of moving bed system, where the oxygen sorbent is circulated between two beds. The Aspen model of the O₂-PC CAR power plant is presented in Figure 4.2.13.

Flue gas, instead of steam extracted from steam turbine, is used as a sweep gas to strip out oxygen from desorption bed. Note that flue gas contains many contaminants such as fly ash, SO_x, NO_x, etc. that may be harmful to the perovskite sorbents used in the CAR process and future experimental studies will be required to quantify this effect.

The flue gas from the boiler transfers heat to the oxygenated flue gas in an air-to-air heat exchanger and then is further cooled down to 150°F by feedwater economizers. After cooling, the flue gas is boosted to a pressure to overcome the pressure drop across the CAR oxygen desorption equipment. Exit gas from desorption bed, containing about 25-45% of oxygen, is then cooled down to 280°F through the sweep gas recuperator. This oxygen containing flue gas is then sent to air-to-air heat exchanger to be heated up to 625°F, and then fed to boiler.

Air is compressed to a pressure of 30 psia and then fed to the adsorption bed after pre-heating in the air recuperator. About 90% of O₂ in the air is adsorbed by solids in the bed. The heat released from adsorption increases the system temperature. Adsorption bed exit gas or vitiated air is cooled down to 280°F in the air recuperator before being discharged to the stack. The solids circulated between two the moving beds adsorb and release oxygen nearly reversibly.

The system net efficiency for the CAR integrated with the O₂-PC power plant is 35.2%. Heat input from natural gas is about 2.7% of the total heat input. Table 4.2.7 lists a comparison among different air separation technologies in efficiency drop and CO₂ energy removal penalty. OITM has less energy penalty than CAR due to the process gain associated with the gas turbine expander (see 4.2.2.1).

Table 4.2.7 – O₂ PC Efficiency with Different O₂ Separation Techniques

Air separation method		Cryo	OITM	CAR
Efficiency Drop	% pts.	6.5	3.3	4.3
CO ₂ removal energy	kWh/k1bCO ₂	99	42	64

Figure 4.2.12 – Integration of CAR Process into O2-PC

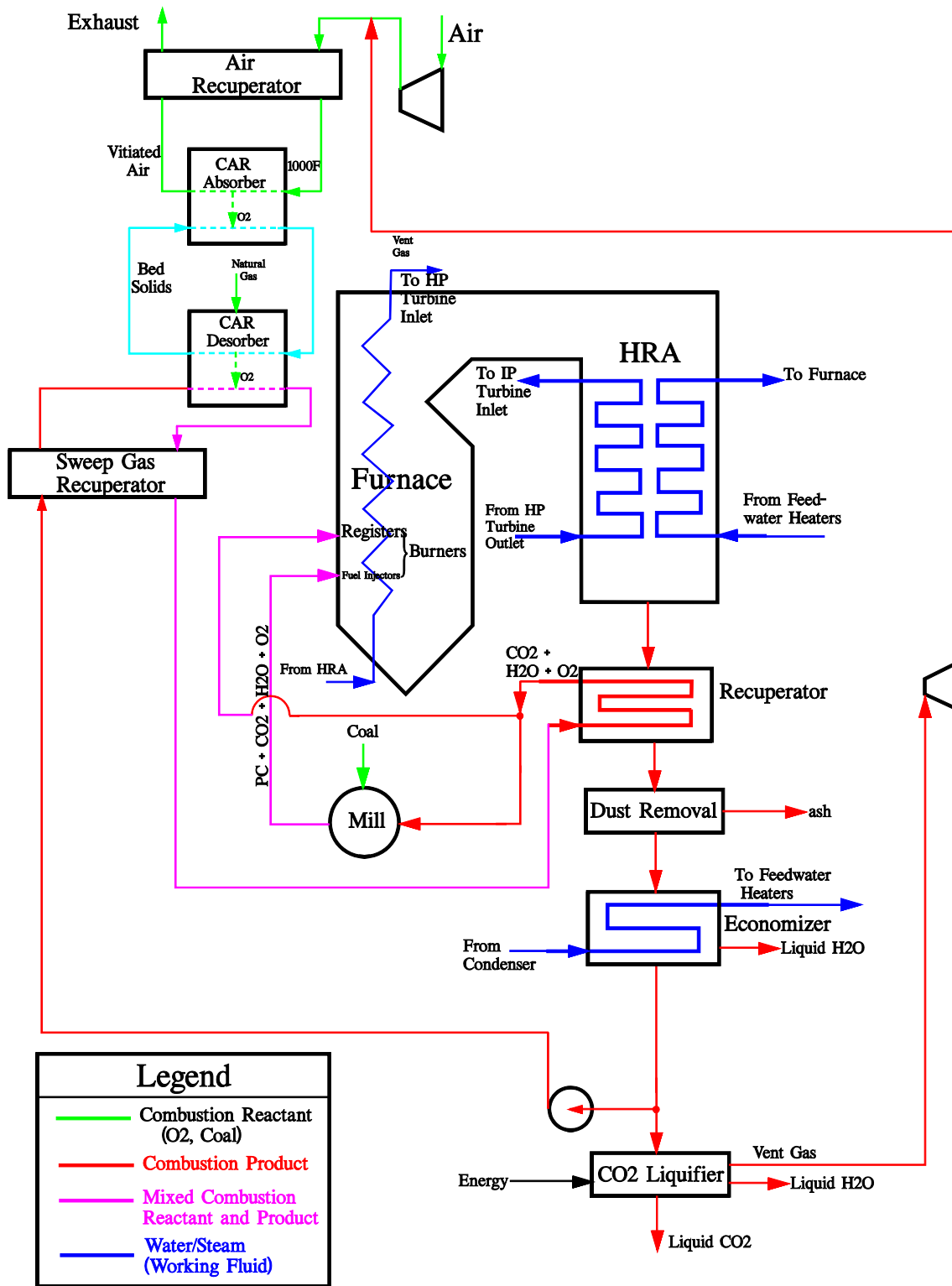
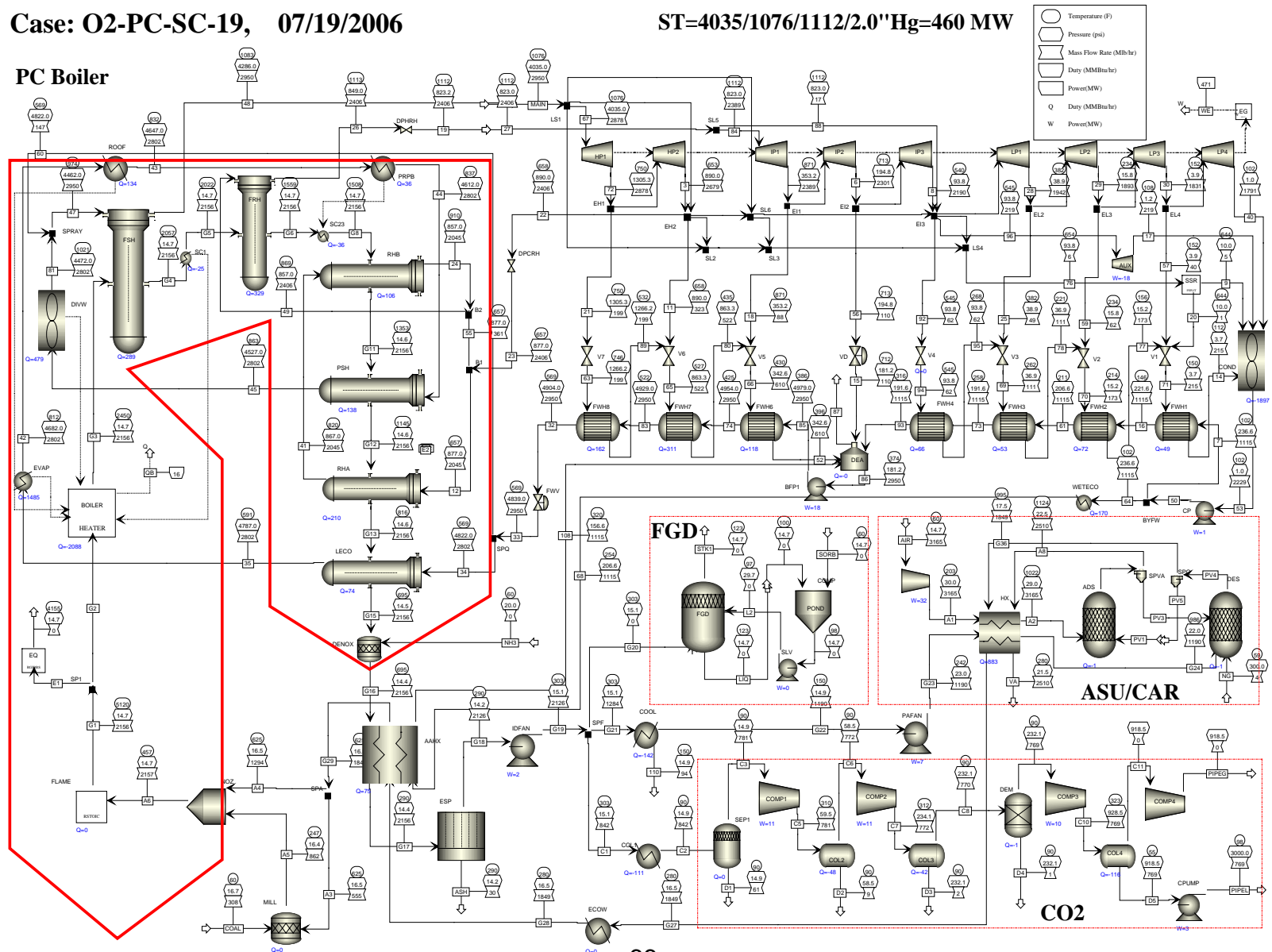


Figure 4.2.13 - O2-PC with CAR

Case: O2-PC-SC-19, 07/19/2006

ST=4035/1076/1112/2.0"Hg=460 MW



4.2.4 Comparisons

CO₂ cannot be captured and sequestered without incurring an energy penalty because of the potential energy stored in the pressurized liquid CO₂. A minimum of 40 kWh/klb_{CO2} additional auxiliary power is required for CO₂ compression. The difference between technologies lies in the difference in power requirements of the different CO₂ or O₂ separation techniques, and the process gain when advanced power generation is integrated, such as power generation from OITM through hot gas expansion.

Table 4.2.8 shows that compared to CAR, the OITM results in higher system efficiency and significantly more in power because of the process gain of the hot compressed air expanding through the gas turbine (gains are in reference to the cryogenic ASU O₂-PC). When the OITM technology is integrated with O₂-fired combustion, a conventional Rankine cycle power plant is upgraded to a combined cycle power plant. This improvement makes the OITM technology attractive for economic CO₂ removal.

Table 4.2.8 - Gains from OITM and CAR Compared to Cryogenic ASU

	Efficiency gain (% points)	Power gain (MW)
OITM	3.2	117
CAR/steam sweep gas	0.7	20
CAR/flue gas sweep gas	2.6	50

The OITM faces more technical challenges than does the CAR process because it operates under higher pressure and temperature. In addition to the OITM development itself, the integration and design of the boiler air heater presents a challenge (see Section 4.3.2.2.3). An alternative to the furnace air heater is to provide the air heating by a natural gas duct burner, although the high heat required (the ratio of heat absorbed by OITM to heat input by the coal is 22%) may preclude duct firing. For the CAR process, the heat input from natural gas is only 2.7% to the total energy input.

In general, CO₂ can be removed by means of:

- Post-combustion capture - Amine process or other
- Pre-combustion capture - IGCC
- Oxygen-combustion – cryogenic ASU, OITM, CAR

Table 4.2.9 compares the efficiency drop and specific power requirement of the various CO₂ removal technologies. Similar to the O₂-PC designs employing

cryogenic ASU and OITM, the O₂-PC CAR power plant is designed to include liquid CO₂ pumping, wet-end heat recovery, increased flame temperature, and hot gas recycle.

Table 4.2.9 – Comparison of CO₂ Removal Technologies

Boiler Type Removal Technique		post comb.	PC O ₂ fired			IGCC pre comb.
			cryo. ASU	OITM	CAR	
Efficiency drop	% pnts	11.6	6.5	3.3	4.3	7.2
CO ₂ removal penalty	kWh/klbCO ₂	188	99	42	64	116

From Table 4.2.9, it is clear that the O₂-fired PC integrated with advanced oxygen separation technology has significant advantages over both the post combustion and pre-combustion CO₂ techniques since the separation of oxygen from air is a physical process and involves less energy than the chemical separation of CO₂ from flue gas or syngas.

4.3 Furnace and Heat Recovery Area Design and Analysis

4.3.1 Furnace Design and Analysis

4.3.1.1 FW-FIRE Computer Program Description

FW-FIRE (Fossil fuel, Water-walled Furnace Integrated Reaction and Emission Simulation) simulates furnace combustion, heat transfer and pollutant formation based on fundamental principles of mass, momentum, and energy conservation [9]. FW-FIRE is an extended and enhanced version of PCGC-3, which was developed over a period of ten years by the Advanced Combustion Engineering Research Center (ACERC), operated jointly by Brigham Young University and the University of Utah. The FW-FIRE computer program incorporates the latest state-of-art coal combustion/gasification, pollutant formation, and physical analysis techniques based on extensive empirical research.

The FW-FIRE code performs general three dimensional multiphase gas combustion steady state analysis of reactive fluid flows. The program is fully capable of analyzing gas-fired and coal-fired boilers although FW-FIRE was initially tailored for pulverized coal combustion and gasification.

The FW-FIRE program models the gas flow field as a three dimensional (Cartesian or cylindrical) turbulent reacting continuum that is described locally by the Newtonian form of the Navier-Stokes equations coupled with the energy equation and other appropriate constitutive equations. These equations are solved in Eulerian framework to predict gas properties such as pressure, temperature, velocity, and pollutants and other species concentrations.

The Reynolds stress terms, which result from Favre-averaging of the conservation equations, are approximated using the Boussinesq assumption and effective eddy viscosity. The value of the eddy viscosity and subsequent closure of the turbulence equations is made using either a linear or non-linear k - ϵ two-equation model. The effects of turbulence of the flow field on the combustion reactions are included.

The turbulent flow field is also coupled with the combustion chemistry. Since gaseous reactions are limited by mixing rates and not reaction kinetics, the process chemistry is calculated using locally instantaneous equilibrium based on the degree of mixing of the species. Rate constants for processes such as devolatilization (two step process) and char oxidation are built-in to the program based on empirical testing.

A Lagrangian model of the particle conservation equations is used to predict particle transport by characterizing the particle field as a series of discrete particle trajectories through the gas continuum. Particles interact with the gas

field via mass, momentum, and energy exchange. Particle properties such as burnout, velocities, temperatures, and particle component compositions are obtained by integrating the governing equations along the trajectory paths. The program possesses the capability to input a particle size distribution and chemical composition.

In a pulverized coal flame, the radiation field is a multi-component, non-uniform, emitting, absorbing, gas-particle system. The coal particles cause anisotropic and multiple scattering, and the flame is surrounded by non-uniform, emitting, reflecting, absorbing surfaces. The radiation field calculations are based on an energy balance on a beam of radiation passing through a volume element containing the absorbing-reflecting-emitting medium. An Eulerian framework using a discrete-ordinates approach is used to model this process. Heat transfer via radiation and convection to waterwall and tube banks is determined by specifying a local wall temperature and emissivity.

The set of non-linear differential equations is discretized and combined by a upwind and weighted central-differencing scheme. The resulting gas flow field finite difference equations are solved using variations of the SIMPLE/SIMPER algorithm.

FW-FIRE contains a sub-model for the prediction of nitrogen pollutant emissions. This sub-model has the capability of predicting both fuel and thermal NO_x formation. Fuel NO formation can proceed directly to N₂ and NO (such as in the case of char) or through HCN and NH₃ which are oxidized to form NO and reduced to N₂ (such as in the case of volatiles). Global reaction rates are based on work by de Soete and Bose. Thermal NO formation is governed by the extended Zeldovich mechanism.

4.3.1.2 Model Geometry

A simulation was made for both the reference air-fired case and for the oxygen-fired case. The FW-FIRE model simulates the furnace, in height from the bottom of the hopper to the roof, in depth from the front wall to the rear wall, and in width from the left side wall to the right side wall. Furnace partial division walls are also included in the model. Finer meshes are used to model the burners and over-fire air (OFA) ports. The air-fired model contains 528,840 (117x113x40) nodes and is shown in Figure 4.3.1. The oxygen-fired model contains 484,160 (136x89x40) nodes and is shown in Figure 4.3.2.

4.3.2 Boundary Conditions

Boundary conditions are based on ASPEN simulations of the power plant [Sect. 4.1 and Sect. 4.2]. The air-fired, oxygen-fired with ASU and oxygen-fired with OITM ASPEN reference cycle diagrams are presented in Figure 4.1.1, Figure 4.1.9, and Figure 4.2.10, respectively. The input data required by FW-FIRE include fuel analysis, coal particle size distribution (mass percentage for each size bin), waterwall fluid temperatures, and the velocities, flow rates and temperatures of primary and secondary gas streams. Boundary conditions are detailed in Figure 4.3.3, Figure 4.3.4, and Figure 4.3.5.

The waterwalls of the furnace are assumed to be gray and diffusive. The wall temperature at each location is calculated based on the fluid temperature and the heat flux at the wall cell.

For coal devolatilization kinetic properties, Ubhayakar rate parameters were employed for bituminous coal. For bituminous char oxidation, Sandia kinetic and burning mode parameters were applied for Illinois #6 coal.

The selected quantity of flue gas recycle produces a 600°F higher equilibrium temperature in O₂-firing than air-firing. This may increase the potential for slagging in the furnace depending on the ash fusion characteristics. Consequently, for a dry bottom furnace design a minimum flue gas recycling flow may be required to avoid slagging depending on fuel type. Alternatively a wet-bottom or slag type furnace could be used to resolve ash deposition and removal problems.

4.3.2.1 Air-Fired Reference Case

The general layout drawing of the air-fired reference case is shown in Figure 4.3.6. The furnace has a total 24 opposed wall-fired burners (3 vertical x 4 horizontal x 2 walls) and 10 overfire air ports. 30% of the total combustion air is injected through the over-fire air ports located at one burner pitch above the top burner row. The radiant heat transfer surface consists of 2.75" OD tube waterwalls and five 2.0" OD tube partial divisional wall panels. Water is circulated in the furnace by forced circulation.

The boundary conditions were applied to the computational model and FW-FIRE was run until steady state conditions were achieved. The modeling results are summarized in Figure 4.3.7. The coal burnout shown in the table is the percentage of dry ash-free based coal burned. The furnace exit gas temperature (FEGT) shown in the table is the average temperature of flue gas before the platen superheater. The energy absorption listed is the total energy absorbed by water walls and partial division walls prior to the platen superheater. Total furnace absorption and FEGT predicted by FW-FIRE and ASPEN match closely.

Figure 4.3.8 is a plot of the flue gas velocity magnitude in a vertical plane through the second burner column. It can be seen that the gas velocity near the burners accelerates to greater than 130 ft/s due to the reduced gas density after particle ignition. Figure 4.3.9 presents a plot of gas temperature in a vertical plane through the second burner column. The maximum flue gas temperature is approximately 3350°F. The mole fraction of O₂ through the second burner column is presented in Figure 4.3.10.

The heat flux at the furnace water wall is shown in Figure 4.3.11. The maximum heat flux is approximately 70,000 Btu/hr-ft² and is located on the side wall at the top of the burner zone. The total heat absorbed by the furnace walls before the furnace exit is 1770 MM Btu/hr. Figure 4.3.12 displays temperatures of the furnace walls and roof. The maximum temperature of the waterwalls is approximately 870°F and of the division walls is approximately 1000°F. Figure 4.3.13 presents the CO concentration at the wall, peaks at approximately 10% due to the sub-stoichiometric conditions of the lower furnace (without overfire air the wall CO would be below 2%).

The trajectories of the 72-micron particles are plotted in Figure 4.3.14 with colors in each trajectory representing the mass fraction of char in the particle. Char is formed from devolatilization and consumed by oxidation. The maximum char mass fraction is usually less than the mass fraction of fixed carbon in a proximate analysis. Figure 4.3.14 shows that all of the 72-micron particles are completely burned before the furnace exit. The trajectories of 176-micron particles are plotted in Figure 4.3.15. It can be observed from Figure 4.3.15 that some particles are not completely burned at the exit of the furnace, causing unburned carbon in the fly ash. Total burnout of all particle sizes is 99.66% (2.61% LOI). Average NO_x concentration at the furnace outlet is 276 ppmvw (0.38 lb/MMBtu).

4.3.2.2 Oxygen-Fired Design Case

The preliminary size of the furnace heat transfer area was based on a calculation of average wall heat flux using the Foster Wheeler computer program, EMISS [11]. The EMISS computer program calculates radiative heat flux of CO₂ and H₂O gases. A three dimensional CFD run was then made using FW-FIRE to more accurately determine the total heat absorption. Based on the CFD results, the height of the furnace model was adjusted until the total heat absorption approximately matched that required in the ASPEN oxygen-fired design case. Figure 4.3.16 shows a comparison between the sizes of the resultant oxygen-fired furnace and the air-fired reference furnace. Compared to the air-fired furnace, the oxygen furnace has only approximately 65% of the surface area and approximately 45% of the volume. Figure 4.3.17 presents the oxygen-fired design general layout drawing for the cryogenic ASU design and Figure 4.3.18 for the OITM design.

The oxygen-fired furnace has a total 24 opposed wall-fired burners (4 vertical x 3 horizontal x 2 walls) and 8 overfire gas ports. The burner designs (including 0.5 primary air swirl) are based on the subcritical O₂-PC burner design [3]. The radiant heat transfer surface consists of 2.75" OD tube waterwalls and ten 2.0" OD tube partial divisional wall panels. Water is circulated in the furnace by forced circulation.

Two designs were simulated: 1) with cryogenic ASU and 2) with OITM. The designs differ as follows:

Radiant Superheater: In the cryogenic ASU design, radiant superheat (downstream of the primary superheater) is provided by the partial division walls, whereas in the OITM design radiant superheat is provided by the waterwalls above 100' and the furnace roof. No division wall surface is required in the OITM design due to the increased coal-firing such that less evaporator surface (below 100') is required (in addition, in the OITM design the overall furnace height is reduced by 5').

Air Heater: A tubular convective air heater is included in the OITM to provide the necessary air heating for the membrane separation process.

The modeling results are summarized in Figure 4.3.7. The coal burnout for the oxygen-fired cases is 100% due to the high furnace temperature and high concentration of O₂. Total furnace absorption and FEGT predicted by FW-FIRE and ASPEN match well. NO_x is reduced by oxygen firing (compared to air-firing) by about a factor of two from 0.38 lb/MMBtu to 0.18 lb/MMBtu.

4.3.2.2.1 Cryogenic ASU – Full Load

Figure 4.3.19 is a plot of the flue gas velocity magnitude in a vertical plane through the middle burner column. It can be seen that the gas velocity near the burners accelerates to nearly 150 ft/s due to the reduced gas density after particle ignition. Figure 4.3.20 presents a plot of gas temperature in a vertical plane through the middle burner column. The maximum flue gas temperature is approximately 3900°F. The mole fraction of O₂ through the middle burner column is presented in Figure 4.3.21. The mixed primary/secondary gas O₂ content (before combustion) is 41%.

The heat flux at the furnace water wall is shown in Figure 4.3.22. The maximum heat flux is approximately 171,000 Btu/hr-ft² and is located on the side wall at the top of the burner zone. This maximum heat flux is approximately 2.5 times the air-fired case due to the higher flame temperature and higher H₂O and CO₂ concentrations. The total heat absorbed by the furnace walls before the furnace exit is 2287 MM Btu/hr. Figure 4.3.23 displays temperatures of the furnace walls and roof. The maximum temperature of the waterwalls is approximately 1035°F

and of the division walls is approximately 1050°F. Because of the higher temperature of the oxygen-fired case compared to the air-fired case, furnace water wall material was upgraded from 0.22" thick SA-213-T2 to 0.20" thick SA-213-T92. Figure 4.3.24 presents the CO concentration at the wall, which is significantly greater than for the air-fired case (Figure 4.3.13) and its effects on corrosion are modeled analytically in Section 4.3.4, but will also need to be measured empirically in future work.

The trajectories of the 69-micron particles are plotted in Figure 4.3.25 with colors in each trajectory representing the mass fraction of char in the particle. Figure 4.3.25 shows that all of the 69-micron particles are completely burned before the furnace exit. The trajectories of 169-micron particles are plotted in Figure 4.3.26. Note that due to the higher temperature and O₂ concentration all the 169-micron particles are completely burned as compared to the air-fired case (Figure 4.3.15) where there is some residual unburned char at the outlet.

4.3.2.2.2 Cryogenic ASU – Part Load

Since the boiler is a supercritical once-through sliding pressure unit, part load operation must be evaluated with thermal/hydraulic and structural criteria. Three part loads were selected for evaluation: 72%, 50%, and 25% (minimum BENSON load). Boundary conditions were based on the ASPEN System Analysis. Figure 4.3.27 presents the corresponding recycle flow versus load. The modeling results are summarized in Figure 4.3.28. Figure 4.3.29 presents the gas temperature in a vertical plane through the middle burner column for the part load cases. The heat flux at the furnace water wall is shown for the part load cases in Figure 4.3.30. The average and peak heat flux versus height is presented in Figure 4.3.31.

4.3.2.2.3 Integration of Oxygen Ion Transport Membrane

Figure 4.3.32 is a plot of the flue gas velocity magnitude in a vertical plane through the middle burner column. It can be seen that the gas velocity near the burners accelerates to nearly 150 ft/s due to the reduced gas density after particle ignition. Figure 4.3.33 presents a plot of gas temperature in a vertical plane through the middle burner column. The maximum flue gas temperature is approximately 3850°F. The mole fraction of O₂ through the middle burner column is presented in Figure 4.3.34. The mixed primary/secondary gas O₂ content (before combustion) is 39%.

The heat flux at the furnace water wall is shown in Figure 4.3.35. The maximum heat flux is approximately 180,000 Btu/hr-ft² and is located on the side wall at the top of the burner zone. This maximum heat flux is approximately 2.5 times the air-fired case due to the higher flame temperature and higher H₂O and CO₂ concentrations. The total heat absorbed by the furnace walls before the furnace

exit is 2029 MM Btu/hr. Figure 4.3.36 displays temperatures of the furnace walls and roof. The maximum temperature of the evaporator waterwalls is approximately 1060°F, of the radiant superheater is approximately 1100°F, and of the air heater is approximately 1800 °F. Because of the higher temperature of the oxygen-fired case compared to the air-fired case, furnace water wall material was upgraded from 0.22" thick SA-213-T2 to 0.23" thick SA-213-T92. The air heater, which constructed from Incoloy MA956 material, is described in detail in Section 4.3.5.4. Figure 4.3.37 presents the CO concentration at the wall, which is significantly greater than for the air-fired case (Figure 4.3.13) and its effects on corrosion will need to be studied in future work.

The trajectories of the 69-micron particles are plotted in Figure 4.3.38 with colors in each trajectory representing the mass fraction of char in the particle. Figure 4.3.38 shows that all of the 69-micron particles are completely burned before the furnace exit. The trajectories of 169-micron particles are plotted in Figure 4.3.39. Note that due to the higher temperature and O₂ concentration all the 169-micron particles are completely burned as compared to the air-fired case (Figure 4.3.15) where there is some residual unburned char at the outlet.

Figure 4.3.1 – Computational Model of Air-Fired Furnace (with right side wall removed)

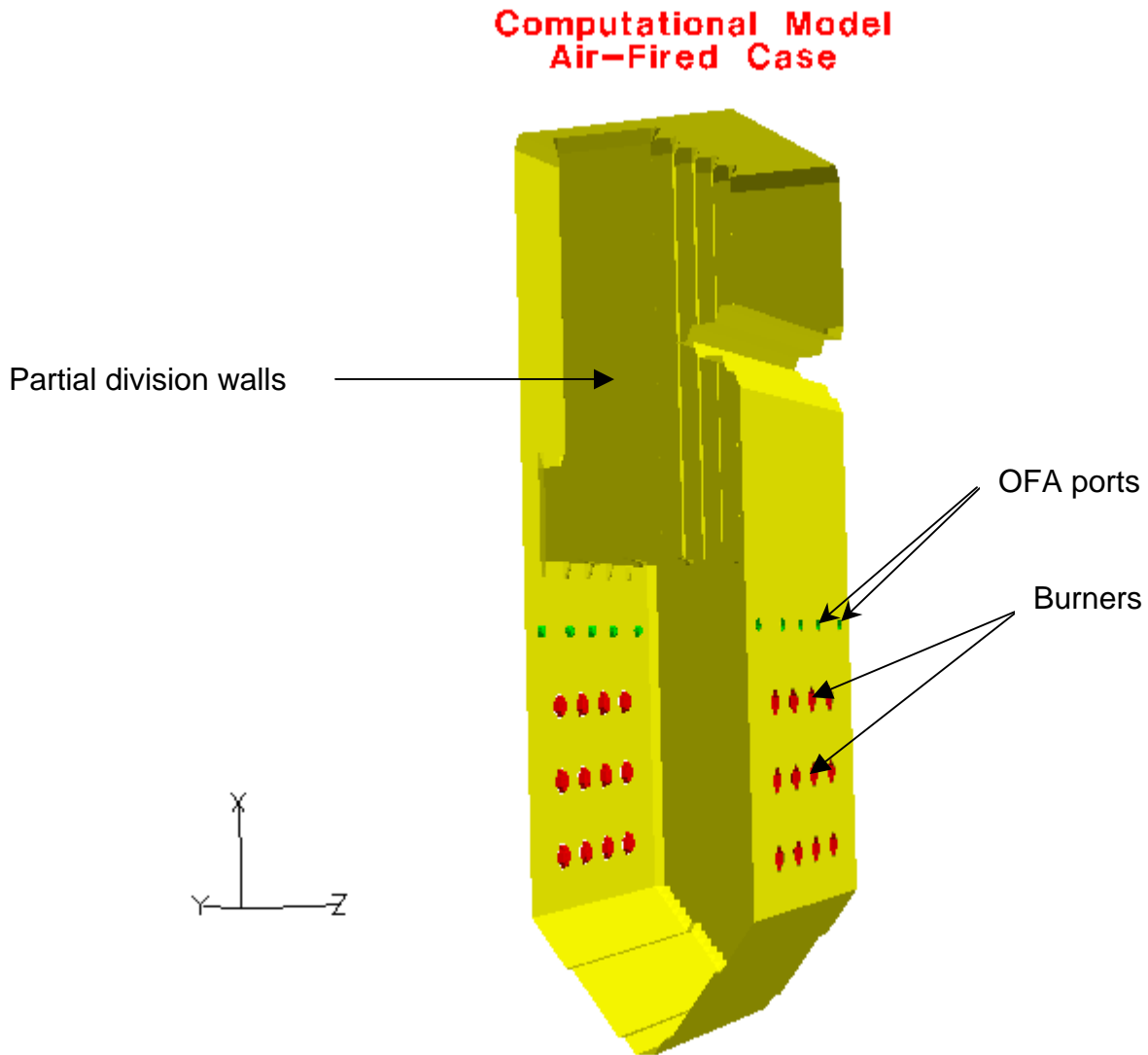


Figure 4.3.2 – Computational Model of Oxygen-Fired Furnace With OFA

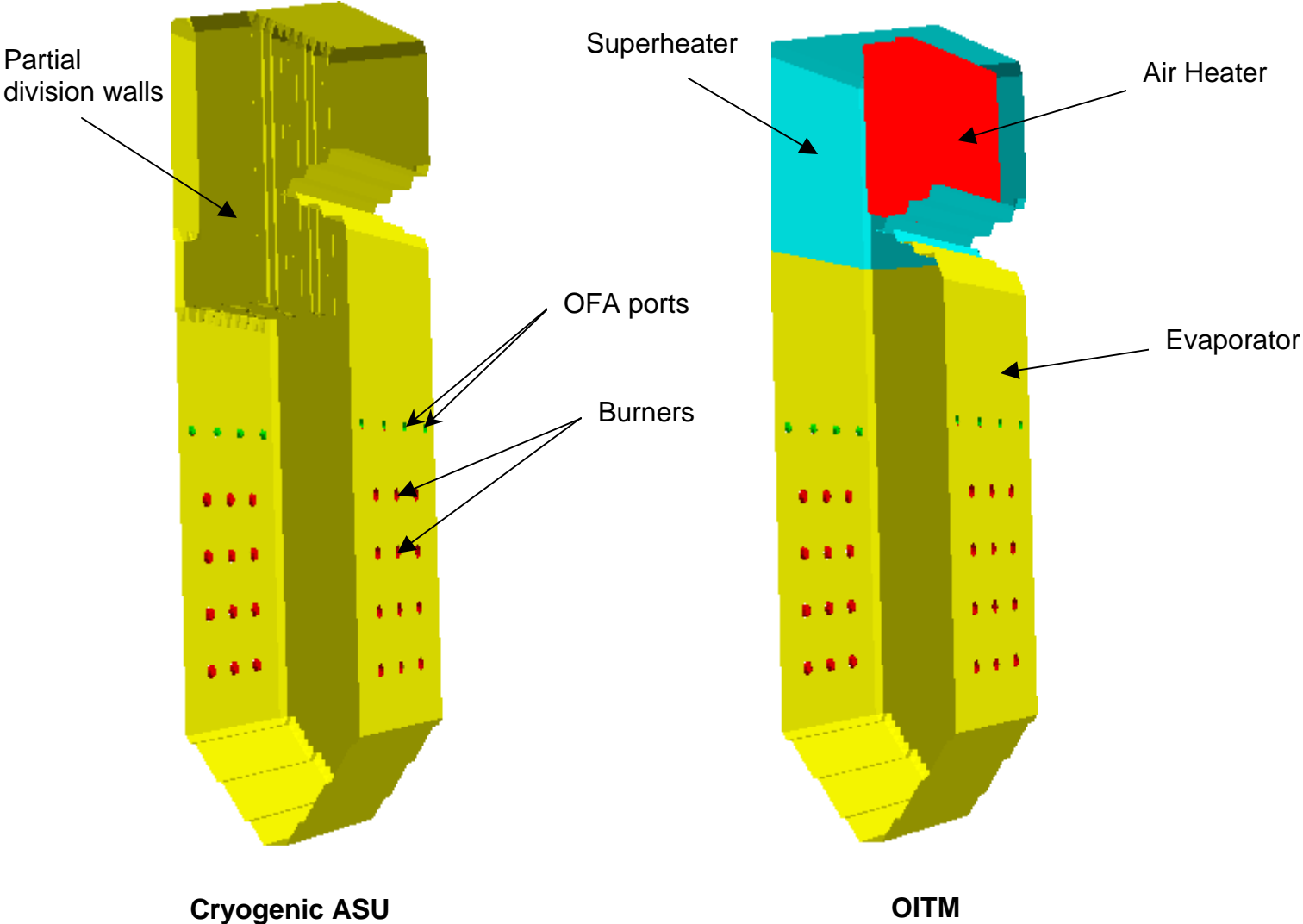


Figure 4.3.3 – Air-Fired Boundary Conditions

Coal			Size (micron)		Mass Percent					
Ultimate Analysis			Distribution							
Ash	%	9.99%	9.3	%	28.9	<table border="1"> <tr> <td>Coal Flow</td> <td>319,000</td> </tr> <tr> <td>Moisture in Coal</td> <td>35,473</td> </tr> </table>	Coal Flow	319,000	Moisture in Coal	35,473
Coal Flow	319,000									
Moisture in Coal	35,473									
S	%	2.51%	33.7	%	27.3					
H	%	4.50%	71.7	%	23.9					
C	%	63.75%	121.8	%	10.7					
H2O	%	11.12%	175.5	%	9.2					
N	%	1.25%	Total		100.0					
O	%	6.88%								
Total	%	100.00%	< 75 micron	%	70					
Volatile Matter (daf)	%	44.35%	< 150 micron	%	99					
Density	lb/ft3	80.0								
HHV, as received	Btu/lb	11,666			<table border="1"> <tr> <td>Heat Input</td> <td>3721.45 MM Btu/hr</td> </tr> </table>	Heat Input	3721.45 MM Btu/hr			
Heat Input	3721.45 MM Btu/hr									

TCA	lb/hr	3,299,687
Excess O2	%	11.0
OFA	%	20.0%

Divwall	Temp (F)	Temp (K)
Inlet	854	730
Outlet	964	791

WW	Temp (F)	Temp (K)
Inlet	638	610
Outlet	810	705

	Flow Rate		Temperature F	Density lb/ft3	Inner Diam. in	Outer Diam. in	Area per Port ft2	No. of Ports	Axial Velocity ft/sec	Tan./Axial Velocity	Rad./Axial Velocity	Coal Flow lb/hr
	lb/hr	%										
Primary	550,000	16.5	219	0.059	13.100	22.750	1.887	24	57.1	0.00	0.00	283,527
Inner Sec. Air	425,044	12.7	580	0.039	23.750	33.375	2.999	24	42.5	0.00	0.21	
Outer Sec. Air	1,700,178	51.0	580	0.039	33.875	49.000	6.837	24	74.6	0.41	0.41	
Tertiary Air	0	0.0	580	0.039	0.000	12.100	0.799	24	0.0	0.00	0.00	
Overfire Air - Inner	335,664	10.1	580	0.039	0.000	19.000	1.969	10	122.7	0.00	0.00	
Overfire Air - Outer	324,274	9.7	580	0.039	19.500	27.000	1.902	10	122.7	0.00	0.21	
	3,335,159	100.0										

Figure 4.3.4 – Oxygen-Fired Boundary Conditions (Cryogenic ASU)

Coal			Size (micron) Distribution		Mass Percent	
Ultimate Analysis						
Ash	%	9.99%	10.7	%	29.5	
S	%	2.51%	33.7	%	38.2	Coal Flow 308,000
H	%	4.50%	69.3	%	25.9	Moisture in Coal 34,250
C	%	63.75%	118.2	%	5.5	
H2O	%	11.12%	169.2	%	1.0	
N	%	1.25%	Total	%	100.0	
O	%	6.88%				
Total	%	100.00%	< 75 micron	%	85	
			< 150 micron	%	99	
Volatile Matter (daf)	%	44.35%				
Density	lb/ft3	80.0				
HHV, as received	Btu/lb	11,666				Heat Input 3593.13 MM Btu/hr

TCA	lb/hr	1,809,811
Excess O2	%	11.0
OFA	%	20.0%

Divwall	Temp (F)	Temp (K)
Inlet	837	720
Outlet	974	796

WW	Temp (F)	Temp (K)
Inlet	593	585
Outlet	825	714

	Flow Rate		Temperature F	Density lb/ft3	Inner Diam. in	Outer Diam. in	Area per Port ft2	No. of Ports	Axial Velocity ft/sec	Tan./Axial Velocity	Rad./Axial Velocity	Coal Flow lb/hr
	lb/hr	%										
Primary	495,000	26.8	257	0.073	9.500	15.000	0.735	24	106.3	0.50	0.00	273,750
Inner Sec. Air	197,420	10.7	625	0.046	16.000	20.750	0.952	24	52.6	0.00	0.21	
Outer Sec. Air	789,679	42.8	625	0.046	21.750	29.000	2.007	24	99.8	0.41	0.41	
Tertiary Air	0	0.0	625	0.046	0.000	8.500	0.394	24	0.0	0.00	0.00	
Overfire Air - Inner	170,790	9.3	625	0.046	0.000	13.500	0.994	8	130.8	0.00	0.00	
Overfire Air - Outer	191,172	10.4	625	0.046	14.000	20.000	1.113	8	130.8	0.00	0.21	
	1,844,061	100.0										

Figure 4.3.5 – Oxygen-Fired Boundary Conditions (OITM)

Coal			Size (micron)		Mass Percent	
Ultimate Analysis			Distribution			
Ash	%	9.99%	10.7	%	29.5	
S	%	2.51%	33.7	%	38.2	
H	%	4.50%	69.3	%	25.9	
C	%	63.75%	118.2	%	5.5	
H2O	%	11.12%	169.2	%	1.0	
N	%	1.25%	Total		%	100.0
O	%	6.88%				
Total	%	100.00%	< 75 micron	%	85	
Volatile Matter (daf)	%	44.35%	< 150 micron	%	99	
Density	lb/ft3	80.0				
HHV, as received	Btu/lb	11,666				

Coal Flow	375,400
Moisture in Coal	41,744

Heat Input	4379.42 MM Btu/hr
------------	-------------------

TCA	lb/hr	2,306,255
Excess O2	%	11.0
Drum Pressure	psia	
OFA	%	20.0%

Divwall	Temp (F)	Temp (K)
Inlet	837	721
Outlet	970	794

WW	Temp (F)	Temp (K)
Inlet	599	588
Outlet	830	716

	Flow Rate		Temperature F	Density lb/ft3	Inner Diam. in	Outer Diam. in	Area per Port ft2	No. of Ports	Axial Velocity ft/sec	Tan./Axial Velocity	Rad./Axial Velocity	Coal Flow lb/hr
	lb/hr	%										
Primary	600,000	25.6	236	0.076	9.500	15.000	0.735	24	125.1	0.50	0.00	333,656
Inner Sec. Air	257,350	11.0	625	0.046	16.000	20.750	0.952	24	68.6	0.00	0.21	
Outer Sec. Air	1,029,399	43.8	625	0.046	21.750	29.000	2.007	24	130.1	0.41	0.41	
Tertiary Air	0	0.0	625	0.046	0.000	8.500	0.394	24	0.0	0.00	0.00	
Overfire Air - Inner	217,639	9.3	625	0.046	0.000	13.500	0.994	8	166.6	0.00	0.00	
Overfire Air - Outer	243,612	10.4	625	0.046	14.000	20.000	1.113	8	166.6	0.00	0.21	
	2,347,999	100.0										

Figure 4.3.6 – Air-Fired Boiler Design

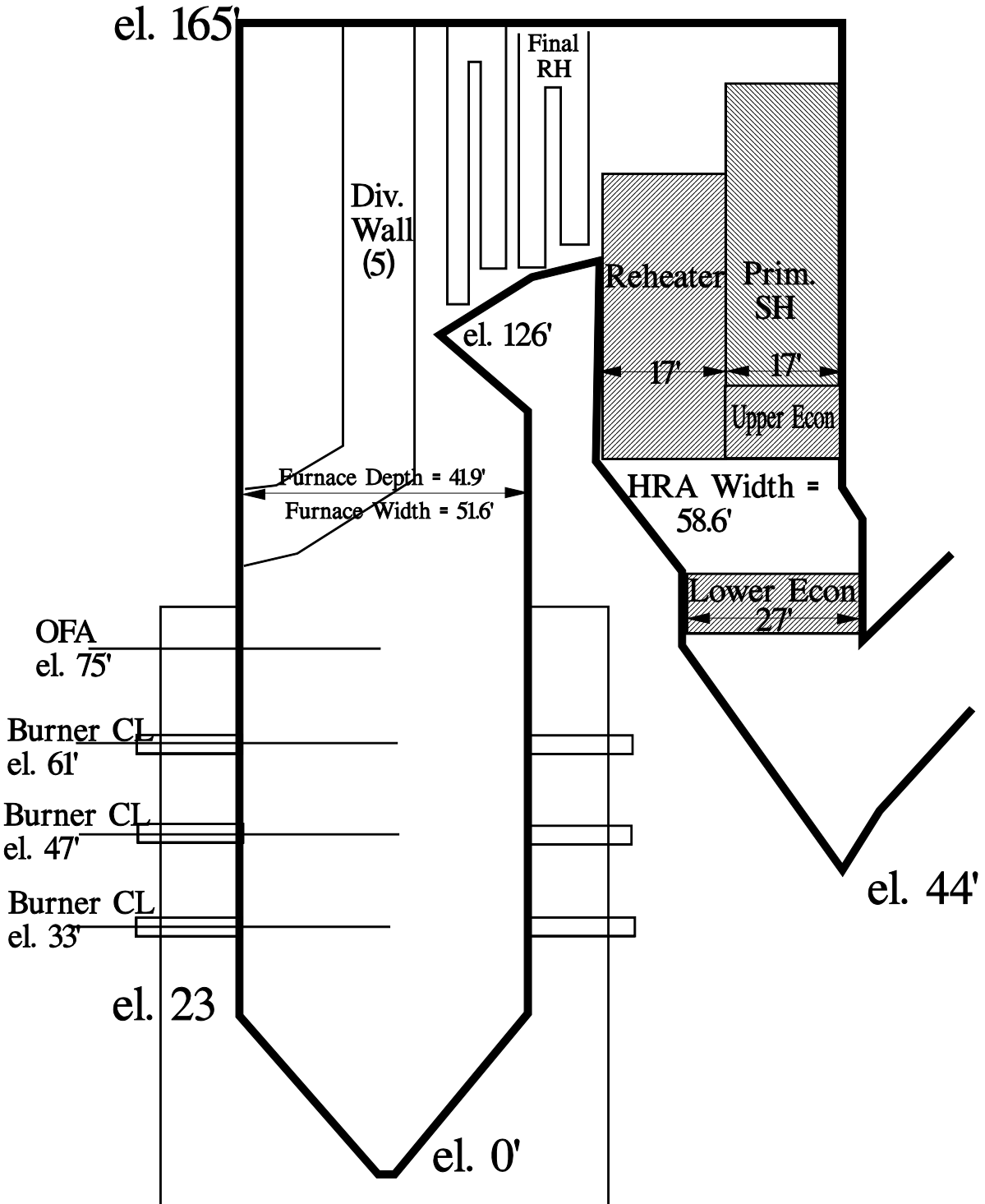


Figure 4.3.7 – Summary of FW-FIRE Furnace Modeling Results

Air-Fired

		FW-FIRE	ASPEN
Burnout	%	99.6	99.0
LOI	%	2.76	7.32
Total Furnace Absorption	M Btu/hr	1770	1751
Division Wall Absorption	M Btu/hr	445	451
FEGT	F	2107	2185
NOx	ppmvw	276	
	lb/MMBtu	0.38	

Oxygen-Fired (Cryogenic ASU)

		FW-FIRE	ASPEN
Burnout	%	100.0	99.9
LOI	%	0.00	0.78
Total Furnace Absorption	M Btu/hr	2096	2089
Division Wall Absorption	M Btu/hr	548	485
FEGT	F	2266	2450
NOx	ppmvw	261	
	lb/MMBtu	0.18	

Oxygen-Fired (OITM)

		FW-FIRE	ASPEN
Burnout	%	100.0	99.9
LOI	%	0.00	0.78
Total Furnace Absorption	M Btu/hr	2029	1961
Radiant SH Absorption	M Btu/hr	458	502
Air Heater Absorption	M Btu/hr	935	970
FEGT	F	1822	2185
NOx	ppmvw	273	
	lb/MMBtu	0.20	

Figure 4.3.8 – Gas Velocity for Air-Fired Case

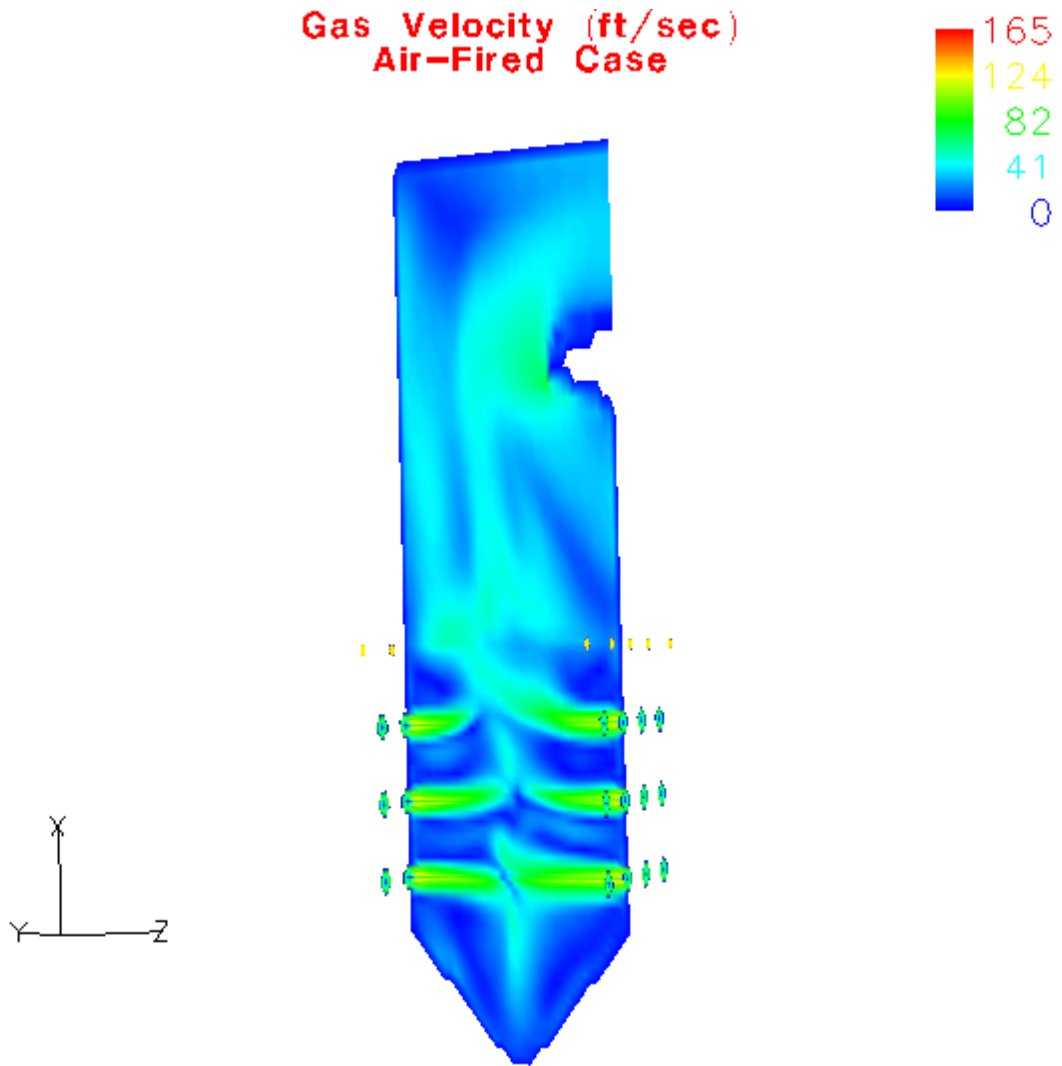


Figure 4.3.9 – Gas Temperature for Air-Fired Case

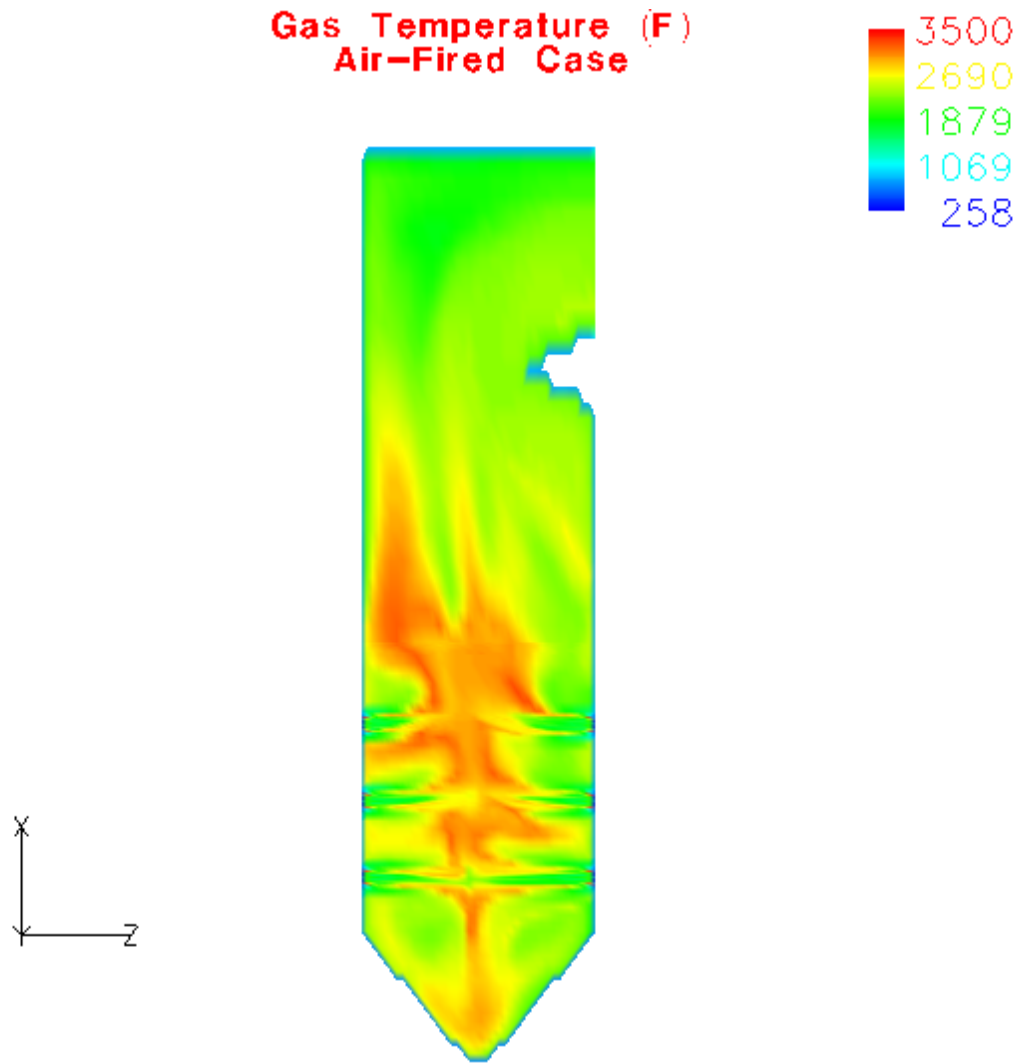


Figure 4.3.10 – O₂ Mole Fraction for Air-Fired Case

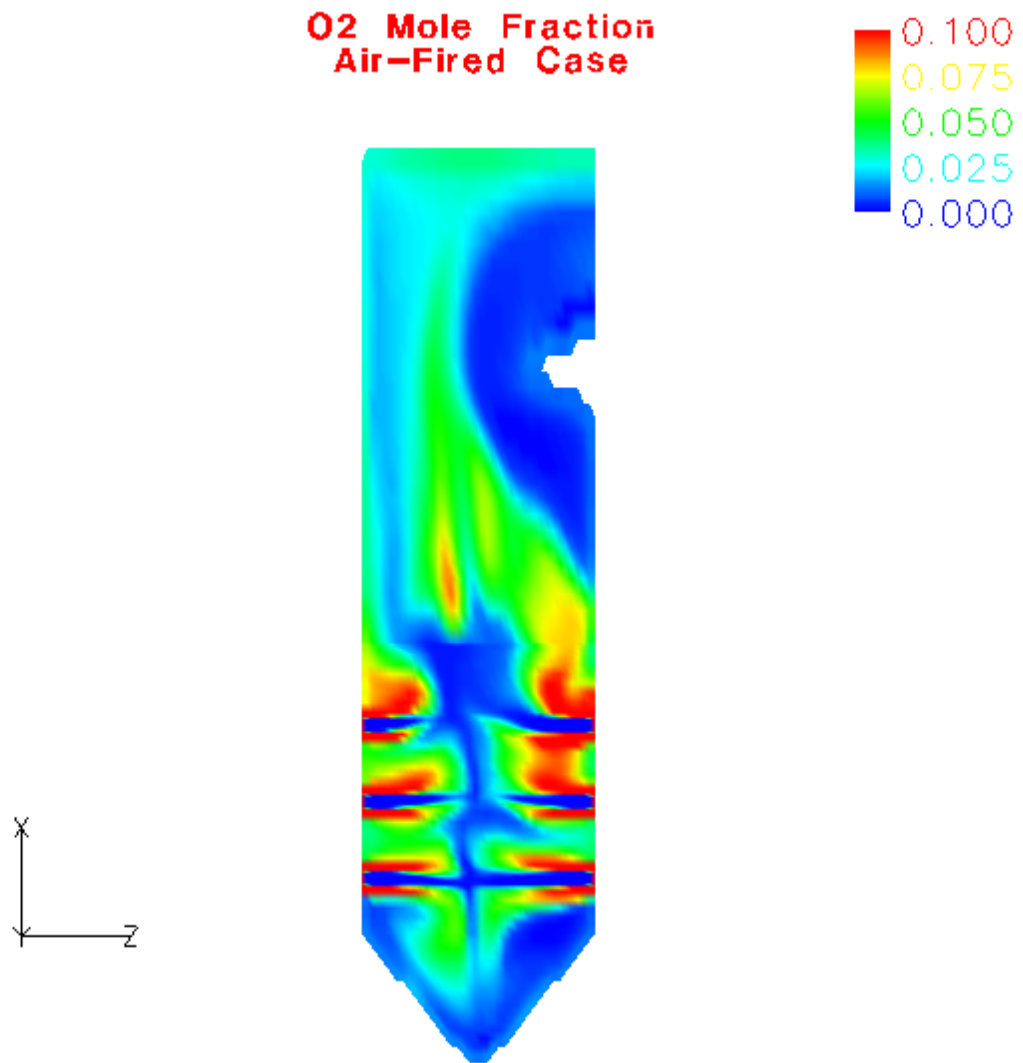


Figure 4.3.11 – Wall Heat Flux for Air-Fired Case

Wall Heat Flux (Btu/hr-ft²)
Air-Fired Case

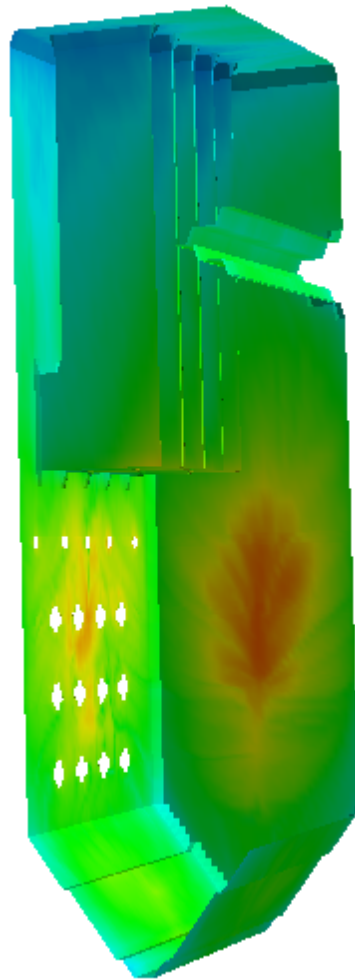
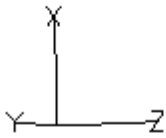


Figure 4.3.12 – Wall Temperature for Air-Fired Case

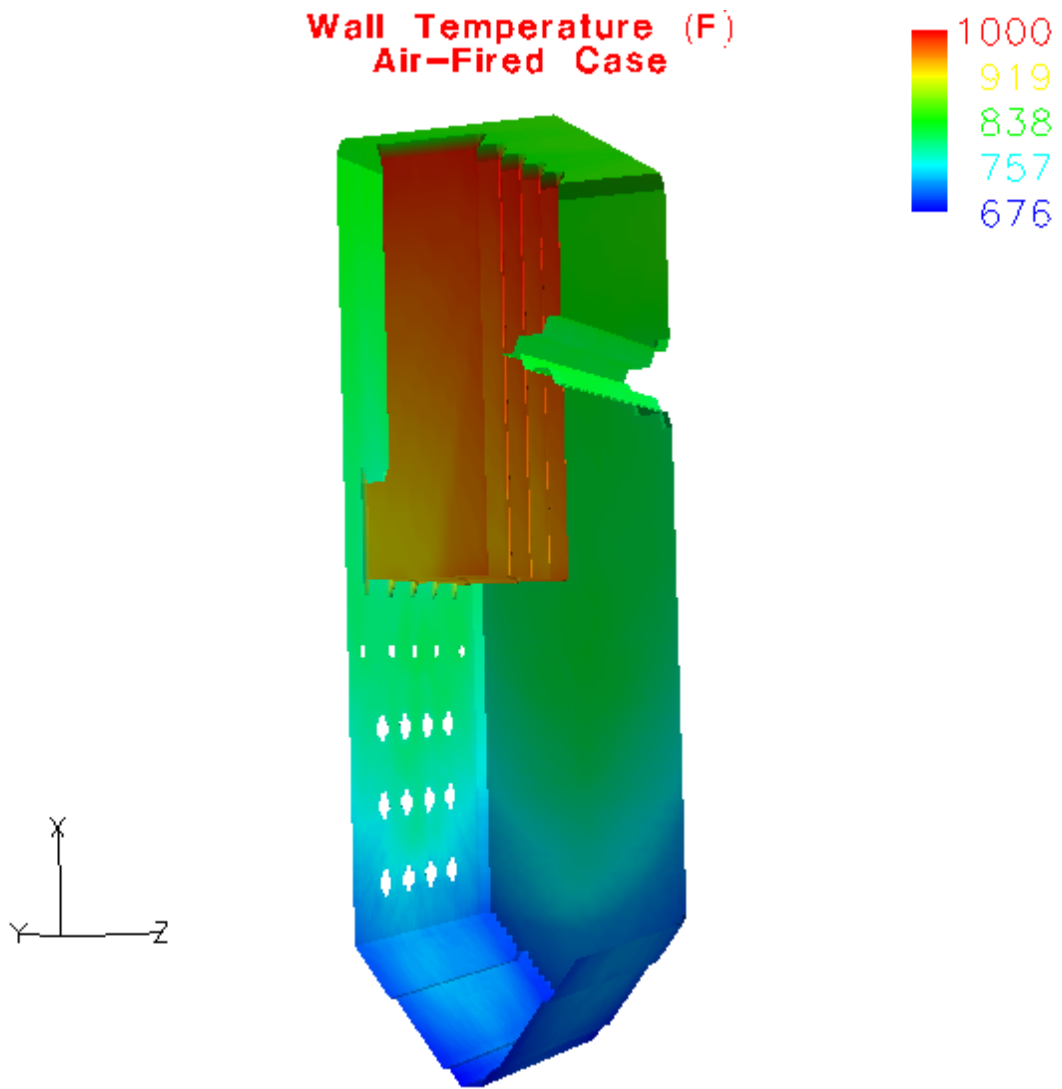


Figure 4.3.13 – Wall CO for Air-Fired Case

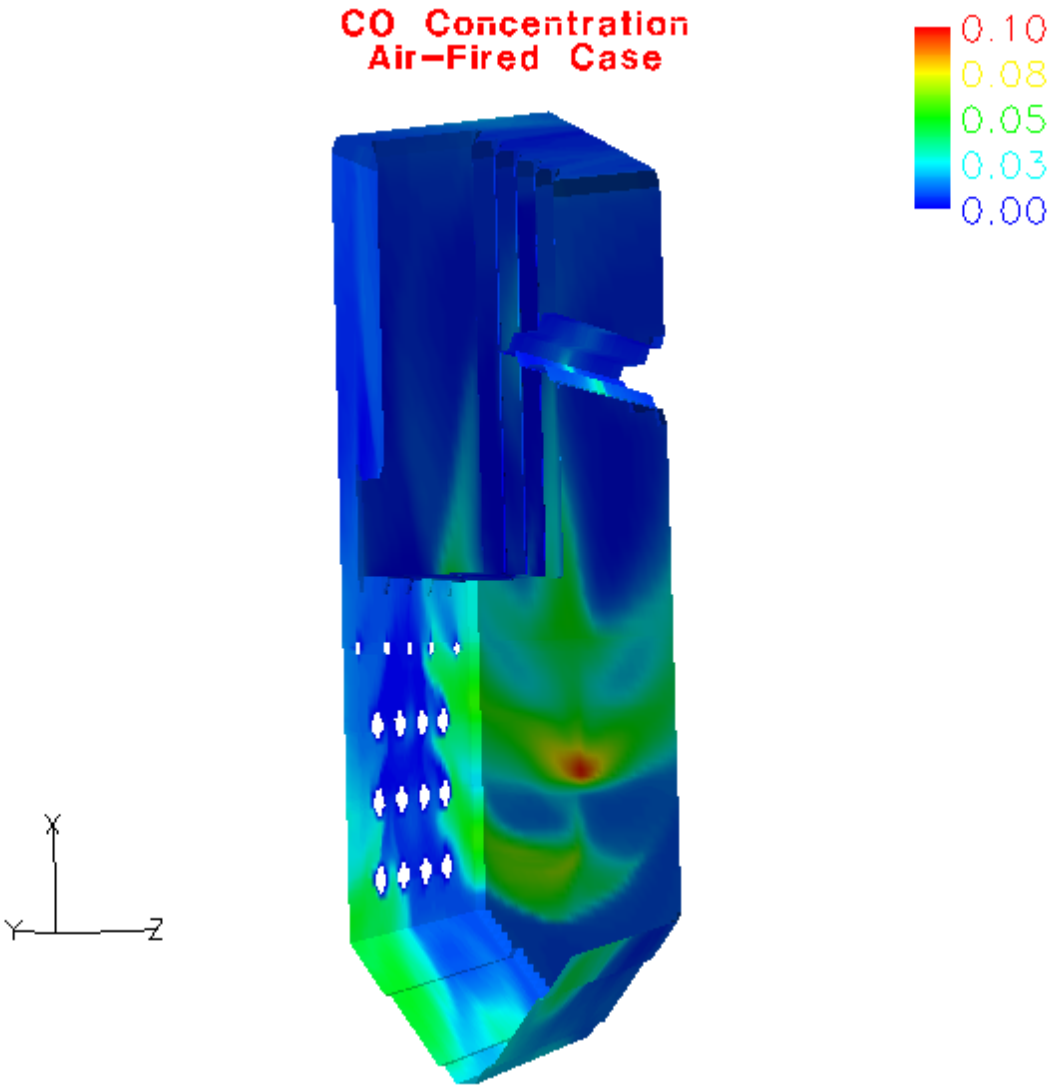


Figure 4.3.14 – Char Mass Fraction (72 microns) for Air-Fired Case

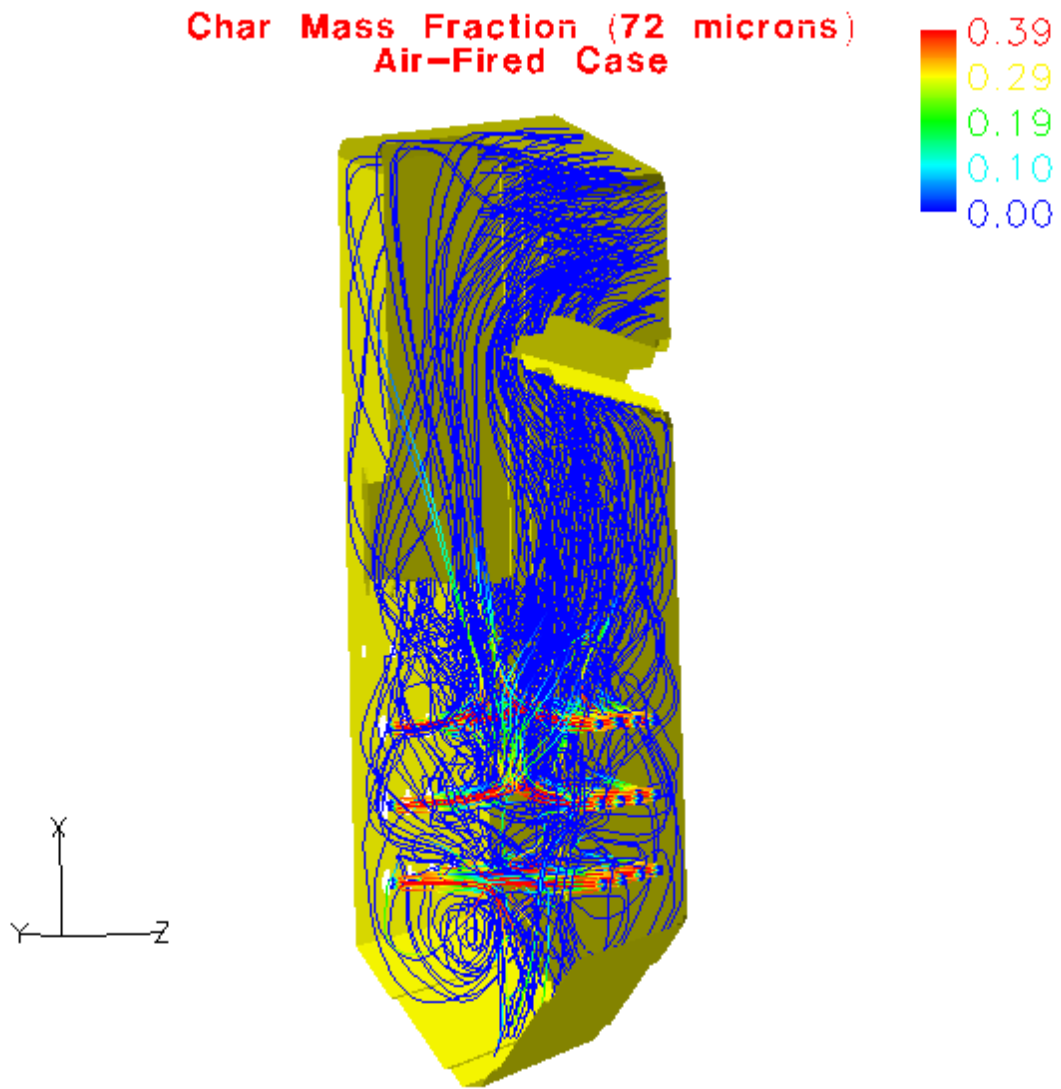


Figure 4.3.15 – Char Mass Fraction (176 microns) for Air-Fired Case

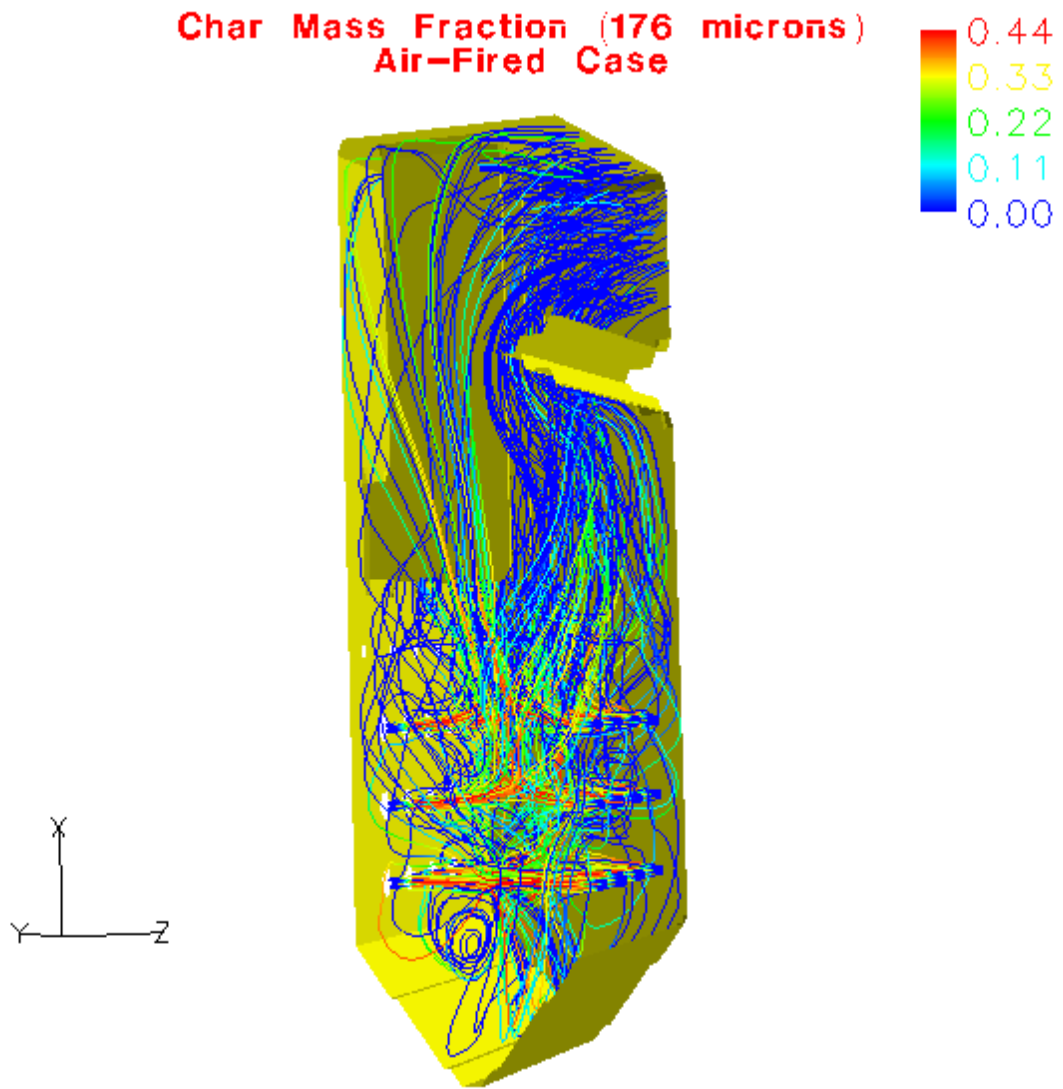


Figure 4.3.16 – Air-Fired and Oxygen-Fired Boiler Outlines
(Black = Air-Fired, Red = Oxygen Fired)

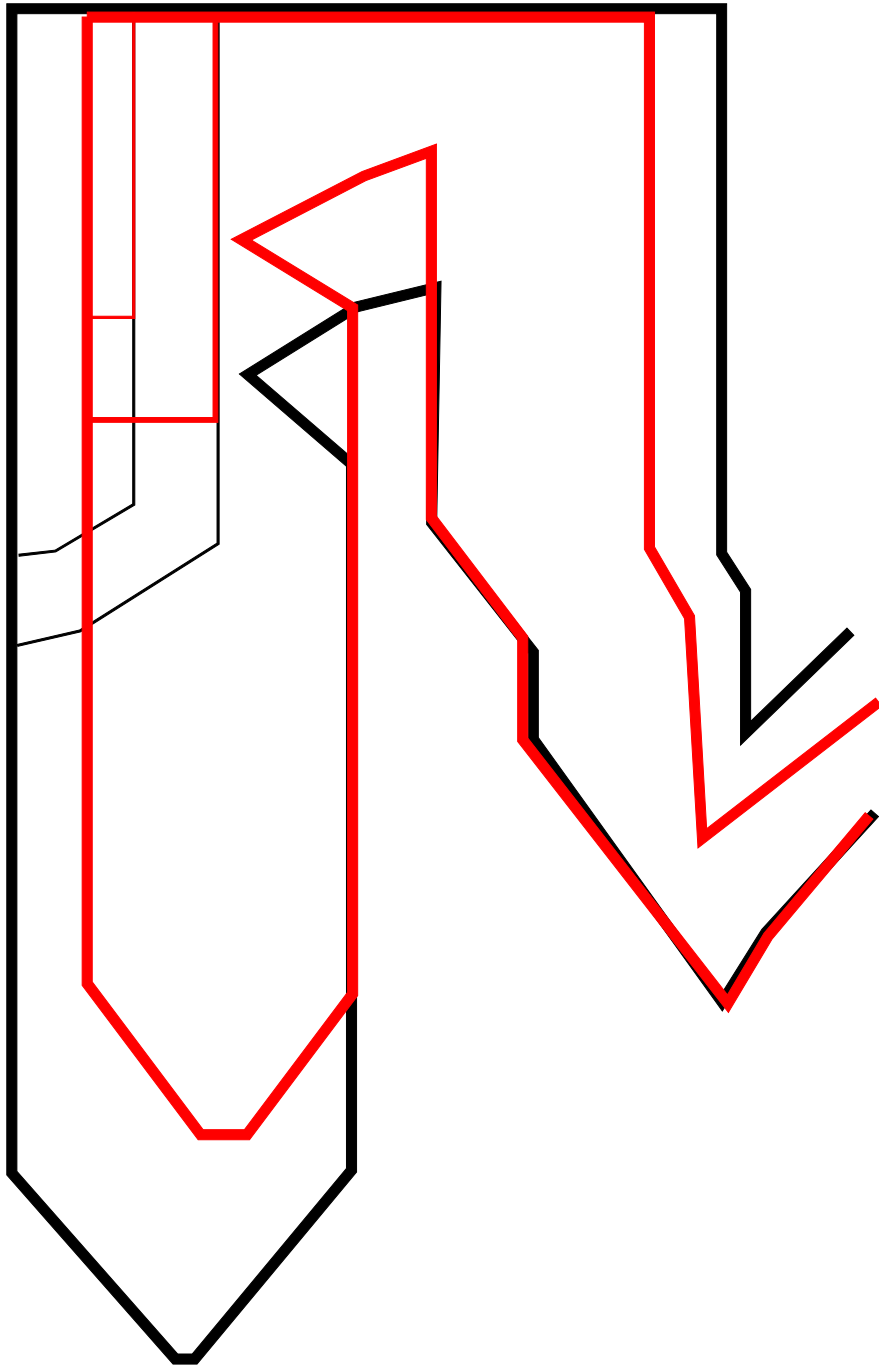


Figure 4.3.17 – Oxygen-Fired Boiler Design (Cryogenic ASU)

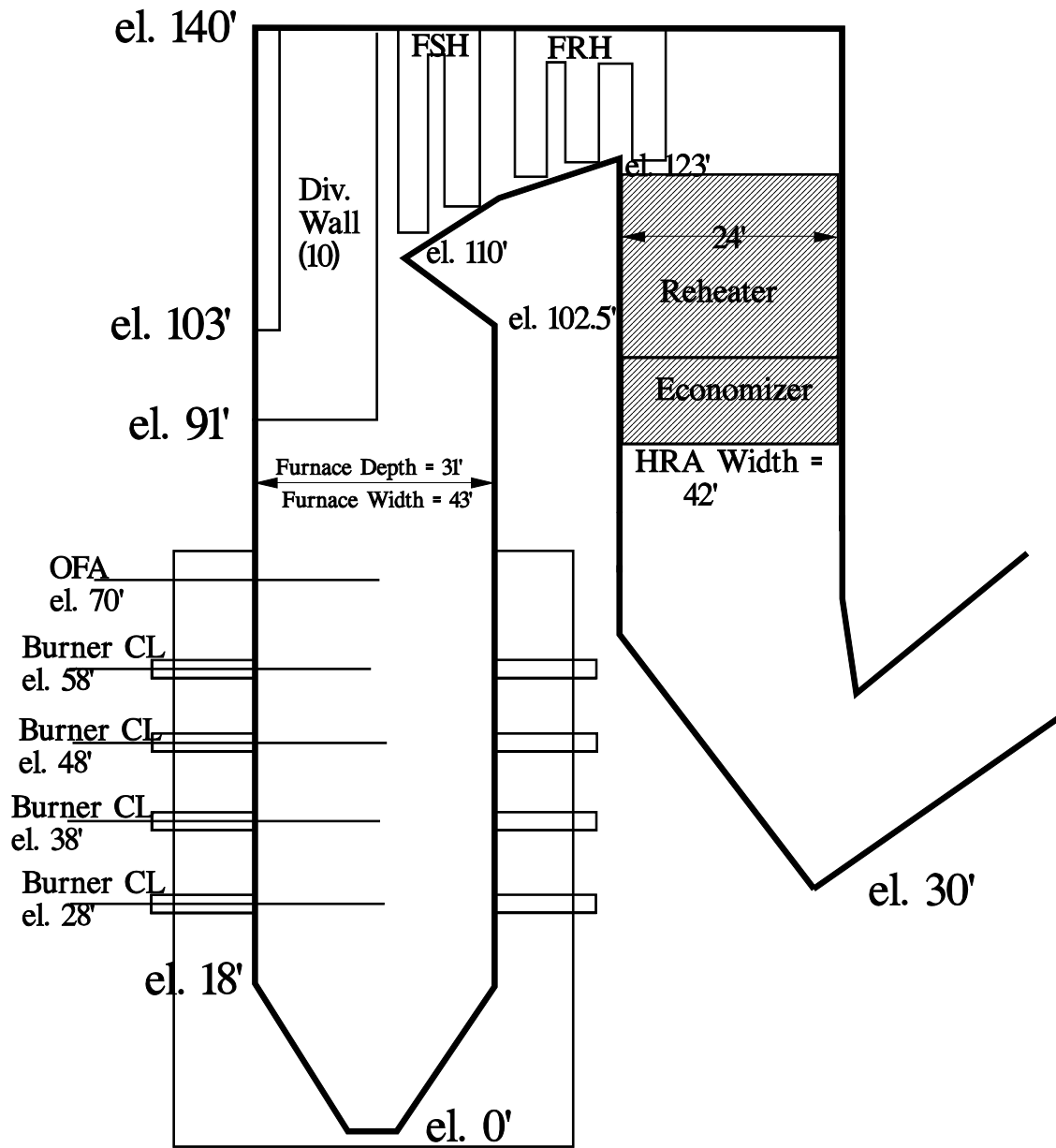


Figure 4.3.18 – Oxygen-Fired Boiler Design (OITM)

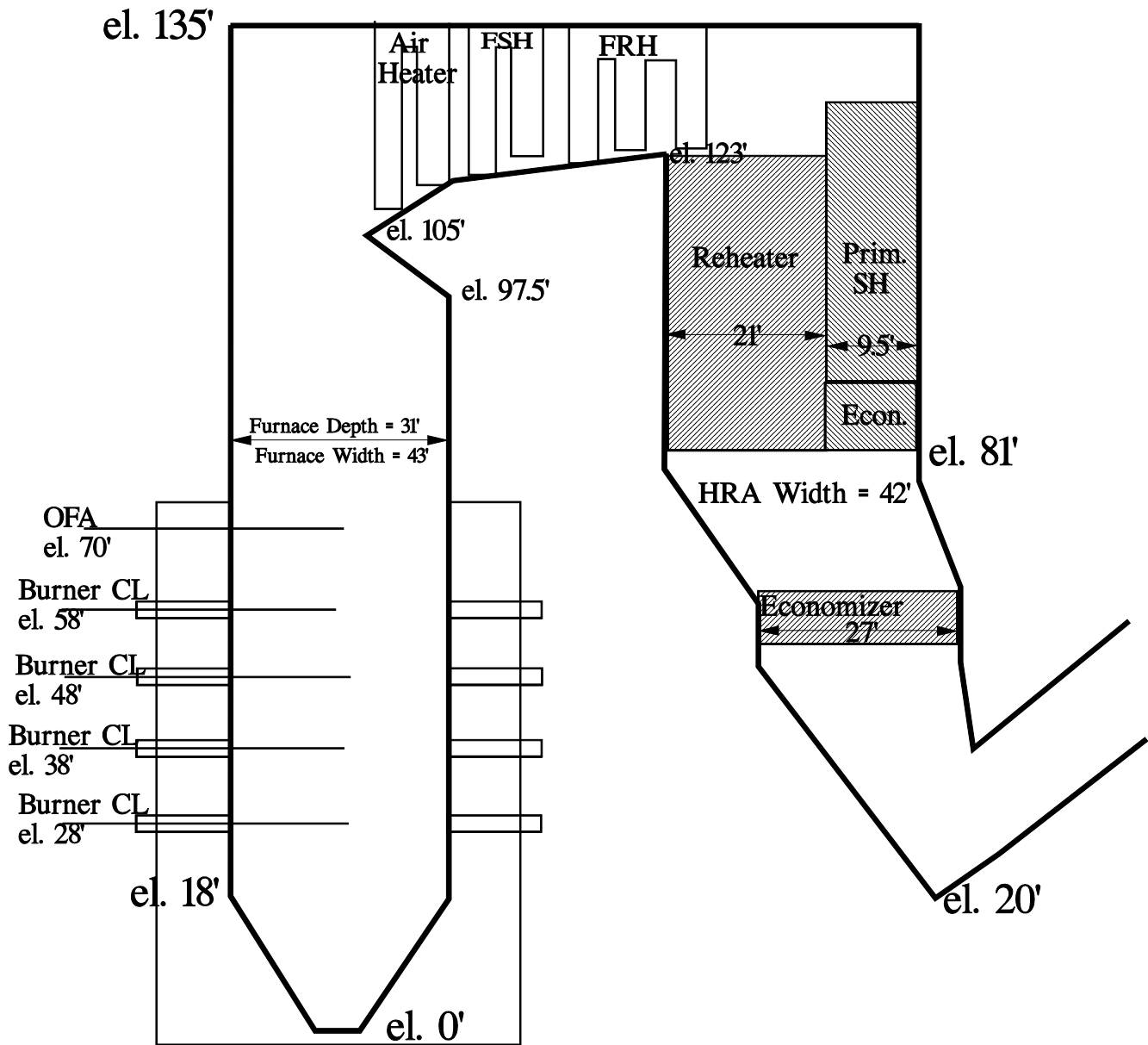


Figure 4.3.19 – Gas Velocity for O₂-Fired Case

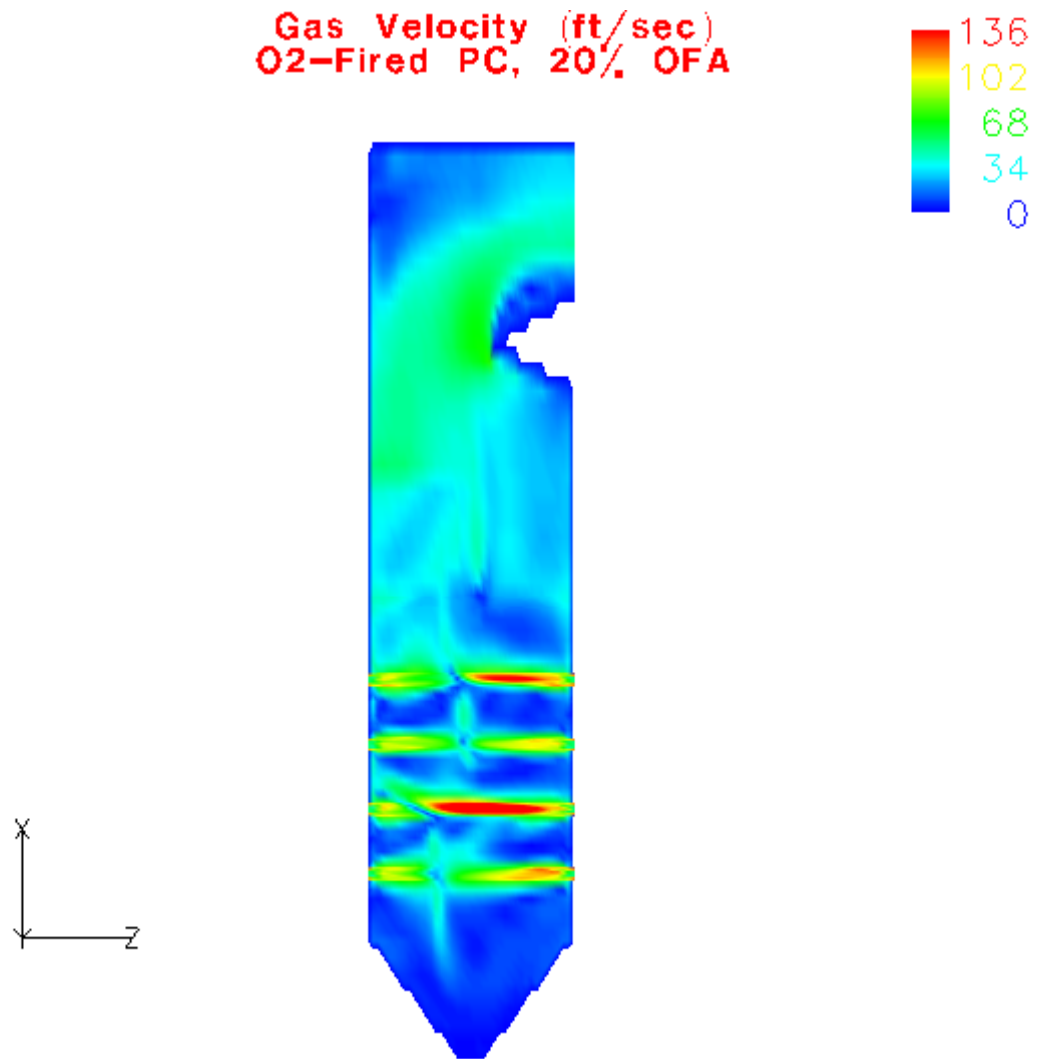


Figure 4.3.20 – Gas Temperature for O₂-Fired Case

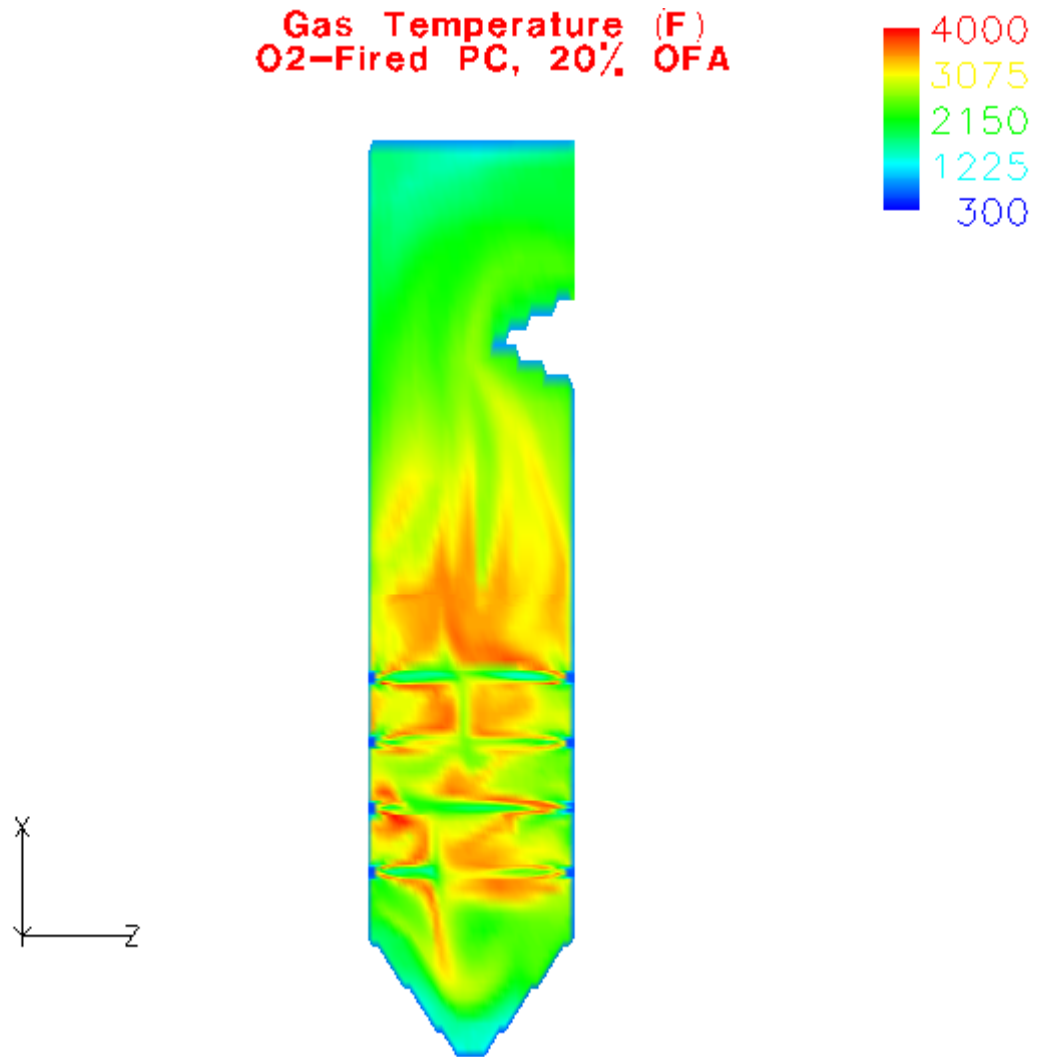


Figure 4.3.21 – O₂ Mole Fraction for O₂-Fired Case

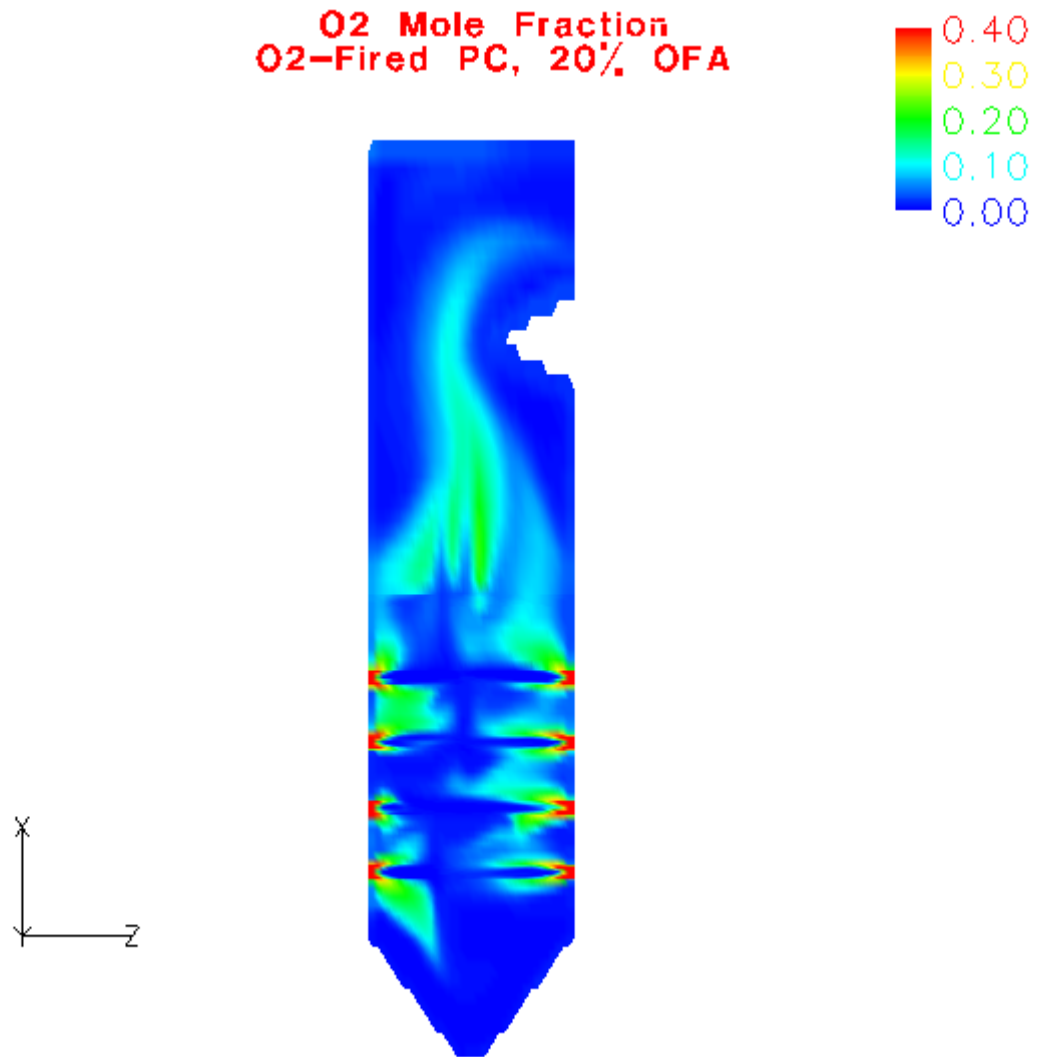


Figure 4.3.22 – Wall Heat Flux for O₂-Fired Case

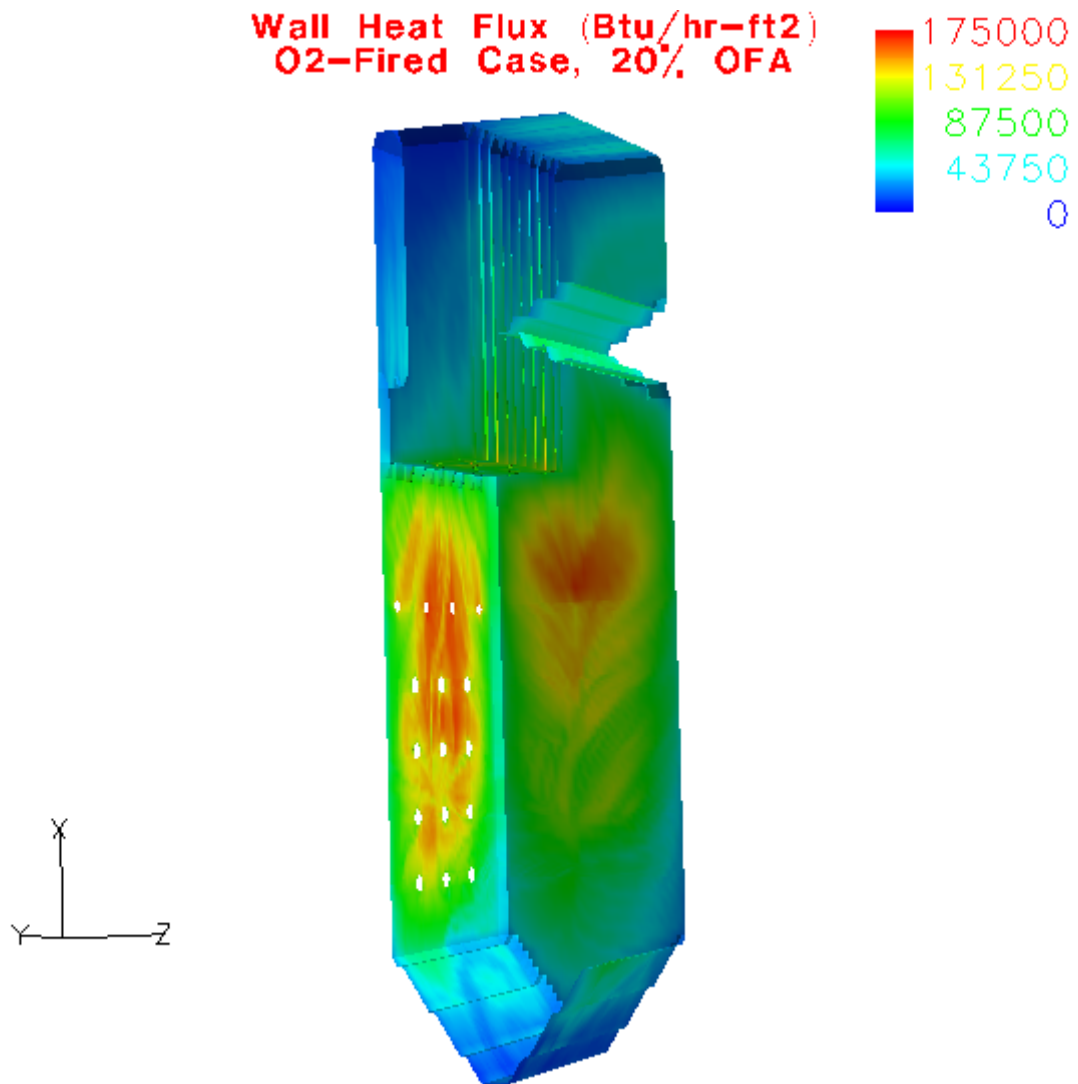


Figure 4.3.23 – Wall Temperature for O₂-Fired Case

Wall Temperature (F)
O₂-Fired Case, 20% OFA

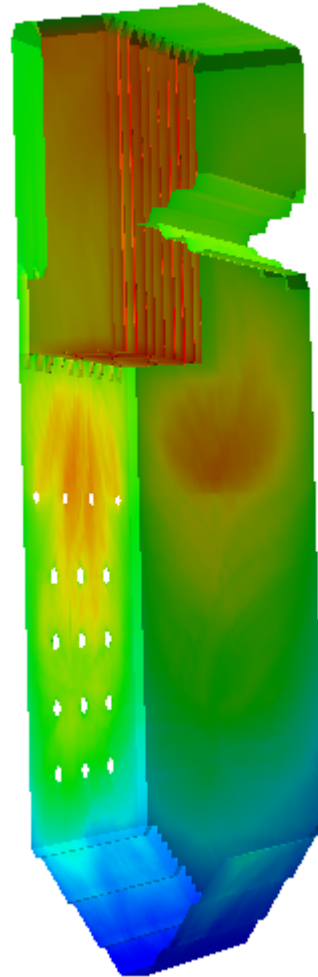
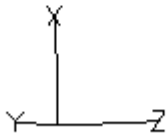


Figure 4.3.24 – Wall CO for O₂-Fired Case

CO Concentration
O₂-Fired Case, 20% OFA

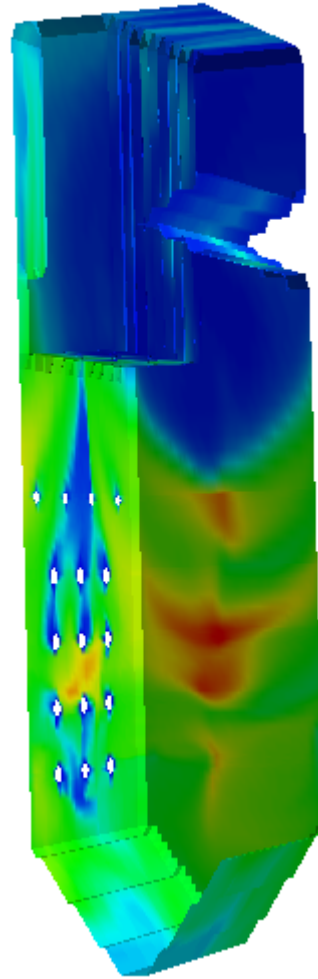
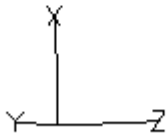


Figure 4.3.25 – Char Mass Fraction (69 micron) for O₂-Fired Case

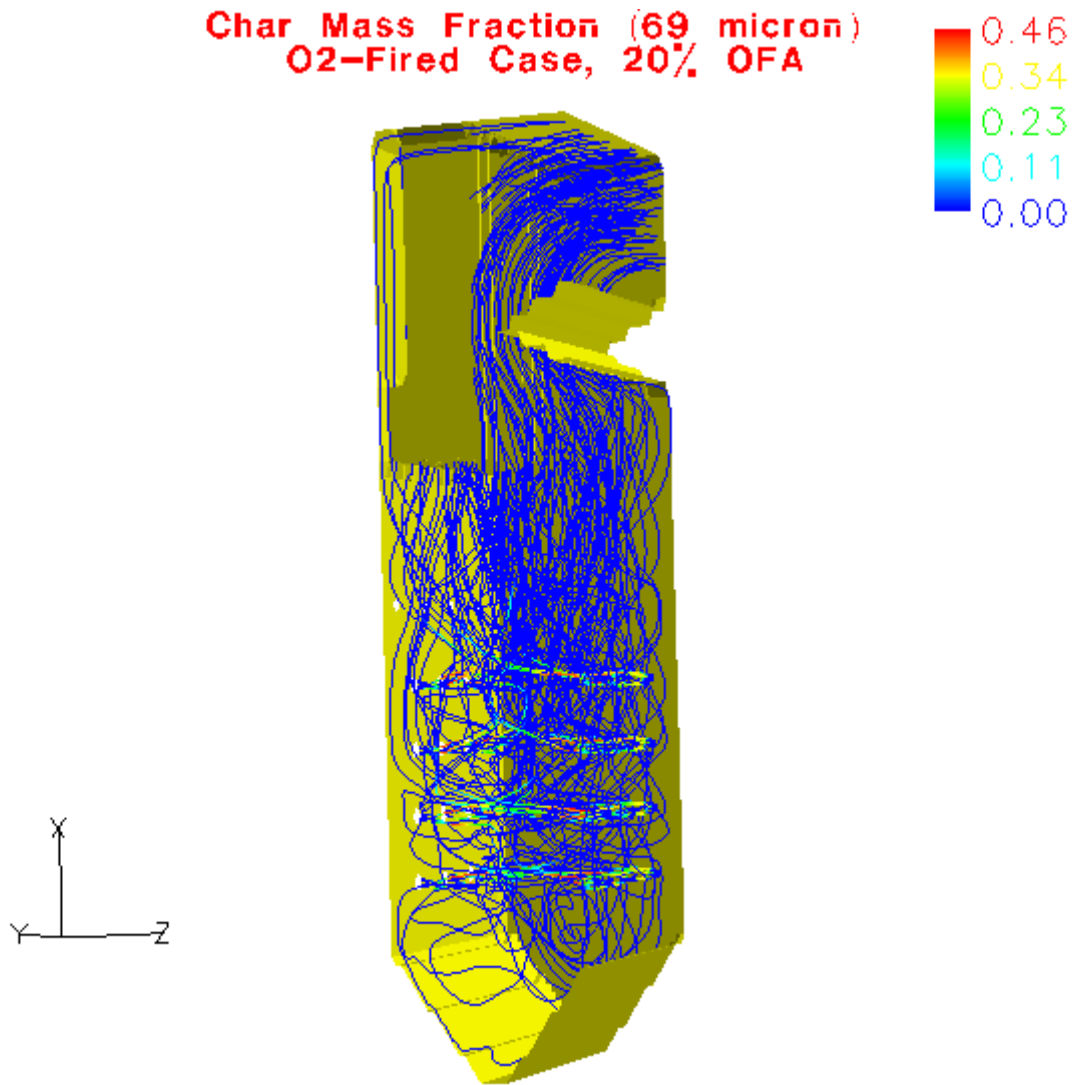


Figure 4.3.26 – Char Mass Fraction (169 micron) for O₂-Fired Case

Char Mass Fraction (169 micron)
O₂-Fired Case, 20% OFA

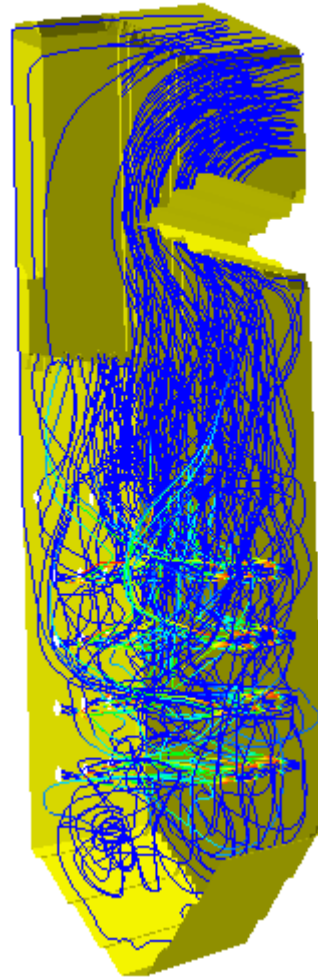
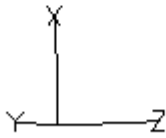


Figure 4.3.27 - Flue gas recycle flow vs. part load operation

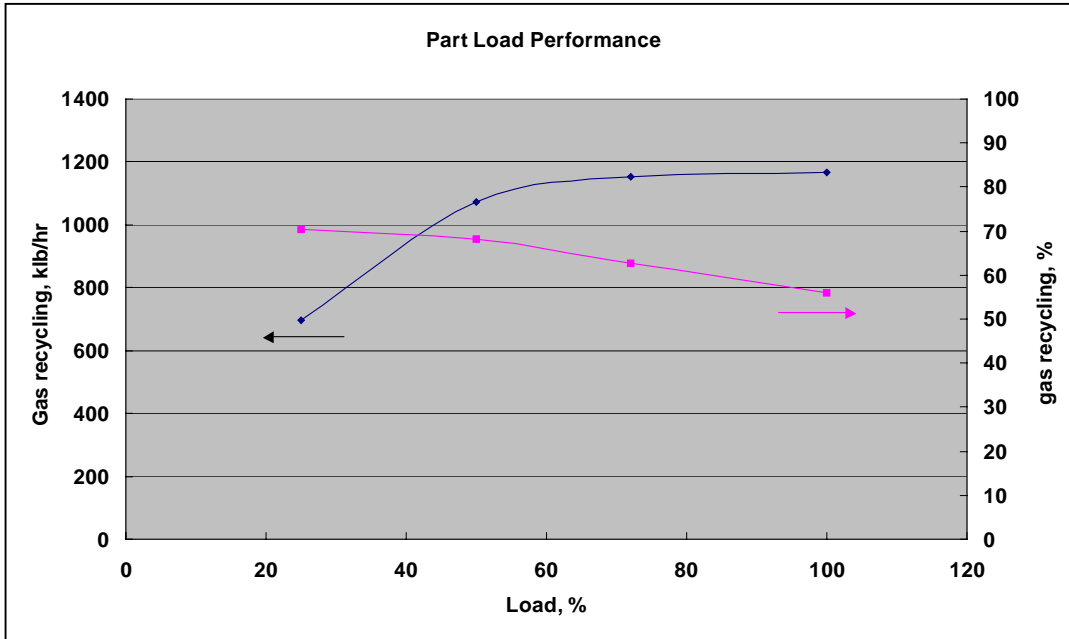


Figure 4.3.28 – Summary of O₂-Fired Part Load Results, Cryogenic ASU

		100% Load	72% Load	50% Load	25% Load
Burnout	%	100.00	100.00	100.00	99.81
LOI	%	0.00	0.00	0.00	1.48
Total Furnace Absorption	MM Btu/hr	2096	1572	1073	747
Division Wall Absorption	MM Btu/hr	548	380	248	193
FEGT	F	2266	2069	1912	1658

Figure 4.3.29 – Gas Temperature for O₂-Fired Part Load, Cryogenic ASU

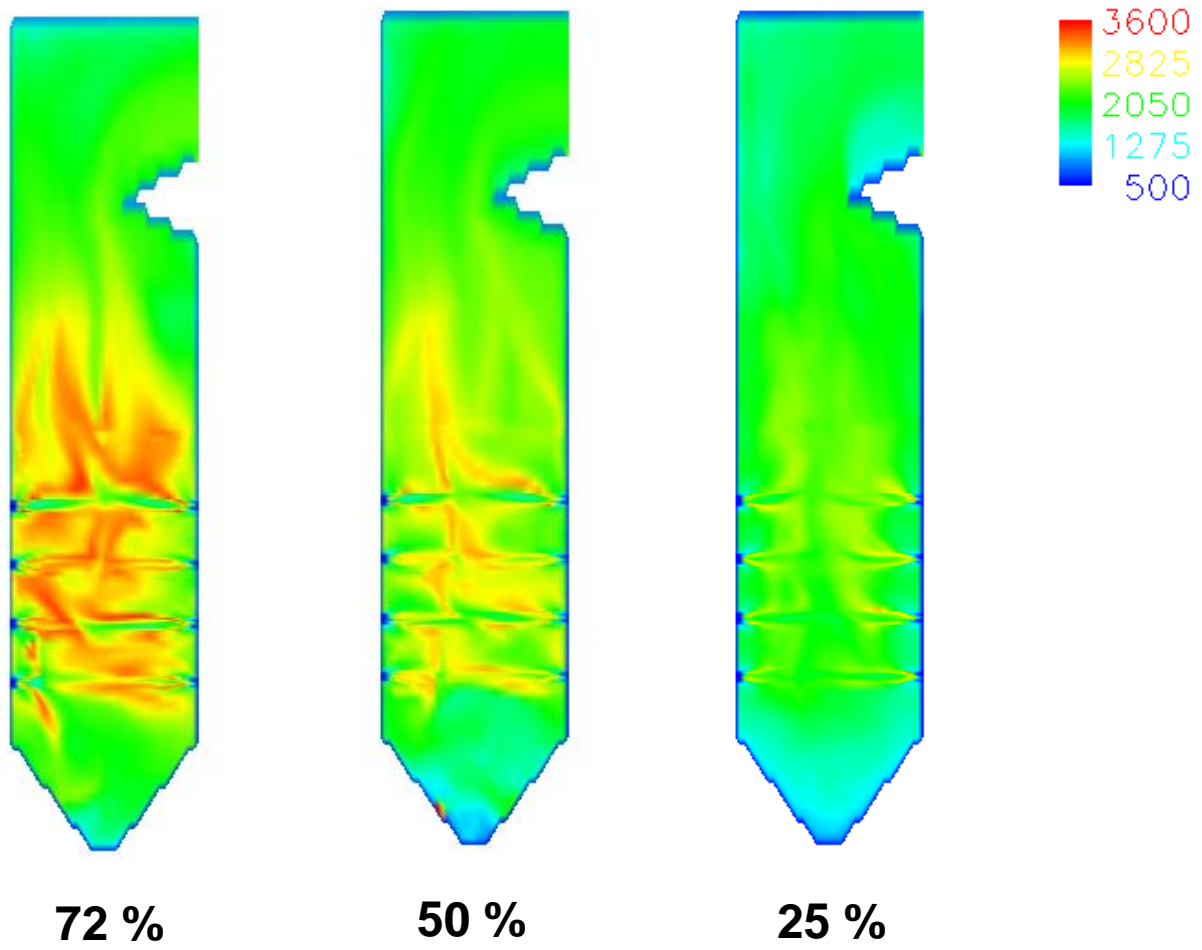


Figure 4.3.30 – Wall Heat Flux for O₂-Fired Part Load, Cryogenic ASU

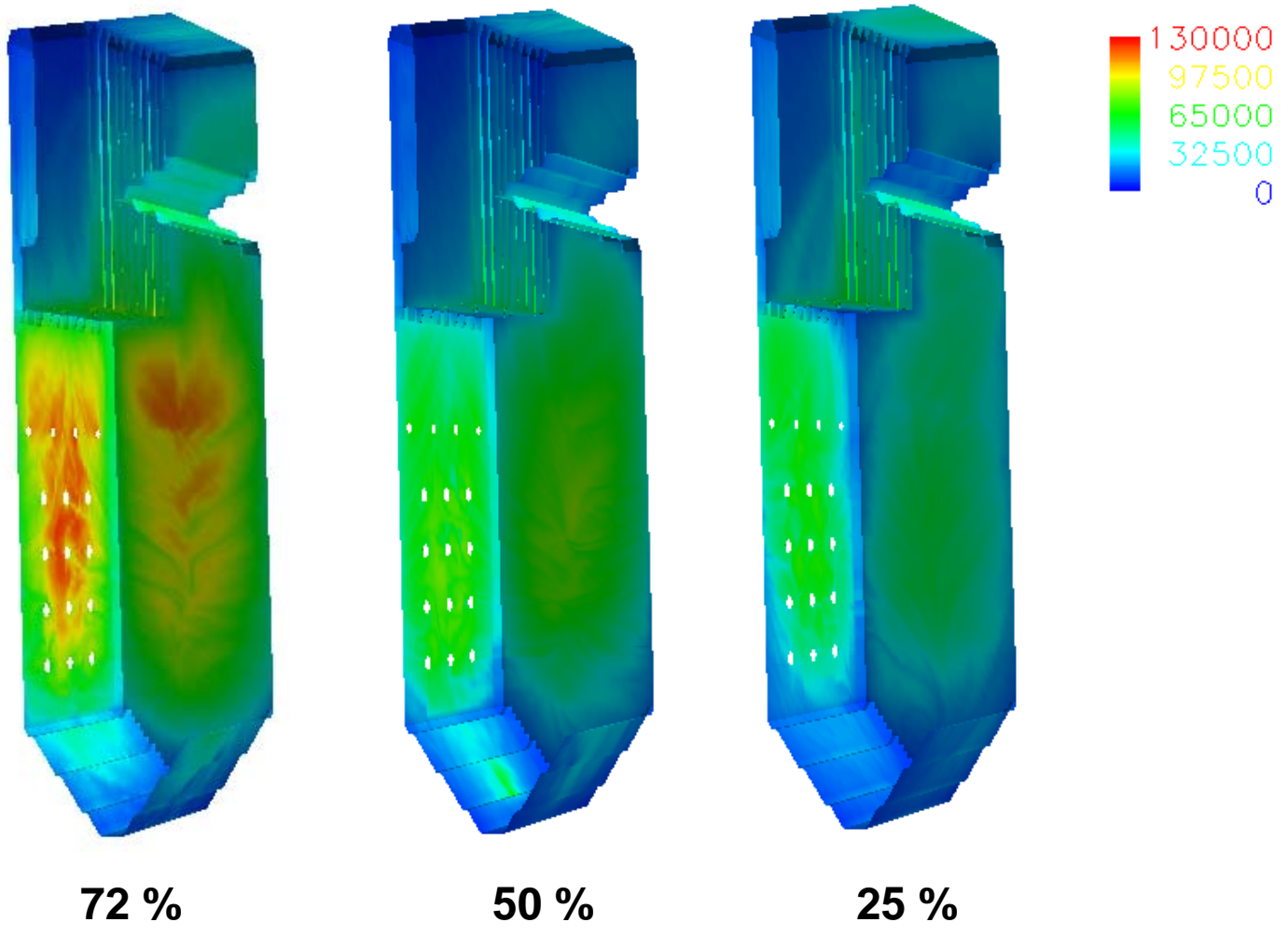


Figure 4.3.31 – Average and Peak Heat Flux in Waterwalls

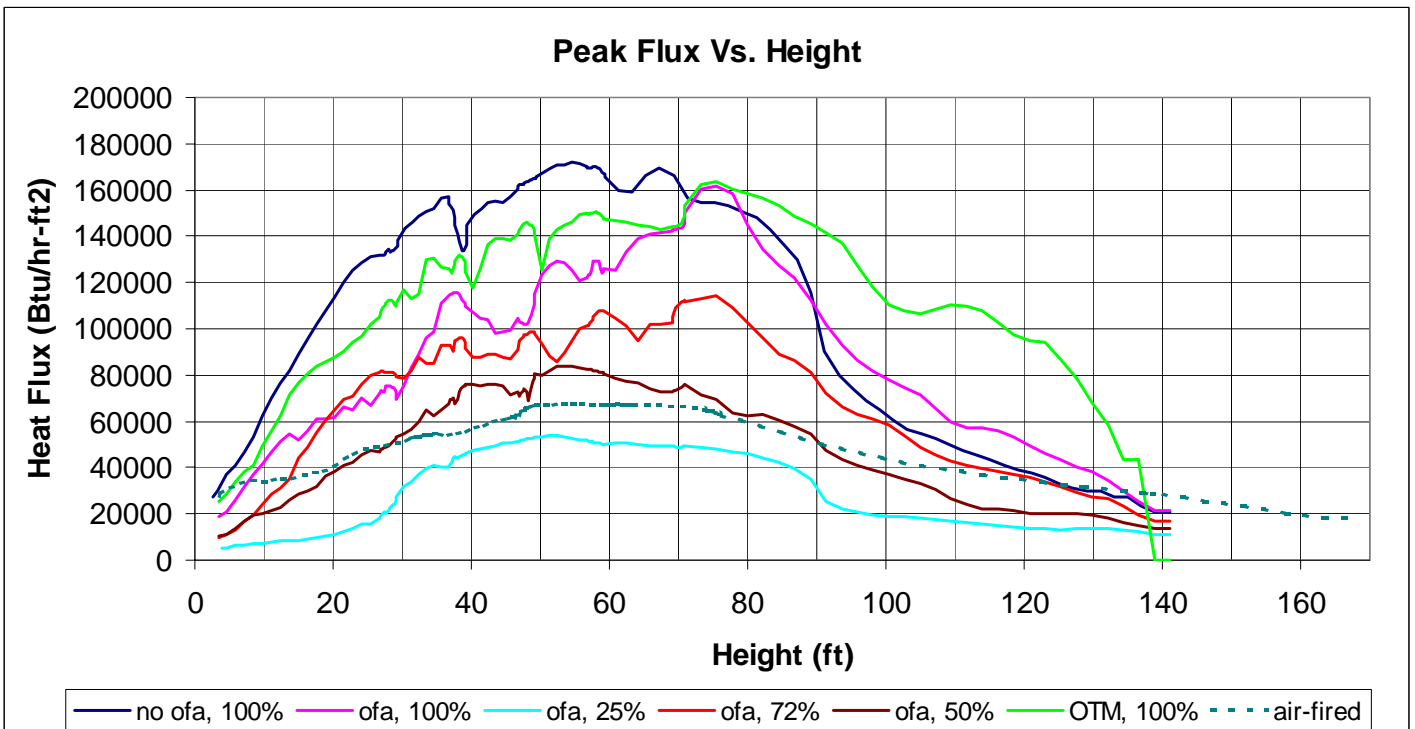
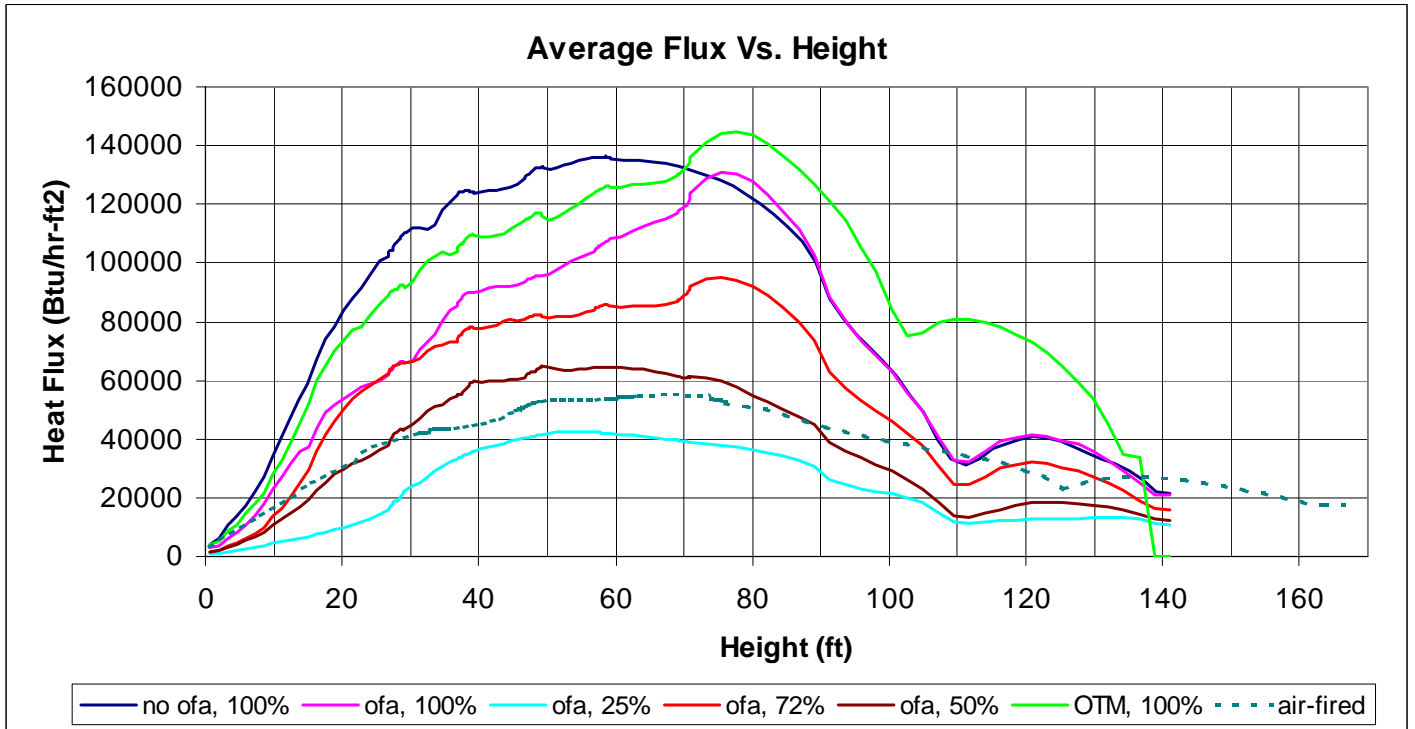


Figure 4.3.32 – Gas Velocity for O₂-Fired with OITM

Gas Velocity (ft/sec)
O₂-Fired PC, 20% OFA

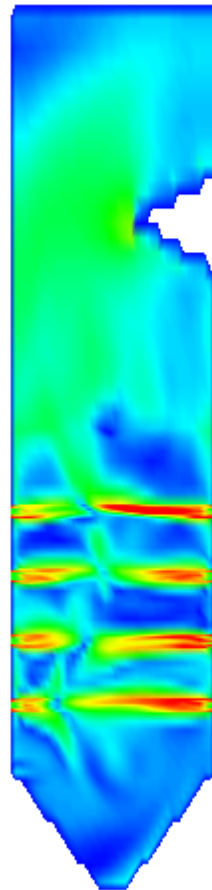
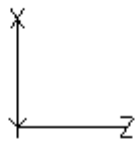


Figure 4.3.33 – Gas Temperature for O₂-Fired Case With OITM

Gas Temperature (F)
O₂-Fired PC, 20% OFA

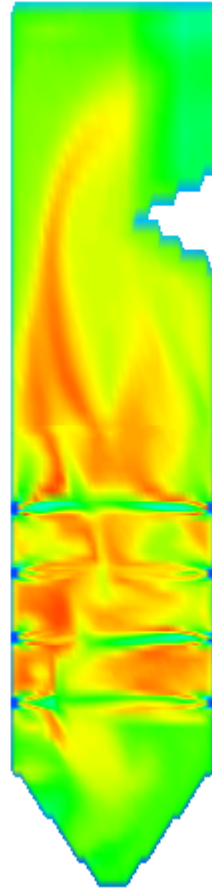
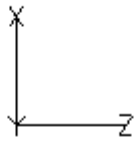


Figure 4.3.34 – O₂ Mole Fraction for O₂-Fired Case With OITM

O₂ Mole Fraction
O₂-Fired PC, 20% OFA

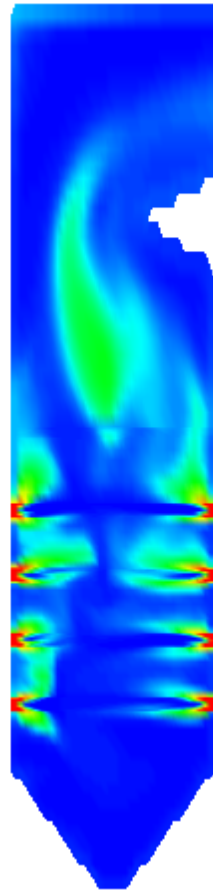
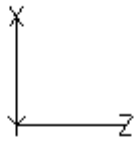
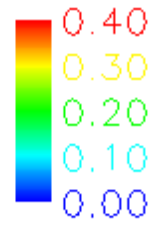


Figure 4.3.35 – Wall Heat Flux for O₂-Fired Case With OITM

Wall Heat Flux (Btu/hr-ft²)
O₂-Fired Case, 20% OFA

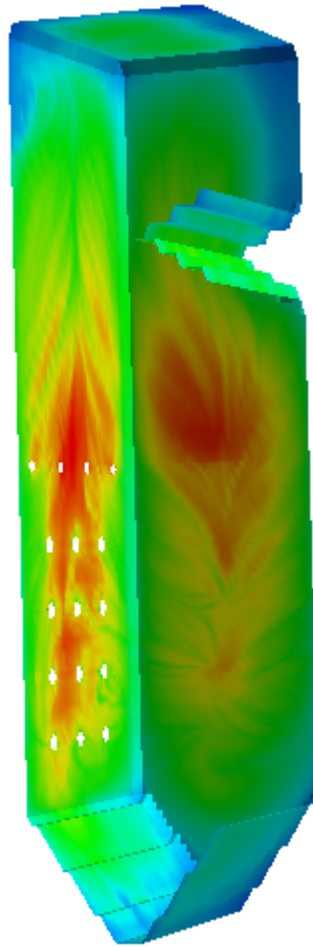
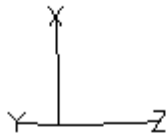
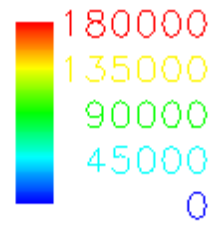


Figure 4.3.36 – Wall Temperature for O₂-Fired Case With OITM

Wall Temperature (F)
O₂-Fired Case, 20% OFA

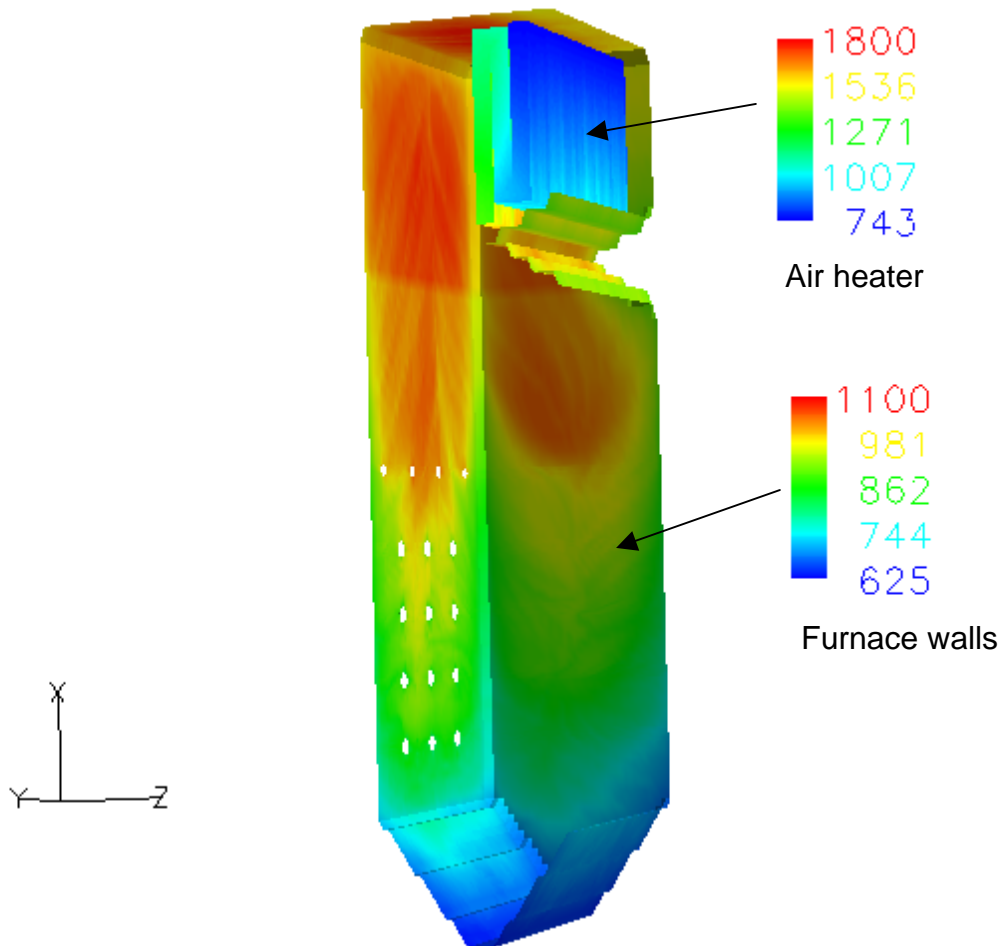


Figure 4.3.37 – Wall CO for O₂-Fired Case With OITM

CO Concentration
O₂-Fired Case, 20% OFA

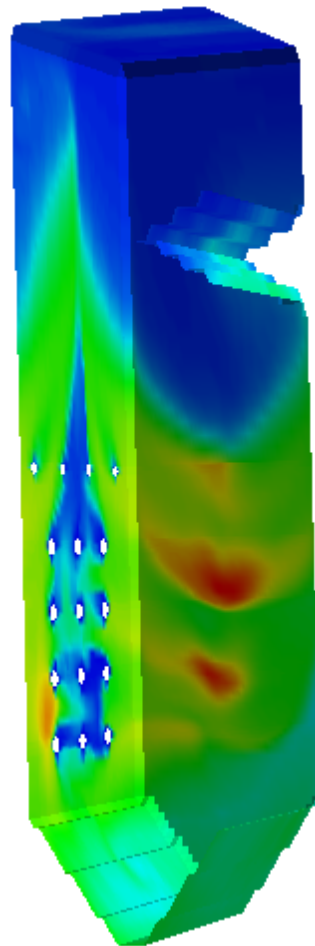
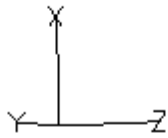


Figure 4.3.38 – Char Mass Fraction (69 micron) for O₂-Fired Case, OITM

Char Mass Fraction (69 micron)
O₂-Fired Case, 20% OFA



0.44
0.33
0.22
0.11
0.00

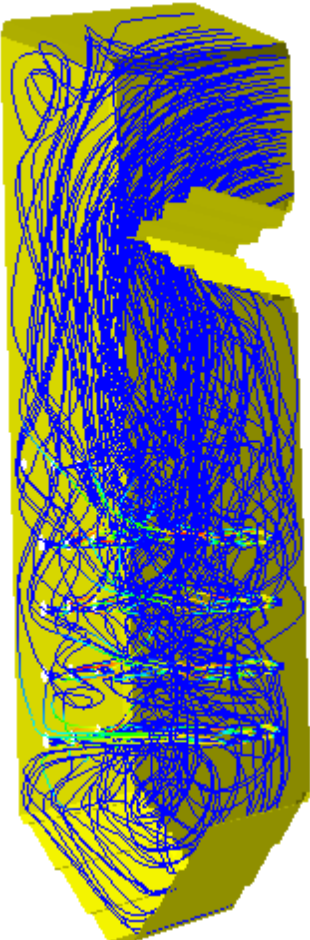
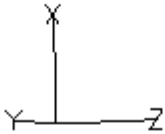
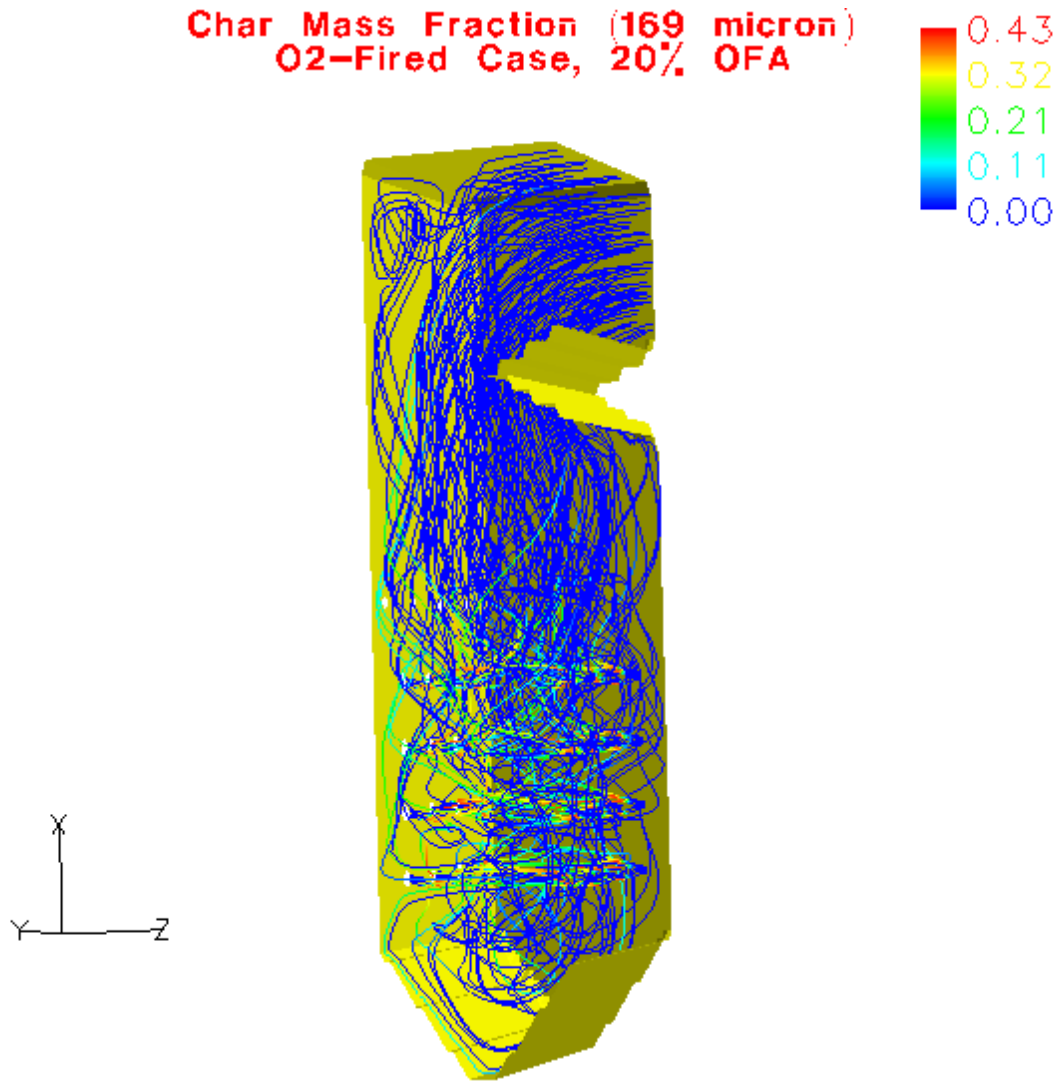


Figure 4.3.39 – Char Mass Fraction (169 micron) for O₂-Fired Case, OITM



4.3.3 Furnace Waterwall and Division Wall Design

The O₂-PC supercritical boiler incorporates the state-of-the-art once-through utility (OTU) BENSON Vertical technology, which uses low fluid mass flow rates in combination with optimized rifled tubing and offers the following advantages:

“Natural Circulation” Flow Characteristic: By designing for low mass flow rates that minimize frictional pressure losses, high heat flux tubes receive more flow to minimize temperature unbalances (see Figure 4.3.40).

Improved Heat Transfer Coefficient: By using optimized rifled tubing, departure from nucleate boiling (DNB) when operating near the critical pressure can be suppressed, even with relatively low fluid mass flow rates, and dryout can be prevented from occurring until steam qualities of greater than 90% are achieved. This lowers the wall temperature permitting the use of thinner wall less expensive materials (see Figure 4.3.41).

Simple Configuration: A standard, simple support system can be used to support the vertical tube panels so that interconnecting piping and headers between multiple passes are not required.

Low Pressure Losses: The low mass flow rates significantly reduce pressure loss, which reduces auxiliary power and therefore increases cycle efficiency. The boiler design pressure can also be lowered.

The furnace heat transfer tube design utilizing optimized rifled tubes is summarized in Figure 4.3.42.

4.3.3.1 Tube Wall Temperature and Pressure Loss

Thermal/hydraulic modeling of the waterwalls and division walls was performed using the Siemens computer program, Stade2 [12]. Stade2 creates a one-dimensional model of the tube panels to determine inside heat transfer, wall temperatures, and pressure loss and to perform linear dynamic and static stability analyses.

Stade2 models of the waterwalls and division walls were created and the average heat flux (Figure 4.3.31) and average mass flow were applied to establish the net pressure difference between the inlet and outlet headers. Models of the peak heat flux tubes were then created and Stade2 was used to determine the increased mass flow rate corresponding to the average pressure drop (due to the natural circulation characteristic of the optimized rifled tube geometry). For example, for the cryogenic O₂-PC design, the average heat flux and average mass flux (832 kg/m²-sec) produced a pressure loss of 33.7 psi. To match this pressure loss for the peak heat flux tube requires a mass flux of 966 kg/m²-sec (0.71 MM lb/ft²-hr). Due to the increased mass flow rate the maximum tube wall temperature of the peak heat flux tube is reduced. Figure 4.3.43 presents the

outside wall temperature of the peak heat flux waterwalls and division walls for the air-fired and O₂-fired designs.

Based on the maximum outside wall temperatures of Figure 4.3.43 the minimum tube wall thickness is computed using stress allowables from the ASME Boiler and Pressure Vessel Code as follows (design pressure = 5000 psi):

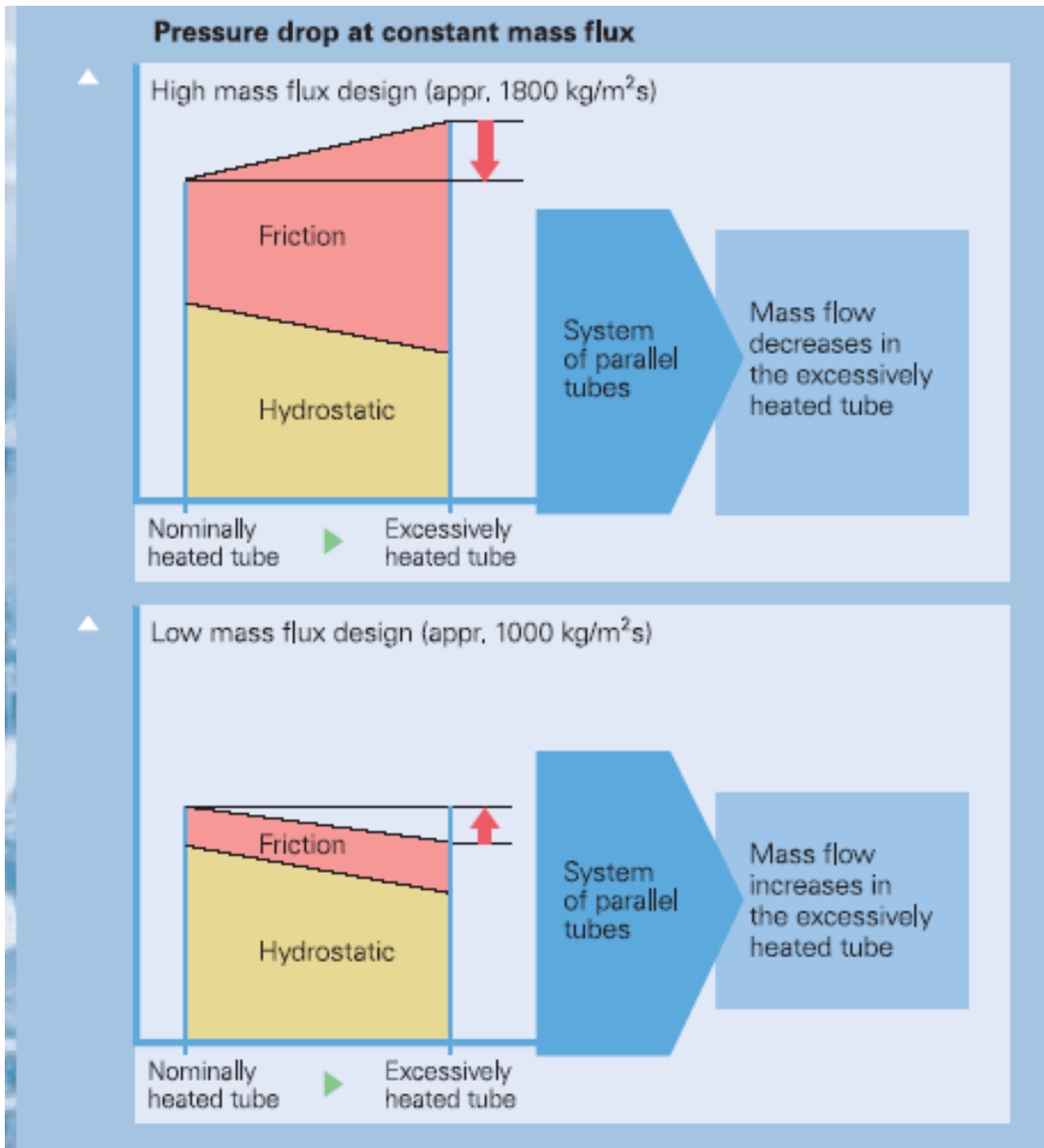
Air-Fired:	Material = SA-213-T2, min. wall thickness = 0.22"
O ₂ -Fired Cryo.:	Material = SA-213-T92, min. wall thickness = 0.20"
O ₂ -Fired OITM:	Material = SA-213-T92, min. wall thickness = 0.23"

4.3.3.2 Tube Panel Stability

The waterwall and division wall designs were determined by Stade2 to be statically and linearly dynamically stable at full and part loads (although the 25% load case appears to be near the dynamically unstable region). A more thorough treatment of dynamic stability was performed using the Siemens program, Dynastab [13]. Dynastab performs calculations for a single tube within a greater number of parallel tubes. The calculation starts from steady state and compares the flow behavior of a single tube, with slightly changed conditions (e.g. heat input, tube geometry), with the mean tubes of the heating surface. The mass flow of the single tube is stimulated by a distinct disturbance (e. g. global or local heating factor, inlet enthalpy), while pressure drop is kept constant. If this disturbance causes continuous oscillations, the tube is dynamically unstable; whereas if the disturbance results in a (new) steady state condition, the tube is dynamically stable.

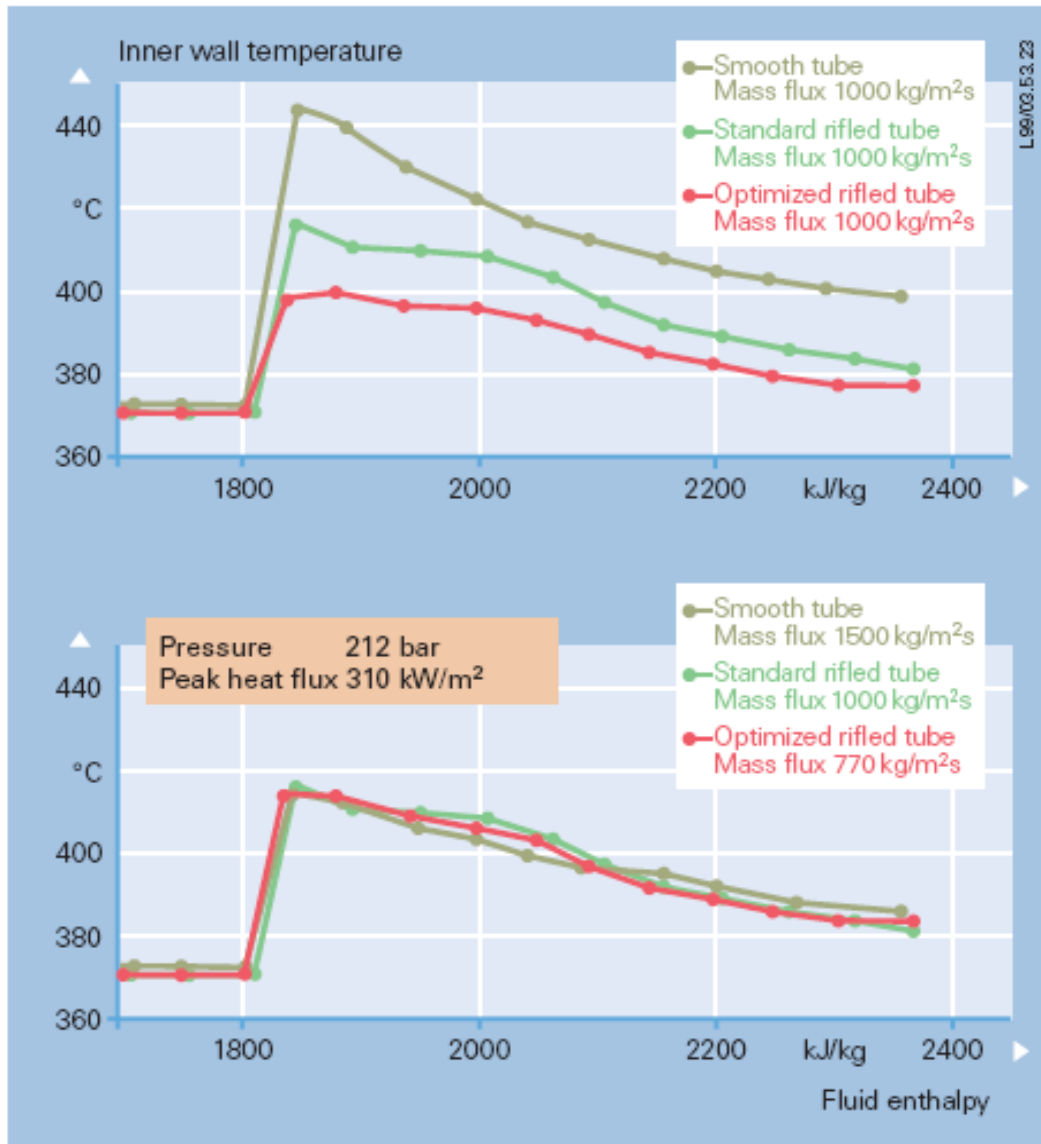
A 10% step increase in heat flux was applied to the single tube model. Figure 4.3.44 presents the transient results of inlet mass flow versus time (although a single tube was modeled the flow per entire furnace is presented). The 100% and 72% loads are stable, the 50% load is marginally stable, and the 25% load is unstable. To ensure stable operation at low loads, a pressure equalization header is added to the design at an elevation of 80' and the resultant dynamic stability response is shown in Figure 4.3.45. With the pressure equalization header all loads are dynamically stable.

Figure 4.3.40 – Advantage of Low Mass Flux Design



In the high mass flux design, mass flow through a tube with higher heat input decreases, while in the low mass flux design it increases,

Figure 4.3.41 – Tube Wall Temperature with Smooth, Standard Rifled, and Optimized Rifled Tubes



The outstanding heat transfer characteristics of the optimized rifled tube can be utilized to reduce either tube wall temperatures or mass fluxes in rifled tubes.

Figure 4.3.42 – Rifled Tube Design

		Air-Fired	O2 PC SC Cryogenic	O2 PC SC OITM
Material		SA-213-T2	SA-213-T92	SA-213-T92
OD	in	1.40	1.40	1.40
t _{wall}	in	0.22	0.20	0.23
ID	in	0.96	1.00	0.94
Pitch	in	2.00	2.00	2.00
Ligament	in	0.60	0.60	0.60
Ligament Width	in	0.25	0.25	0.25
Number of waterwall tubes		1218	888	888
Number of radiant superheater tubes		618	720	666
Number of ribs		6	6	6
Rib Height	in	0.048	0.050	0.048

Figure 4.3.43 – Outside Tube Wall Temperature with Peak Heat Flux

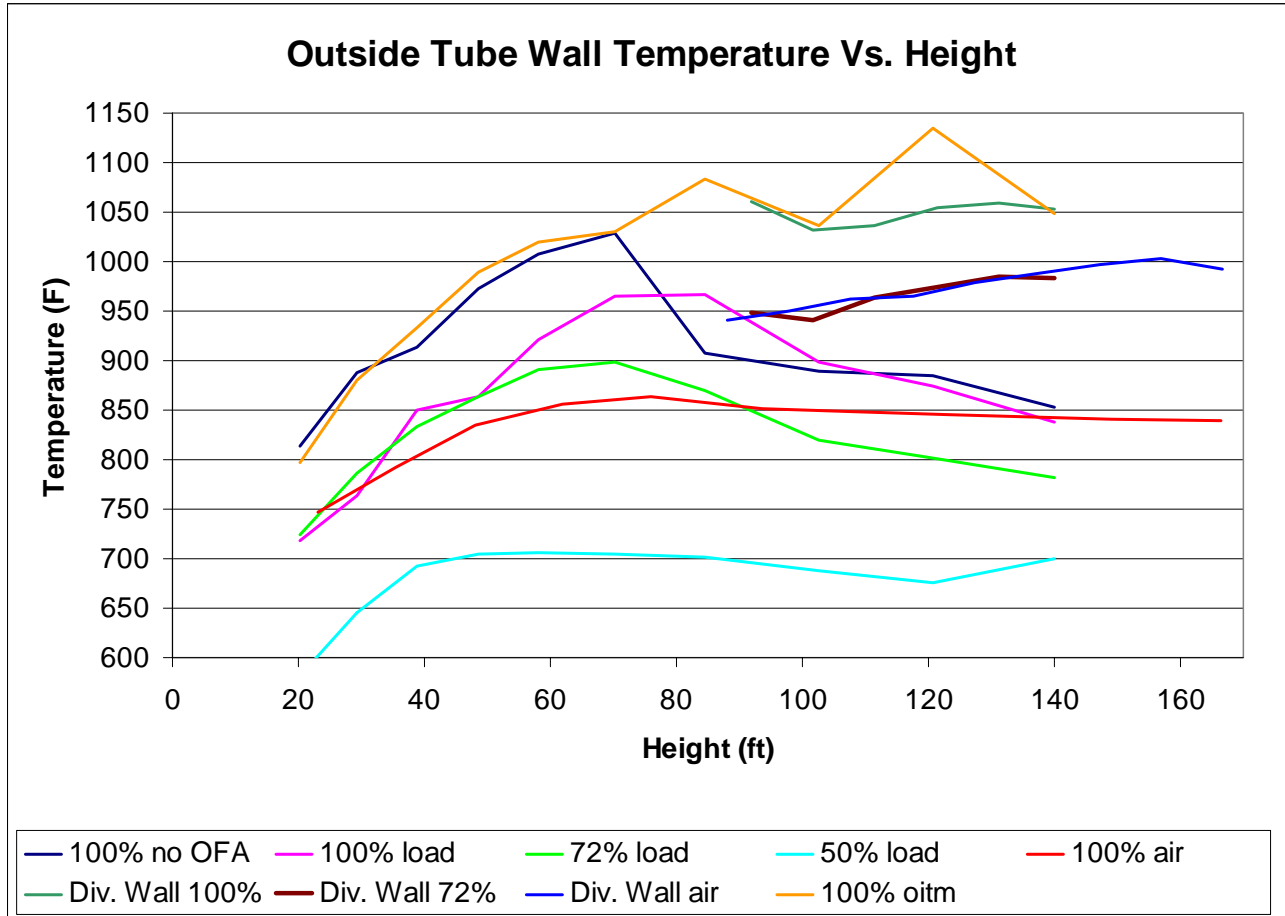


Figure 4.3.44 – Tube Inlet Mass Flow With a 10% Heat Flux Step Increase (No Pressure Equalization Header)

Flow Vs. Time: No Pressure Equalization Header

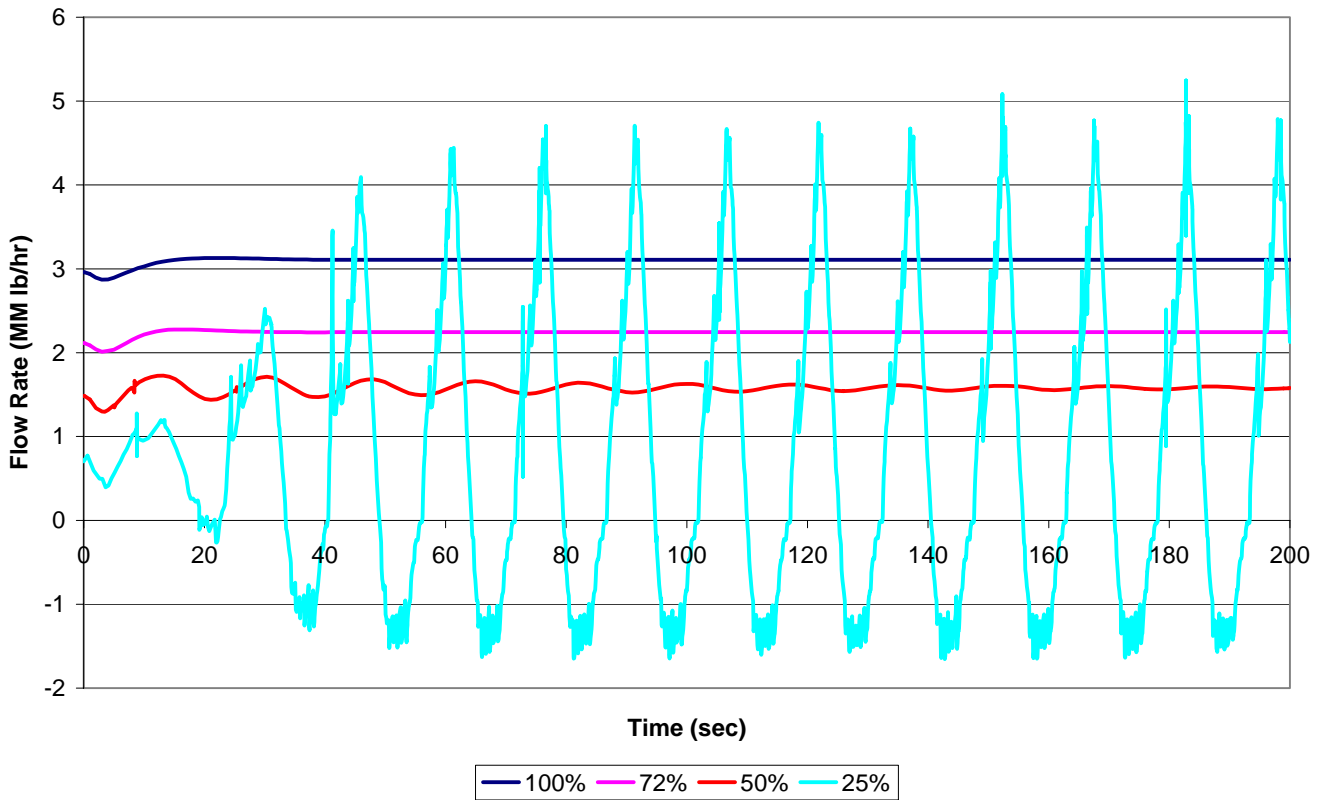
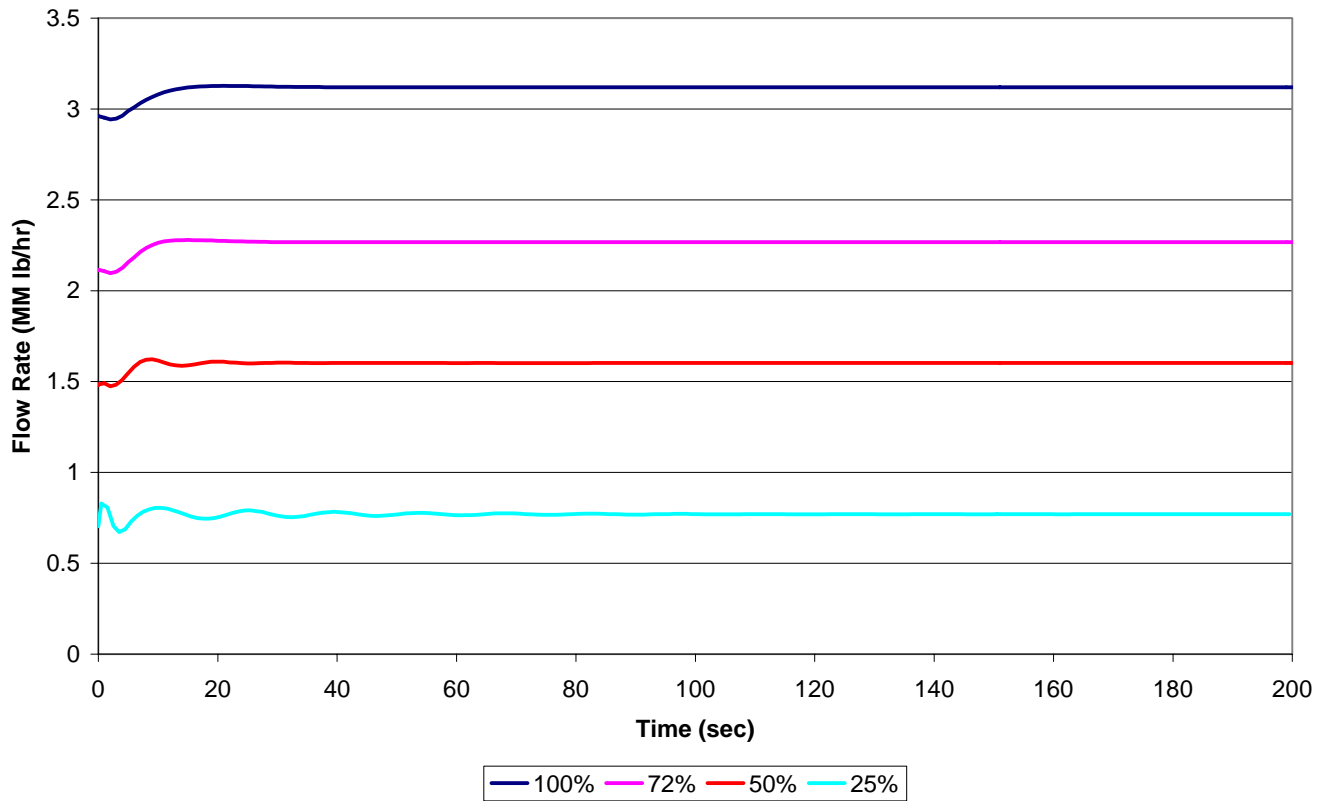


Figure 4.3.45 – Tube Inlet Mass Flow With a 10% Heat Flux Step Increase (With Pressure Equalization Header at 80')

Flow Vs. Time: With Pressure Equalization Header at 80'



4.3.4 Furnace Waterwall Corrosion

Waterwall corrosion is caused by sulfidation from a sub-stoichiometric gas containing H₂S and from deposits containing carbon and iron sulfide. Corrosion is especially significant at the high waterwall surface temperatures of a supercritical and ultra-supercritical boiler. In the O₂-PC without FGD, recycling of the flue gas will increase the H₂S concentration of the furnace by a factor of 1/(1 – recycle fraction). For example for a recycle flow rate of 55%, the H₂S concentration is increased by a factor of 2.2. An empirical EPRI formula was developed to predict the magnitude of waterwall corrosion due to the presence of H₂S as follows:

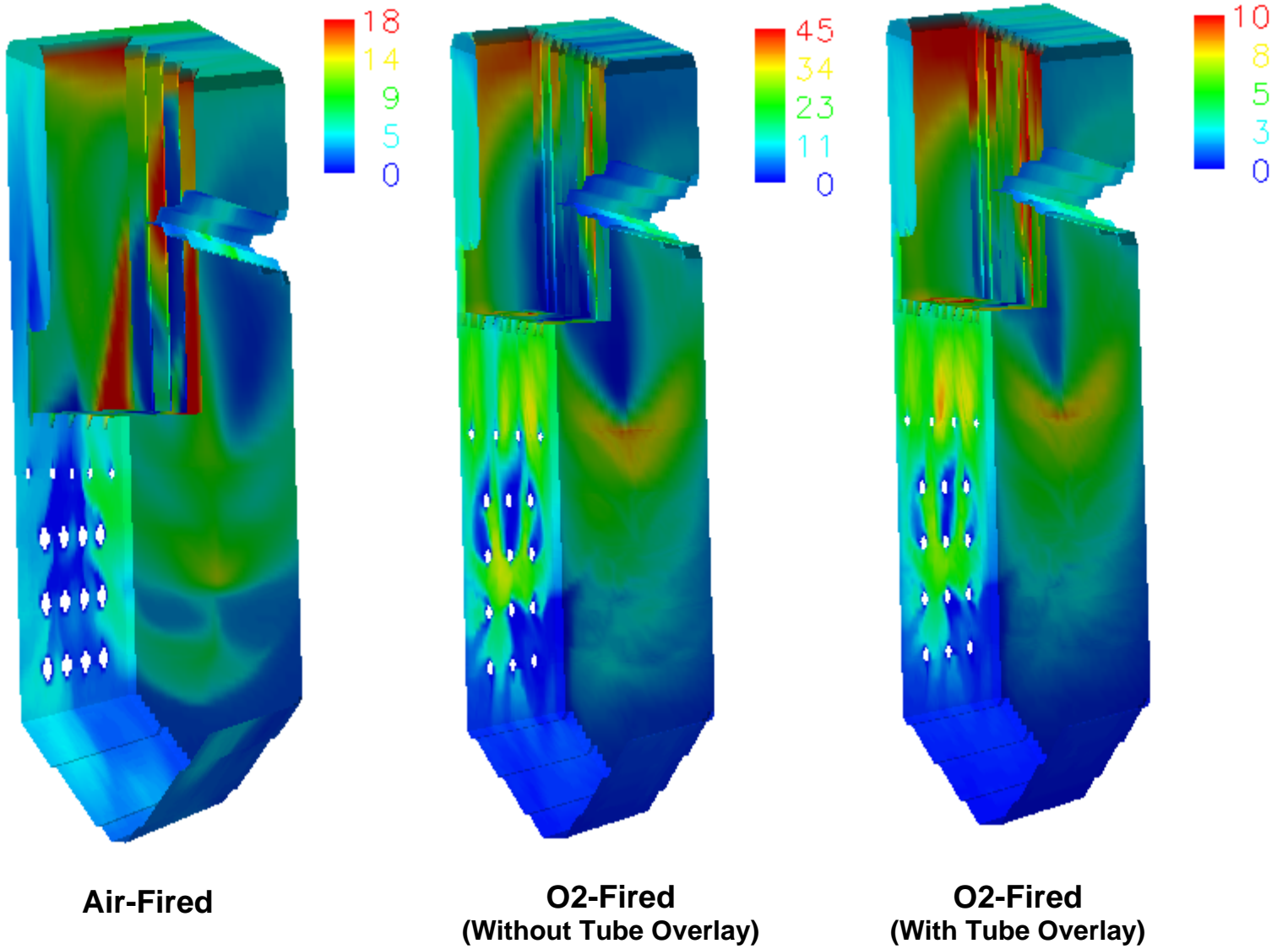
$$CR = 3.2 \times 10^5 \exp\left(-\frac{15818}{1.987T}\right) [H_{2S}]^{0.574} \frac{1}{(Cr\% + 10.5)^{1.234}} \quad (Cr \text{ wt}\% < 10)$$

$$CR = 1.04 \times 10^7 \exp\left(-\frac{19230}{1.987T}\right) [H_{2S}]^{0.29} \frac{1}{(Cr\% - 1.40)^{1.37}} \quad (Cr \text{ wt}\% > 16)$$

where, CR = corrosion rate (mil/year)
 T = metal temperature, K
 H₂S = H₂S flue gas concentration, ppm
 Cr% = Cr concentration of the metal

Figure 4.3.46 shows the predicted corrosion rate for the air-fired and O₂-fired cases. For the air-fired case the maximum corrosion on the waterwalls is 12 mil/yr and on the division walls is 18 mil/yr (maximum H₂S concentration is 1600 ppm). For the oxygen-fired case maximum corrosion on the waterwalls is 35 mil/yr and on the division walls is 45 mil/yr (maximum H₂S concentration is 5600 ppm). Note that for the O₂-fired case the corrosion is increased by the higher water wall temperature, higher concentration of H₂S, but is reduced by the higher chromium content of T92 vs. T2. To reduce the corrosion in the O₂-PC, weld overlays with high Nickel and Chromium contents are proposed. This will be much more cost-effective than adding an FGD system, which will be substantially more costly and reduce the corrosion by only a factor of 1.6 (by reducing the H₂S by a factor of 2.2). Applying alloy 622 (20% Cr) as a weld overlay significantly reduces the corrosion rate as shown in Figure 4.3.46 to less than 10 mil/yr. Note that other alternatives to weld overlays include upgrading the base tube metal and thermal spray coatings.

Figure 4.3.46 – Predicted Wall Corrosion (mil/yr) in Air-Fired and O₂-Fired Furnaces



4.3.5 Heat Recovery Area Design and Analysis

4.3.5.1 HEATEX Program Description

HEATEX [10] is a Foster Wheeler general-purpose program for thermal/hydraulic analysis of tube banks. The program performs heat transfer calculations on a local basis by dividing the tube bundle into a number of small heat transfer elements.

4.3.5.2 Air-Fired Reference Case

HEATEX was used to determine the heat recovery area (HRA) design of the convective tube banks between the furnace exit and the SCR/air heater. These tube banks include the finishing superheater, finishing reheater, primary superheater, primary reheater, upper economizer, and lower economizer. Flue gas exits the furnace at 2185°F and flows over the finishing superheater and finishing reheater tube bundles where it heats the main steam and reheat steam to 1083°F and 1113°F, respectively. The gas flow is then split into two parallel flows: one passing over the primary reheater and the other passing over the primary superheater and upper economizer. The gas split is controlled by dampers to achieve the proper reheater outlet temperature. Attemperating spray is used to control superheat temperature. The flue gas is combined downstream of the dampers and flows over the lower economizer, which receives water from the last feedwater heater stage. Flue gas exits the lower economizer at 720°F and is sent to the SCR and then to the air heater. Figure 4.1.1 presents the heat transfer requirements of the HRA banks. Figure 4.3.47 presents the corresponding design of the HRA banks. Total surface area of all convective banks is 335,025 ft². The performance of HRA tube banks is shown in Figure 4.3.48. The total heat transferred to the water/steam is 1431 MM Btu/hr as 3.59 MM lb/hr of flue gas is cooled from 2185°F to 720°F.

4.3.5.3 Oxygen-Fired Case, Cryogenic ASU

Due to the 40% lower flue gas flow rate of the cryogenic ASU oxygen-fired case versus the air-fired case, the cross sectional area of the HRA is reduced to maintain the same gas side velocity (and pressure drop). HEATEX was used to determine the heat recovery area design of the convective tube banks between the furnace exit and the gas recuperator. These tube banks include the finishing superheater, finishing reheater, primary reheater, and lower economizer. Flue gas exits the furnace at 2450°F and flows over the finishing superheater and finishing reheater tube bundles where it heats the main steam and reheat steam to 1083°F and 1113°F, respectively. Because of the reduced flue gas flow and lower HRA duty, the HRA is designed in series instead of parallel to produce a more compact design. After exiting the finishing reheater the flue gas flows over the primary reheater and then the lower economizer, which receives water from the last feedwater heater stage. Flue gas exits the lower economizer at 695°F and is sent to the gas recuperator.

Figure 4.1.9 presents the heat transfer requirements of the HRA banks. Figure 4.3.47 presents the corresponding design of the HRA banks. Total surface area of all convective banks is 218,693 ft². The performance of HRA tube banks is shown in Figure 4.3.48. The total heat transferred to the water/steam is 1151 MM Btu/hr as 2.12 MM lb/hr of flue gas is cooled from 2450°F to 695°F. The total heat transfer surface required in the oxygen-fired HRA is 35% less than the air-fired HRA due to the following main reasons:

1. More heat is absorbed in the oxygen-fired furnace (2089 MM Btu/hr) than the air-fired furnace (1751 MM Btu/hr) due to the higher adiabatic temperature and the greater specific heat of the oxygen-fired furnace flue gas. This requires less heat transfer duty in the HRA (as a consequence the upper economizer is not needed)
2. A higher heat transfer coefficient can be achieved in the oxygen-fired HRA than the air-fired HRA for the same flue gas pressure loss due to greater molecular weight (38 mol/lb-mol vs. 29 mol/lb-mol) of the oxygen-fired flue gas.

The HRA tube materials and wall thicknesses are nearly the same for the air-fired and oxygen-fired design (except for the finishing superheater where the 0.42" wall thickness of the air-fired case is increased to 0.46" for the oxygen-fired case) since the flue gas and water/steam temperature profiles encountered by the heat transfer banks are very similar.

4.3.5.4 Oxygen-Fired Case, OITM

Due to the 25% lower flue gas flow rate of the OITM oxygen-fired case versus the air-fired case, the cross sectional area of the HRA is reduced to maintain the same gas side velocity (and pressure drop). HEATEX was used to determine the heat recovery area design of the convective tube banks between the furnace exit and the gas recuperator. These tube banks include the finishing superheater, finishing reheater, primary superheater, primary reheater, upper economizer, and lower economizer. Flue gas exits the furnace at 2185°F and flows over the finishing superheater and finishing reheater tube bundles where it heats the main steam and reheat steam to 1083°F and 1113°F, respectively. The flue gas is then used to heat the air used for the OITM process. The gas flow is then split into two parallel flows: one passing over the primary reheater and the other passing over the primary superheater and upper economizer. The gas split is controlled by dampers to achieve the proper reheater outlet temperature. Attemperating spray is used to control superheat temperature. The flue gas is combined downstream of the dampers and flows over the lower economizer, which receives water from the last feedwater heater stage. Flue gas exits the lower economizer at 695°F and is sent to the gas recuperator.

Figure 4.2.10 presents the heat transfer requirements of the HRA banks. Figure 4.3.47 presents the corresponding design of the HRA banks. Total surface area of all

convective banks is 291,150 ft² (242,510 ft² without the air heater). The total heat transfer surface required in the oxygen-fired OITM HRA is 13% less than the air-fired HRA (28% less not including the air heater). The performance of HRA tube banks is shown in Figure 4.3.48. The total heat transferred to the water/steam is 1181 MM Btu/hr and to the air is 990 MMBtu/hr as 2.68 MM lb/hr of flue gas is cooled to 695°F. The total furnace + HRA heat transfer surface area for the OITM O₂-PC is 309,799 ft² as compared to 382,574 ft² for the air-fired PC and 252,002 ft² for the cryogenic ASU O₂-PC.

The HRA tube materials and wall thicknesses are nearly the same for the air-fired and OITM oxygen-fired design (except for the finishing superheater where the 0.42" wall thickness of the air-fired case is increased to 0.46" for the oxygen-fired case) since the flue gas and water/steam temperature profiles encountered by the heat transfer banks are very similar.

The air heater is constructed Incoloy MA956 which is an iron-chromium-aluminum alloy. Incoloy MA956 has been used in advanced gas turbine engines and is resistant to creep, oxidation, and corrosion at temperatures up to 2200°F. The furnace air heater is a three pass tubular design situated above the furnace nose to reduce radiation and maximum metal temperature. Air is heated from 745 to 1650°F as the flue gas is cooled from 2950 to 2185°F. Maximum metal temperature is approximately 1900°F.

Figure 4.3.47 – HRA Tube Bank Design

		Air-Fired	O2 PC SC Cryogenic	O2 PC SC OITM
<u>Air Heater</u>				
Length	ft			28.0
No. of Tubes Deep				42
No. of Tubes Wide				79
Total Number of Tubes				3,318
Tube Outside Diameter	in			2.000
Tube Thickness	in			0.06
Tube Material				MA956
Design Pressure	psi			250
Design Temperature	F			2000
Stress Allowable	psi			8200
Min. Wall	in			0.040
Total Surface Area	ft2			48,640
<u>Finishing Superheater</u>				
Length	ft	36.0	24.0	24.0
No. of Tubes Deep		44	56	40
No. of Tubes Wide		30	32	32
Total Number of Tubes		1,320	1,792	1,280
Tube Outside Diameter	in	2.000	2.000	2.000
Tube Thickness	in	0.42	0.47	0.47
Tube Material		SA-213-T92	SA-213-T92	SA-213-T92
Design Pressure	psi	5000	5000	5000
Design Temperature	F	1150	1180	1180
Stress Allowable	psi	10200	8379	8379
Min. Wall	in	0.414	0.470	0.470
Total Surface Area	ft2	26,539	24,021	17,152
<u>Vertical Reheater</u>				
Length	ft	30.5	20.0	20.0
No. of Tubes Deep		40	72	60
No. of Tubes Wide		63	51	51
Total Number of Tubes		2,520	3,672	3,060
Tube Outside Diameter	in	2.250	2.250	2.250
Tube Thickness	in	0.165	0.165	0.165
Tube Material		SA-213-T92	SA-213-T92	SA-213-T92
Design Pressure	psi	1000	1000	1000
Design Temperature	F	1200	1200	1200
Stress Allowable	psi	7990	7330	6730
Min. Wall	in	0.173	0.173	0.173
Total Surface Area	ft2	45,270	43,260	36,050
<u>Primary Superheater</u>				
Length	ft	17.0		9.5
No. of Tubes Deep	0	96		64
No. of Tubes Wide	0	63		90
Total Number of Tubes	0	6,048		5,760
Tube Outside Diameter	in	2.250		2.250
Tube Thickness	in	0.42		0.42
Tube Material		SA-213-T2		SA-213-T2
Design Pressure	psi	5000		5000
Design Temperature	F	925		925
Stress Allowable	psi	11550		11550
Min. Wall	in	0.412		0.412
Total Surface Area	ft2	63,252		33,662

Figure 4.49 – HRA Tube Bank Design (Continued)

		Air-Fired	O2 PC SC Cryogenic	O2 PC SC OITM
<u>Horizontal Reheater</u>				
Length	ft	17.0	24.0	21.0
No. of Tubes Deep		70	75	75
No. of Tubes Wide		125	90	90
Total Number of Tubes		8,750	6,750	6,750
Tube Outside Diameter	in	2.250	2.250	2.250
Tube Thickness	in	0.165	0.165	0.165
Tube Material		SA-213-T2	SA-213-T2	SA-213-T2
Design Pressure	psi	1000	1000	1000
Design Temperature	F	950	950	950
Stress Allowable	psi	9200	9200	9200
Min. Wall	in	0.127	0.127	0.127
Total Surface Area	ft2	93,461	101,792	89,067
<u>Upper Economizer</u>				
Length	ft	17.0	0.0	9.5
No. of Tubes Deep		30	0	36
No. of Tubes Wide		126	0	90
Total Number of Tubes		3,780	0	3,240
Tube Outside Diameter	in	2.250	0.000	2.250
Tube Thickness	in	0.34	0	0.32
Tube Material		SA-210-A1	0	SA-210-A1
Design Pressure	psi	5000	0	5000
Design Temperature	F	700	0	650
Stress Allowable	psi	15600	0	17100
Min. Wall	in	0.322	0	0.298
Total Surface Area	ft2	40,373	0	19,339
<u>Lower Economizer</u>				
Length	ft	27.0	24.0	27.0
No. of Tubes Deep		33	39	33
No. of Tubes Wide		126	90	90
Total Number of Tubes		4,158	3,510	2,970
Tube Outside Diameter	in	2.250	2.250	2.250
Tube Thickness	in	0.32	0.32	0.32
Tube Material		SA-210-A1	SA-210-A1	SA-210-A1
Design Pressure	psi	5000	5000	5000
Design Temperature	F	650	650	650
Stress Allowable	psi	17100	17100	17100
Min. Wall	in	0.298	0.298	0.298
Total Surface Area	ft2	66,130	49,620	47,240
Total HRA Surface Area	ft2	335,025	218,693	291,150
Total Furnace + HRA Surface Area	ft2	382,574	252,002	309,799

Figure 4.3.48 – HRA Tube Bank Performance

	Bank	Surface Area (ft ²)	Heat Trans. Coeff. (Btu/hr-ft ² -F)	Mean Temp. Diff. (F)	Heat Transfer (MM Btu/hr)	Gas Press. Drop (in H ₂ O)
O2 PC OITM	Air Heater	48,640	17.1	1189	990	0.38
Air PC	Finishing Superheater	26,539	11.4	1038	315	0.12
O2 PC	Finishing Superheater	24,021	14.7	1173	414	0.19
O2 PC OITM	Finishing Superheater	17,157	16.0	1026	281	0.20
Air PC	Primary Superheater	63,252	8.6	356	194	0.29
O2 PC	Primary Superheater	0				0.00
O2 PC OITM	Primary Superheater	33,662	11.2	268	101	0.44
Air PC	Finishing Reheater	45,270	10.2	722	333	0.18
O2 PC	Finishing Reheater	43,260	12.2	629	331	0.35
O2 PC OITM	Finishing Reheater	36,050	14.1	658	334	0.47
Air PC	Primary Reheater	93,461	9.1	402	341	0.47
O2 PC	Primary Reheater	101,792	10.8	290	320	0.58
O2 PC OITM	Primary Reheater	89,067	10.9	353	342	0.55
Air PC	Upper Economizer	40,373	7.5	367	111	0.20
O2 PC	Upper Economizer	0				0.00
O2 PC OITM	Upper Economizer	19,339	15.6	367	111	0.19
Air PC	Lower Economizer	66,130	9.9	196	128	0.35
O2 PC	Lower Economizer	49,620	9.8	177	86	0.27
O2 PC OITM	Lower Economizer	47,240	10.4	165	81	0.28
Air PC	Total	335,025			1431	1.61
O2 PC	Total	218,693			1151	1.39
O2 PC OITM	Total	291,155			2171	2.51

4.4 Economic Analysis

Economic analysis was performed for three cases: air-fired (reference), O₂-fired with cryogenic ASU, and O₂-fired with OITM. Economic analysis was not performed for the O₂-fired PC with CAR since detailed cost information on the CAR process was not available in the literature nor was it provided by the vendor (BOC).

4.4.1 Main Assumptions

The economic analysis was performed based on the DOE/NETL guidelines [14] using the EPRI Technical Assessment Guide (TAG) methodology. Plant capital costs were compiled under the Code of Accounts developed by EPRI.

The estimate basis and major assumptions are listed below:

- Total plant costs were estimated in January 2006 dollars.
- Plant book life was assumed to be 20 years.
- The net power output of the reference air-fired plant is 430.2 MWe versus 347.0 MWe for the ASU oxygen-based plant and 463.3 MWe for the OITM oxygen-based plant.
- The plants operate with a capacity factor of 85 per cent (Plant operates at 100 per cent load 85 per cent of the time).
- Cost of electricity (COE) was determined on a levelized constant dollar basis.
- Average annual ambient air conditions for material balances, thermal efficiencies and other performance related parameters are at a dry bulb temperature of 60°F and an air pressure of 14.7 psia.
- The coal is 2.5 per cent sulfur Illinois #6 coal (see Table 4.4.1 for analysis).
- Design CO₂ effluent purity is presented in Table 4.4.2
- Terms used are consistent with the EPRI TAG.

Economic study assumptions are detailed in Table 4.4.3.

Table 4.4.1 - Coal Properties

Illinois No. 6 Coal		
C	%	63.75%
H	%	4.50%
O	%	6.88%
N	%	1.25%
Cl	%	0.29%
S	%	2.51%
Ash	%	9.70%
H2O	%	11.12%
Total	%	100.00%
LHV	Btu/lb	11,283
HHV	Btu/lb	11,631

Table 4.4.2 - CO₂ Effluent Purity Design Conditions

Constituent	Units	Value
N2	vppm	< 300
H2O	vppm	< 20
O2	vppm	< 50

Table 4.4.3 – Economic Study Assumptions

GENERAL DATA/CHARACTERISTICS

Levelized Capacity Factor / Preproduction (equivalent months):	85%	
Capital Cost Year Dollars (Reference Year Dollars):	2006 (January)	
Design/ Construction Period:	4 years	
Plant Start-up Date (1st year Dollars):	2010 (January)	
Land Area/Unit Cost:	100 acres	\$1,600 / Acre

FINANCIAL CRITERIA

Project Book Life:	20 years
Book Salvage Value:	0 %
Project Tax Life:	20 years
Tax Depreciation Method:	Accel. Based on ACRS Class
Inflation Rate	3.0 %
Property Tax Rate:	1.0 %
Insurance Tax Rate:	1.0 %
Federal Income Tax Rate:	35.0 %
State Income Tax Rate:	4.0 %
Investment Tax Credit/% Eligible	0 %

Economic Basis: Over Book Constant Dollars

Capital Structure	<u>% of Total</u>	<u>Cost (%)</u>
Common Equity	20	12
Preferred Stock	0	
Debt	80	6.5
Weighted Cost of Capital: (after tax)		5.57%

Coal Price Escalation Rate 3.0% (same as general escalation)

Total Capital Requirement

Initial Chemical Inventory 30 days

Startup Costs

2% TPI
30 days of fuel and chemicals
labor and miscellaneous items

Spare Parts

0.5% TPC

Working Capital

30 days fuel and consumables
30 days direct expenses

Consumable Costs

Coal, \$/MMBtu	\$1.34
Limestone, \$/ton	\$15.00
Water, \$/kgal	\$1.00
Water Treatment Chemicals, \$/kgal	\$0.50
Ash/Slag Disposal, \$/ton	\$10.00

Plant Labor

Operating labor

Labor Rate 42.25 \$/hr (includes labor burden)
personnel 14 per shift
Supervisory/clerical 30% of operating + maintenance labor cost

Maintenance Costs

Labor 0.88% TPC
Materials 1.32% TPC

4.4.2 Plant Cost Basis

For each of the plants, heat and material balances (Aspen simulations) were prepared that identified the flow rates and operating conditions of all major flow streams (Sect. 4.1 and Sect. 4.2). These balances also identified each boiler's operating requirements and enabled design calculations to be performed that established the overall boiler dimensions, tube surface areas, materials of construction, weights, and auxiliary equipment requirements. With this information defined, the cost of each boiler, which together with its auxiliary equipment constitutes the plant "boiler island", was determined from Foster Wheeler's cost estimating database.

4.4.2.1 Air-Fired Reference Plant Cost

In [15] Parsons presents a conceptual design of a supercritical pressure PC plant with a net power output of 550.2 MWe. Similar to the air-fired reference plant of this study, the Parsons plant burned 2.5 per cent sulfur Illinois No. 6 coal with air and, to control emissions, the boiler was provided with low NO_x burners, SCR, wet flue gas desulfurization, and a baghouse filter. A detailed EPRI TAG cost estimate of the plant totaled \$745.7 million or \$1355/kW in year 2006 dollars and was broken down into 14 accounts, one of which (Account 4 entitled, "PC Boiler and Accessories") included the cost of the PC boiler and its auxiliaries. Since the primary difference between the Parsons and the FW air-fired reference plant is size, the Parsons balance of plant costs (excluding the boiler island) were scaled down on an account-by-account basis to obtain the reference plant balance of plant costs. As recommended in [16] a scaling exponent of 0.65 applied to flow rate/output was used and a small adjustment to the PC plant's feedwater and steam turbine accounts was made for the slightly higher operating pressure. Boiler island costs were estimated directly by FW based on designs generated in Task 3 (Sect. 4.3). To validate the scaling process, Parsons Account 4 boiler costs were scaled down and determined to be within 6 per cent of Foster Wheeler's directly estimated costs. The results of the scaling, together with Foster Wheeler's determined Account 4 (boiler island) costs, yielded a total plant cost of \$633.0 million or \$1471/kW for the 430.2 MWe reference plant. The account-by-account costs of the air-fired reference plant (case-1, Figure 4.1.1) are presented in Table 4.4.4.

The total plant cost (TPC), also referred to as the plant capital cost is comprised of the following elements:

1. Bare erected plant cost (includes equipment supply and erection)
2. Architect engineering, construction management, and fee
3. Project and process contingencies

The reference plant estimate uses the same erection factors, fees, and contingencies as the Parsons plant estimate (i.e. boiler erection at 80 per cent of equipment supply costs, architect engineering/construction management/home office/fees at 10 per cent

of bare erected costs, and contingency, totaling 10 per cent, applied to the sum of items 1 and 2).

4.4.2.2 Oxygen Based PC Plant Costs

In [7] Parsons presents conceptual designs of two plants that burned 2.5 per cent sulfur Illinois No. 6 coal with oxygen to facilitate CO₂ capture/removal for pipeline transport to a sequestering site. Both plants used flue gas recirculation to control their boiler combustion temperatures and their CO₂ rich exhaust gases were dried and compressed for pipeline transport.

The first plant had a net power output of 132.2 MWe; its oxygen was supplied by a conventional, cryogenic ASU, and the gas flow to the CO₂ processing unit totaled 422.3 Klb/hr. The oxygen was 99 per cent pure and it was delivered to an “air heater” at the boiler where 660°F flue gas heated the oxygen to 610°F for delivery to the boiler at a rate of 327.1 Klb/hr. In the FW study’s ASU based plant, the oxygen from the ASU is also heated by an “air heater” at the boiler but to 625°F with 695°F flue gas; aside from some slight temperature differences, the plant arrangements are similar and their ASUs differ primarily in size/through put.

The second Parsons plant had a net output of 197.4 MWe; its oxygen was supplied at a rate of 398.8 Klb/hr by an ion transport membrane, and the gas flow to CO₂ processing was 515.8 Klb/hr. The OITM operated with 200 psia air that was heated to 1652°F via heat transfer surface placed in the boiler; the hot air was then delivered to the OITM for separation of the oxygen and nitrogen. The oxygen, with a purity of 100 per cent, was then delivered to the boiler, whereas, the nitrogen was passed through a hot gas expander followed by a heat recovery steam generator for power recovery. Excepting for differences in flow rates, the operating conditions of the Parsons OITM plant are essentially identical to the OITM based plant of the FW study.

Praxair Inc, a developer of oxygen transport membranes, participated in the detailed Alstom/Parsons study [7] and, per the Acknowledgement section of their study report, provided detailed design, performance, and cost information on the OITM system. Aside from a difference in flow rate, the FW OITM operates at essentially the same pressure and temperature as that used in the Alstom/Parsons study and, hence, the FW system cost estimate was obtained by scaling their system capital costs. Consequently, individual OITM component designs were not developed in the FW study. It is assumed that Parsons/Praxair selected the operating conditions of the OITM to minimize the overall system cost. Such a sensitivity/optimization cost evaluation of the OITM plant design is beyond the scope of the FW study. Note that there are several variables, which have direct influence on the OITM plant cost and performance (see Sect. 4.2.2.3 for more details). These variables include

O₂ Recovery Percentage: CO₂ removal power penalty is minimum at an O₂ recovery of 85% (The Alstom/Parsons study uses a O₂ recovery of 85%).

Air Pressure: Increasing air pressure reduces OITM size, but also reduces system efficiency. Optimum pressure depends on the relative cost of the OITM.

OITM Temperature: Increasing OITM operating temperature will increase system efficiency, but will increase boiler air heater cost and presumably OITM cost.

A detailed 14 account EPRI TAG cost estimate in year 2003 dollars was prepared by Parsons for each of the two plants; in these estimates the oxygen (ASU or OITM) and CO₂ processing system costs appear, respectively, as separate sub-accounts under the Boiler and Accessories and Flue Gas Clean Up Accounts. Since the arrangement and scope of supply of these systems is essentially identical to that of the FW study's O₂-fired plants, the Parsons costs were used to estimate the costs of Foster Wheeler's two plants. The Parsons ASU system costs were scaled up based on oxygen flow rate raised to the 0.65 exponent and escalated to year 2006 dollars; comparison of the scaled up costs with a vendor supplied budget price yielded good agreement further validating the scale up exponent. Comparison of the gas processing system costs given for Parsons' two plants, however, revealed a greater sensitivity to flow rate and resulted in a scaling exponent of 0.87; this exponent was then used to calculate the CO₂ gas processing system costs of Foster Wheeler's plants.

The Table 4.4.4 air-fired reference plant cost estimate served as a starting point for the determination of O₂ based plant costs. The cost of the air-fired PC boiler package was removed from the Parsons cost estimate and the new value, determined by Foster Wheeler for the particular plant configuration under study, was inserted. Then each balance of plant account and or component was individually scaled based on flow rate/output and adjusted, where necessary, to reflect design differences. Some examples of the changes that were made are removal of SCR systems, limestone systems, flue gas desulfurization systems, etc. and elimination of the stack from the ASU based plant.

Table 4.4.5 and Table 4.4.6 present a detailed cost breakdown of the ASU based O₂ plant (case-9B, Figure 4.1.9) and the OITM based O₂-PC plant (case-18, Figure 4.2.10) and Table 4.4.7 compares the total costs of all three plants. Although the oxygen-based plants use flue gas recirculation to control the boiler combustion temperature, they operate with higher oxygen concentrations than the air-fired reference plant boiler. As a result they produce a higher combustion temperature and a lower flue gas flow rate, which reduce the size of the boiler and its downstream flue gas components. With the SCR eliminated and the flue gas flow rate reduced, the PC boiler cost of the ASU based plant is about \$32 million less than that of the air-fired case. Despite additional savings associated with elimination of some systems/components (e.g. SCR, limestone, FGD, and stack plus a reduction in size of other components, i.e. baghouse filter, ducting, foundations, etc.), the total cost of the cryogenic ASU based plant is approximately \$91 million higher than the air-fired plant because of the high cost of the ASU (\$115.0 million) and CO₂ processing systems (\$111.5 million).

In the OITM based plant, the PC boiler not only meets the steam generation and heating needs of the steam cycle, but it also contains tubing that heats air to 1600°F for delivery to the OITM. Although the boiler flue gas flow rate of the OITM based plant is about 25 per cent less than the air-fired plant, the cost savings it provides is more than negated by the high cost of the air heater tubing; as a result, the OITM based PC boiler costs \$18 million more than that of the air-fired plant. The compressor required to pressurize OITM air to 200 psia, the OITM, the OITM associated heat exchangers and piping, the OITM power recovery system (hot gas expander and HRSG), and a larger CO₂ gas processing system add additional costs to the plant; as a result, the OITM plant costs approximately 50 per cent more than the air-fired reference plant (\$953.0 million versus \$633.0 million) and approximately 32 per cent more than the cryogenic ASU based plant (\$953.0 million versus \$723.3 million). Since the OITM based plant operates with a higher electrical output than the cryogenic ASU based plant (463.3 MWe versus 347.0 MWe), its total plant costs on a dollar per kilowatt basis are slightly lower (\$2,057/kW versus \$2,084/kW) but much higher than the air-fired plant (\$2,057/kW versus \$1,471/kW).

Table 4.4.4 - Cost of 430.2 MWe Air-Fired Supercritical PC Plant (\$1000 Yr 2006)

Account #	Account Title	Bare Erected Costs	Engr, C.M. H.O. & Fee at 10%	Contingency at 10%	Total Plant Costs
1	Coal & Sorbent Handling				
	Coal	12,985	1,299	1,428	15,712
	Limestone	3,114	311	343	3,768
2	Coal and Sorbent Prep & Feed				
	Coal	2,599	260	286	3,145
	Limestone	6,934	693	763	8,390
3	Feedwater & Misc BOP Systems	47,879	4,788	5,267	57,933
4	Boiler and Accessories				
	Boiler with SCR, Air Heater, Fans, Ducts, etc Oxygen Supply; None	155,621	15,562	17,118	188,301 0
5	Flue Gas Clean Up				
	Baghouse & Accessories	17,111	1,711	1,882	20,705
	FGD	58,705	5,871	6,458	71,033
	CO2 Processing	0	0	0	0
6	Combustion Turbine & Accessories				0
7	HRS&G, Ducting, & Stack				
	Duct Work	9,094	909	1,000	11,004
	Stack	9,774	977	1,075	11,827
	Foundations	1,456	146	160	1,762
8	Steam Turbine Generator	88,706	8,871	9,758	107,334
9	Cooling Water System	24,540	2,454	2,699	29,693
10	Slag/Ash Handling Systems	7,746	775	852	9,373
11	Accessory Electric Plant	27,500	2,750	3,025	33,275
12	Instrumentation & Control	12,237	1,224	1,346	14,807
13	Improvements to Site	7,773	777	855	9,405
14	Buildings & Structures	29,353	2,935	3,229	35,517
	Totals	523,126	52,313	57,544	632,984
	\$/kW				1,471

Table 4.4.5 - Cost of 347.0 MWe ASU Based Supercritical PC Plant (\$1000 Yr 2006)

Account #	Account Title	Bare Erected Costs	Engr, C.M. H.O. & Fee at 10%	Contingency at 10%	Total Plant Costs
1	Coal Handling	12,692	1,269	1,396	15,357
2	Coal Prep & Feed	2,540	254	279	3,074
3	Feedwater & Misc BOP Systems	47,879	4,788	5,267	57,933
4	Boiler and Accessories Boiler with Air Heater, Fans, Ducts, etc Oxygen Supply: ASU	129,052	12,905	14,196	156,153 115,005 *
5	Flue Gas Clean Up Baghouse & Accessories FGD CO2 Processing	12,102	1,210	1,331	14,643 0 111,493 *
6	Combustion Turbine & Accessories				0
7	HRSG, Ducting, & Stack Duct Work and Foundations Stack HRSG	6,432	643	707	7,782 0 0
8	Steam Turbine Generator	88,706	8,871	9,758	107,334
9	Cooling Water System	25,966	2,597	2,856	31,419
10	Slag/Ash Handling Systems	7,281	728	801	8,810
11	Accessory Electric Plant	27,885	2,789	3,067	33,741
12	Instrumentation & Control	12,408	1,241	1,365	15,014
13	Improvements to Site	7,882	788	867	9,537
14	Buildings & Structures	29,764	2,976	3,274	36,014
	Totals		41,059	45,165	723,310
	\$/kW				2,084

*Values Scaled from Parsons /Alstom Year 2003 Study and Escalated to 2006 at 5% per Year

**Table 4.4.6 - Cost of 463.3 MWe OITM Based Supercritical PC Plant (\$1000
Yr 2006)**

Account #	Account Title	Bare Erected Costs	Engr, C.M. H.O. & Fee at 10%	Contingency at 10%	Total Plant Costs
1	Coal Handling	14,434	1,443	1,588	17,465
2	Coal Prep & Feed	2,889	289	318	3,496
3	Feedwater & Misc BOP Systems	47,879	4,788	5,267	57,933
4	Boiler and Accessories				
	Boiler, Air Heater, Fans, Ducts, etc	170,902	17,090	18,799	206,791
	Oxygen Supply: OTM				188,031 *
5	Flue Gas Clean Up				
	Baghouse & Accessories	14,113	1,411	1,552	17,077
	FGD				0
	CO2 Processing				131,662 *
6	Combustion Turbine & Accessories				48,627 *
7	HRSO, Ducting, & Stack				
	Duct Work	7,501	750	825	9,076
	Stack				2,680 *
	Foundations				205 *
	HRSO				18,420 *
8	Steam Turbine Generator	88,706	8,871	9,758	107,334
9	Cooling Water System	29,489	2,949	3,244	35,682
10	Slag/Ash Handling Systems	8,344	834	918	10,097
11	Accessory Electric Plant	29,101	2,910	3,201	35,212
12	Instrumentation & Control	12,949	1,295	1,424	15,668
13	Improvements to Site	8,225	823	905	9,953
14	Buildings & Structures	31,061	3,106	3,417	37,584
	Totals		46,559	51,215	952,993
	\$/kW				2,057

*Values Scaled from Parsons /Alstom Year 2003 Study and Escalated to 2006 at 5% per Year

Table 4.4.7 - Comparison of Total Plant Costs (\$1000 Yr 2006)

	Reference Air-Fired Plant	ASU Based Plant	OITM Based Plant
Net Power Output, MWe	430.2	347.0	463.3
Flow Rates, Klb/hr			
Coal	319.0	308.0	375.4
Limestone	26.0	0.0	0.0
Ash	33.0	30.0	37.0
Boiler Flue Gas	3556.0	2087.0	2644.0
Gas to CO2 Processing	0.0	774.0	936.0
Condenser Duty, MMBtu/hr	1696.0	1850.0	2250.0

Account #	Account Title	Plant Costs by Account		
1	Coal and Limestone Handling			
	Coal	15,712	15,357	17,465
	Limestone	3,768	0	0
2	Coal and Limestone Prep & Feed			
	Coal	3,145	3,074	3,496
	Limestone	8,390	0	0
3	Feedwater & Misc BOP Systems	57,933	57,933	57,933
4	Boiler and Accessories			
	Boiler, SCR*, Air Heater, Fans, Ducts, etc	188,301	156,153	206,791
	Oxygen Supply		115,005	188,031
5	Flue Gas Clean Up			
	Baghouse & Accessories	20,705	14,643	17,077
	FGD	71,033	0	0
	CO2 Processing	0	111,493	131,662
6	Combustion Turbine & Accessories	0	0	48,627
7	HRSG, Ducting, & Stack			
	Duct Work	11,004	7,782	9,076
	Stack	11,827	0	2,680
	Foundations	1,762	in duct work	205
	HRSG	0	0	18,420
8	Steam Turbine Generator	107,334	107,334	107,334
9	Cooling Water System	29,693	31,419	35,682
10	Slag/Ash Handling Systems	9,373	8,810	10,097
11	Accessory Electric Plant	33,275	33,741	35,212
12	Instrumentation & Control	14,807	15,014	15,668
13	Improvements to Site	9,405	9,537	9,953
14	Buildings & Structures	35,517	36,014	37,584
	Totals	632,984	723,310	952,993
	\$/kW	1,471	2,084	2,057

4.4.3 Total Plant Investment (TPI)

The TPI at date of start-up includes escalation of construction costs and allowance for funds used during construction (AFUDC). AFUDC includes interest during construction as well as a similar concept for timing of equity funds over the construction period. TPI is computed from the TPC based on a linear draw down schedule and the compounded interest (or implied equity rate) in the percentages of debt and equity. Draw down was over the assumed 48-month construction schedule for all three plants. As the analysis is done in constant 2006 dollars, no escalation was applied. The full AFUDC is used in calculating returns on debt and equity, but only the interest during construction is included in the depreciation base.

4.4.4 Total Capital Requirement (TCR)

The TCR includes all capital necessary to complete the entire project. TCR consists of TPI, prepaid royalties, pre-production (or start-up) costs, inventory capital, initial chemical and catalyst charge, and land cost:

- Royalty Costs have been assumed to be zero, as none apply.
- Start-Up/Pre-Production Costs are intended to cover operator training, equipment checkout, extra maintenance, and use of fuel and other materials during plant start-up. They are estimated as follows:
 - Hiring and phasing-in prior to and during start up of operating and maintenance labor, administrative and support labor, variable operating costs ramped up to full capacity (including fuel, chemicals, water, and other consumables and waste disposal charges. These variable costs are assumed to be compensated by electric energy payments during the start up period.
 - Costs of spare parts usage, and expected changes and modifications to equipment that may be needed to bring the plant up to full capacity.
- Inventory capital is the value of inventories of fuel, other consumables, and by-products, which are capitalized and included in the inventory capital account. The inventory capital is estimated as follows:
 - Fuel inventory is based on full-capacity operation for 30 days.
 - Inventory of other consumables (excluding water) is normally based on full-capacity operation for the same number of days as specified for the fuel.
 - ½ percent of the TPC equipment cost is included for spare parts.
- Initial catalyst and chemical charge covers the initial cost of any catalyst or chemicals that are contained in the process equipment (but not in storage, which is covered in inventory capital). No value is shown because costs are assumed to have been included in the component equipment capital cost.
 1. Land cost is based on 100 acres of land at \$1,600 per acre.

4.4.5 Operating Costs And Expenses

Operating costs were expressed in terms of the following categories:

- Operating Labor
- Maintenance Cost
 - Maintenance labor
 - Maintenance materials
- Administrative and Support Labor
- Consumables
- Fuel Cost

These values were calculated consistent with EPRI TAG methodology. All costs were based on a first year basis in January 2006 dollars. The first year costs do not include start-up expenses, which are included in the TCR.

The cost categories listed above are calculated, on a dollars per year basis, as follows:

- Operating labor is calculated by multiplying the number of operating personnel with the average annual (burdened) compensation per person.
- Maintenance costs are estimated to be 2.2% of the TPC and are divided into maintenance labor and maintenance materials
 - Maintenance labor is estimated to be 40% of the total maintenance cost
 - Maintenance materials are estimated to be 60% of the total maintenance cost
- Administrative and support labor is estimated to be equal to 30% of the sum of operating and maintenance labor.
- Consumables are feedstock and disposal costs calculated from the annual usage at 100 per cent load and 85 per cent capacity factor. The costs is expressed in year 2006 dollars and levelized over 20 years on a constant dollar basis.

Fuel cost is calculated based on a coal delivered cost of \$1.34/MMBtu. Fuel cost is determined on a first year basis and levelized over 20 years on a constant dollar basis. The calculation of first year fuel costs is done as follows:

$$\text{Fuel (tons/day)} = \text{Full Load Coal Feed Rate (lb/hr)} \times 24 \text{ hr/day} / 2000 \text{ lbs/ton}$$

$$\text{Fuel Unit Cost (\$/ton)} = \text{HHV (Btu/lb)} \times 2000 \text{ lb/ton}$$

Fuel Cost (1st year) = Fuel (tons/day) x Fuel Unit Cost (\$/ton) x 365 day/yr x 0.85 (CF)

The operating and maintenance costs, excluding fuel and consumables, are combined and divided into two components: 1) 90 per cent for Fixed O&M, which is independent of power generation, and 2) 10 per cent for Variable O&M, which is proportional to power generation.

4.4.6 Cost Of Electricity (COE)

The COE value is made up of contributions from the capital cost (called the carrying charge), operating and maintenance costs, consumables, and fuel costs. The following relationship is used to calculate COE from these cost components:

$$\text{COE} = \text{LCC} + \text{LFOM} \times 100 / (8760 \times \text{CF}) + \text{LVOM} + \text{LCM} + \text{LFC}$$

LCC = Levelized carrying charge, ¢/kWh

LFOM = Levelized fixed O&M, \$/kW-yr

LVOM = Levelized variable O&M, ¢/kWh

LCM = Levelized consumables, ¢/kWh

LFC = Levelized fuel costs, ¢/kWh

CF = plant capacity factor (0.85)

The CO₂ mitigation cost (MC) shows the cost impact, in dollars per tonne of CO₂ that would otherwise be emitted, of a configuration that allows CO₂ capture relative to the air-fired reference plant.

The MC is calculated as follows:

$$\text{MC} = \frac{\text{COE}_{\text{with removal}} - \text{COE}_{\text{reference}}}{E_{\text{reference}} - E_{\text{with removal}}} \times 0.01 \text{ \$/¢}$$

COE = Cost of electricity in ¢/kWh

E = CO₂ emission in tonnes/kWh

The capital investment and revenue requirements of the three plants are presented in detail in Table 4.4.8 through Table 4.4.10 and summarized in Table 4.4.11.

With the oxygen based plants having higher total plant costs than the air-fired reference plant, their interest during construction is higher and they have higher total plant investment costs; start-up and working capital costs, which are somewhat related to total plant costs are also higher and yield total capital requirement costs that are 14 and 51 per cent higher than the air-fired plant.

The air-fired reference plant incorporates an ammonia based SCR and a limestone based scrubber to control its NO_x and SO_x emissions. Although these systems are not required with the oxygen based plants, the latter incorporates oxygen supply and CO₂ processing systems. Since the number of systems added equaled the number deleted, it was assumed, in the absence of a detailed staffing study, that all three plants required the same number of operating personnel. Although operator costs are identical, maintenance and administration costs, which key off of total plant costs, are higher for the oxygen-based plants. The consumable requirements of the three plants are given in Table 4.4.12. With the SCR and scrubber systems deleted, the consumable costs of the oxygen-based plants are lower (ammonia and limestone costs are eliminated), but because of their lower efficiency, their fuel costs are higher (per net MWe). The higher fuel and higher operating and maintenance costs exceed the lower consumable cost savings and, as a result, the ASU and OITM plants have higher 20 year levelized production costs of \$24.42/MWhr and \$22.27/MWhr, respectively, versus \$20.93/MWhr for the air-fired plant. When added to their respective higher capital carrying costs of \$41.75/MWhr and \$41.21/MWhr versus \$29.48/MWhr, their costs of electricity of \$66.17/MWhr and \$63.48/MWhr are 31 and 26 per cent higher than the air-fired reference plant at \$50.41/MWhr (see Figure 4.4.1). The breakdown of the COE for the three plants is summarized in Figure 4.4.2, where plant capital cost is divided into CO₂ Processing, ASU, Turbines, Boiler, and Balance of Plant (BOP).

The CO₂ mitigation costs of the ASU and OITM based plants were calculated to be \$20.23 and \$16.77 per tonne of CO₂ sent to the pipeline for sequestering (not including transportation cost). With the OITM based plant offering the promise of a lower CO₂ mitigation cost, this analysis has shown that reducing the costs of both the oxygen supply and the CO₂ processing systems are a key to reducing both the cost of electricity and CO₂ mitigation costs of these sequestration ready power plants.

4.4.7 Tube Weld Overlay

As discussed in Section 4.3.4 tube wall weld overlays may be required to mitigate furnace waterwall corrosion. Conservatively assuming weld overlay is applied to the entire furnace adds approximately \$7.5 million to the total plant cost. This increases the COE of the cryogenic O₂-PC to 66.7 \$/MWhr (increase of 0.75%) and the MC to \$20.8 per tonne (increase of 3.0%). The weld overlay increases the COE of the OITM O₂-PC to 63.7 \$/MWhr (increase of 0.3%) and the MC to \$17.0 per tonne (increase of 1.5%). Utilizing weld overlays would be more cost effective in mitigating corrosion than FGD since adding an FGD system (upstream of the recycle split) would increase the COE by approximately 9%. Note that adding an FGD system downstream of the recycle split (to remove SO_x from the pipeline) would increase the COE by approximately 6%.

4.4.8 Reduced Pipeline Pressure

The analysis performed herein was conservatively performed for a pipeline pressure of 3000 psia. The Reference 14 guidelines specify a pipeline pressure of 2200 psia. At 2200 psia system efficiency is increased by 0.1% and COE is reduced by 0.3%. The economic effects of adding tube overlay and reducing the pipeline pressure are shown in Table 4.4.13.

Table 4.4.8 - Air Fired PC Plant Capital Investment & Revenue Requirement

TITLE/DEFINITION			
Case:	Air Fired	Steam Turbine:	4005psig/1076F/1112F
Plant Size:	430.2 MWe (net)	Net Efficiency:	39.5 % HHV
Fuel (type):	Illinois No 6 Coal	Fuel Cost:	\$1.34/MMBtu
Design/Construction:	48 Months	Book Life:	20 Years
TPC (Plant Cost) Year:	Jan-06		
Capacity Factor:	85.0%		
CAPITAL INVESTMENT:		\$x1000	\$/kW
	TOTAL PLANT COST	632,982	1,471
	AFUDC	105,458	
	TOTAL PLANT INVESTMENT	732,440	1,717
Royalty Allowance		0	
Start Up Costs		16,458	
Working Capital		4,795	
Debt Service Reserve		0	
	TOTAL CAPITAL REQUIREMENT	759,693	1,815
OPERATING & MAINTENANCE COSTS (2006)			
Operating Labor		4,921	
Maintenance Labor		5,570	
Maintenance Material		8,355	
Administrative & Support Labor		3,147	
	TOTAL OPERATION & MAINTENANCE (2006)	21,994	
	FIXED O&M (2006)	19,795	
	VARIABLE O&M (2006)	2,199	
CONSUMABLE OPERATING COSTS, LESS FUEL (2006)			
Water and Treatment		1,297	
Limestone		1,452	
Ash Disposal		2,423	
Ammonia		1,768	
Other Consumables		1,005	
	TOTAL CONSUMABLES (2006)	7,945	
BY-PRODUCT CREDITS (2006)		0	
FUEL COST (2006)			
Coal	FUEL COST (2006)	37,131	
		1st Year (2010)	20 Year Levelized
PRODUCTION COST SUMMARY		\$/MWhr	\$/MWhr
	Fixed O&M	6.18	6.18
	Variable O&M	0.69	0.69
	Consumables	2.48	2.48
	By-Product Credit	0.00	0.00
	Fuel	11.59	11.59
	TOTAL PRODUCTION COST (2006)	20.94	20.93
	LEVELIZED 20 YEAR CARRYING CHARGES (Capital)*		29.48
	LEVELIZED 20 YEAR BUSBAR COST OF POWER		50.41
*Levelized Fixed Charge Rate = 12.5%			

Table 4.4.9 - ASU Based PC Plant Capital Investment & Revenue Requirement

TITLE/DEFINITION			
Case:	Oxygen by ASU	Steam Turbine:	4005psig/1076F/1112F
Plant Size:	347.0 MWe (net)	Net Efficiency:	33.0 % HHV
Fuel (type):	Illinois No 6 Coal	Fuel Cost:	\$1.34/MMBtu
Design/Construction:	48 Months	Book Life:	20 Years
TPC (Plant Cost) Year:	Jan-06		
Capacity Factor:	85.0%		
CAPITAL INVESTMENT:			
	TOTAL PLANT COST	\$x1000	\$/kW
		723,310	2,084
	AFUDC	120,507	
	TOTAL PLANT INVESTMENT	843,818	2,432
Royalty Allowance		0	
Start Up Costs		18,806	
Working Capital		5,480	
Debt Service Reserve		0	
	TOTAL CAPITAL REQUIREMENT	868,103	2,502
OPERATING & MAINTENANCE COSTS (2006)			
Operating Labor		4,921	
Maintenance Labor		6,365	
Maintenance Material		9,548	
Administrative & Support Labor		3,386	
	TOTAL OPERATION & MAINTENANCE (2006)	24,220	
	FIXED O&M (2006)	21,798	
	VARIABLE O&M (2006)	2,422	
CONSUMABLE OPERATING COSTS, LESS FUEL (2006)			
Water and Treatment		898	
Limestone		0	
Ash Disposal		1,111	
Ammonia		0	
Other Consumables		1,005	
	TOTAL CONSUMABLES (2006)	3,014	
BY-PRODUCT CREDITS (2006)			
		0	
FUEL COST (2006)			
Coal	FUEL COST (2006)	35,851	
		1st Year (2010))	20 Year Levelized
PRODUCTION COST SUMMARY			
	Fixed O&M	8.43	8.43
	Variable O&M	0.94	0.94
	Consumables	1.17	1.17
	By-Product Credit	0.00	0.00
	Fuel	13.88	13.88
	TOTAL PRODUCTION COST (2006)	24.42	24.42
	LEVELIZED 20 YEAR CARRYING CHARGES (Capital)*		41.75
	LEVELIZED 20 YEAR BUSBAR COST OF POWER		66.17
*Levelized Fixed Charge Rate = 12.5%			

Table 4.4.10 - OITM Based PC Plant Capital Investment & Revenue Requirement

TITLE/DEFINITION			
Case:	Oxygen by Ion Transport Membrane	Steam Turbine:	4005psig/1076F/1112F
Plant Size:	463.3 MWe (net)	Net Efficiency:	36.1 % HHV
Fuel (type):	Illinois No 6 Coal	Fuel Cost:	\$1.34/MMBtu
Design/Construction:	48 Months	Book Life:	20 Years
TPC (Plant Cost) Year:	Jan-06		
Capacity Factor:	85.0%		
CAPITAL INVESTMENT:			
	TOTAL PLANT COST	\$x1000	\$/kW
	AFUDC	952,993	2,057
	TOTAL PLANT INVESTMENT	1,111,767	2,400
Royalty Allowance		0	
Start Up Costs		24,778	
Working Capital		7,220	
Debt Service Reserve		0	
	TOTAL CAPITAL REQUIREMENT	1,143,764	2,469
OPERATING & MAINTENANCE COSTS (2006)			
Operating Labor		4,921	
Maintenance Labor		8,386	
Maintenance Material		12,579	
Administrative & Support Labor		3,992	
	TOTAL OPERATION & MAINTENANCE (2006)	29,879	
	FIXED O&M (2006)	26,891	
	VARIABLE O&M (2006)	2,988	
CONSUMABLE OPERATING COSTS, LESS FUEL (2006)			
Water and Treatment		899	
Limestone		0	
Ash Disposal		1,356	
Ammonia		0	
Other Consumables		1,005	
	TOTAL CONSUMABLES (2006)	3,259	
BY-PRODUCT CREDITS (2006)			
		0	
FUEL COST (2006)			
Coal	FUEL COST (2006)	43,696	
		1st Year (2010)	20 Year Levelized
PRODUCTION COST SUMMARY			
		\$/MWhr	\$/MWhr
	Fixed O&M	7.79	7.79
	Variable O&M	0.86	0.86
	Consumables	0.94	0.94
	By-Product Credit	0.00	0.00
	Fuel	12.67	12.67
	TOTAL PRODUCTION COST (2006)	22.27	22.27
	LEVELIZED 20 YEAR CARRYING CHARGES (Capital)*		41.21
	LEVELIZED 20 YEAR BUSBAR COST OF POWER		63.48
*Levelized Fixed Charge Rate = 12.5%			

Table 4.4.11 - Summary of Plant Economics and CO₂ Mitigation Costs

	Reference Air-Fired Plant	ASU Based Plant	OITM Based Plant
Net Power Output, MWe	430.2	347.0	463.3
Efficiency, % (HHV)	39.5	33.0	36.1
Coal Flow, Klb/hr	319.0	308.0	375.4
CO2 to Stack			
	Klb/hr		
	Tonnes/MW hr		
	739.0		
	0.779		
CO2 to Pipe Line			
	Klb/hr		
	Tonnes/MW hr		
		718.0	866.0
		0.939	0.848
Total Plant Cost			
	Millions of Dollars		
	\$/kW		
	633.0	723.3	953.0
	1,471	2,084	2,057
Total Capital Requirement in Millions of Dollars	760.0	868.1	1143.8
Levelized Production Costs, \$/MW hr			
	Operating & Maintenance		
	Consummables		
	Fuel		
	Total		
	6.86	9.37	8.66
	2.48	1.17	0.94
	11.59	13.88	12.67
	20.93	24.42	22.27
Levelized Capital Carrying Charges, \$/MW hr	29.48	41.75	41.21
Levelized COE, \$/MW hr	50.41	66.17	63.48
CO2 Mitigation Cost, \$/tonne		20.23	16.77

Table 4.4.12 - Plant Daily Consumable Requirements

	Air-Fired	Cryogenic ASU	OITM
Water, 1000s gal/day	3,483	2,414	2,414
Water Treatment Chemicals, lbs/day	17,041	17,041	17,041
Limestone, tons/day	312	0	0
Ammonia (28% NH3), tons/day	25	0	0
Ash Disposal, tons/day	371	358	437
Fuel, tons/day	3,828	3,696	4,505
Fuel, lbs/hr/MWe	741.5	887.6	810.3
Fuel, Btu/hr/kWe	8625	10324	9424

Figure 4.4.1 – Increase in COE of O₂ Plant Above Air-Fired Reference Plant

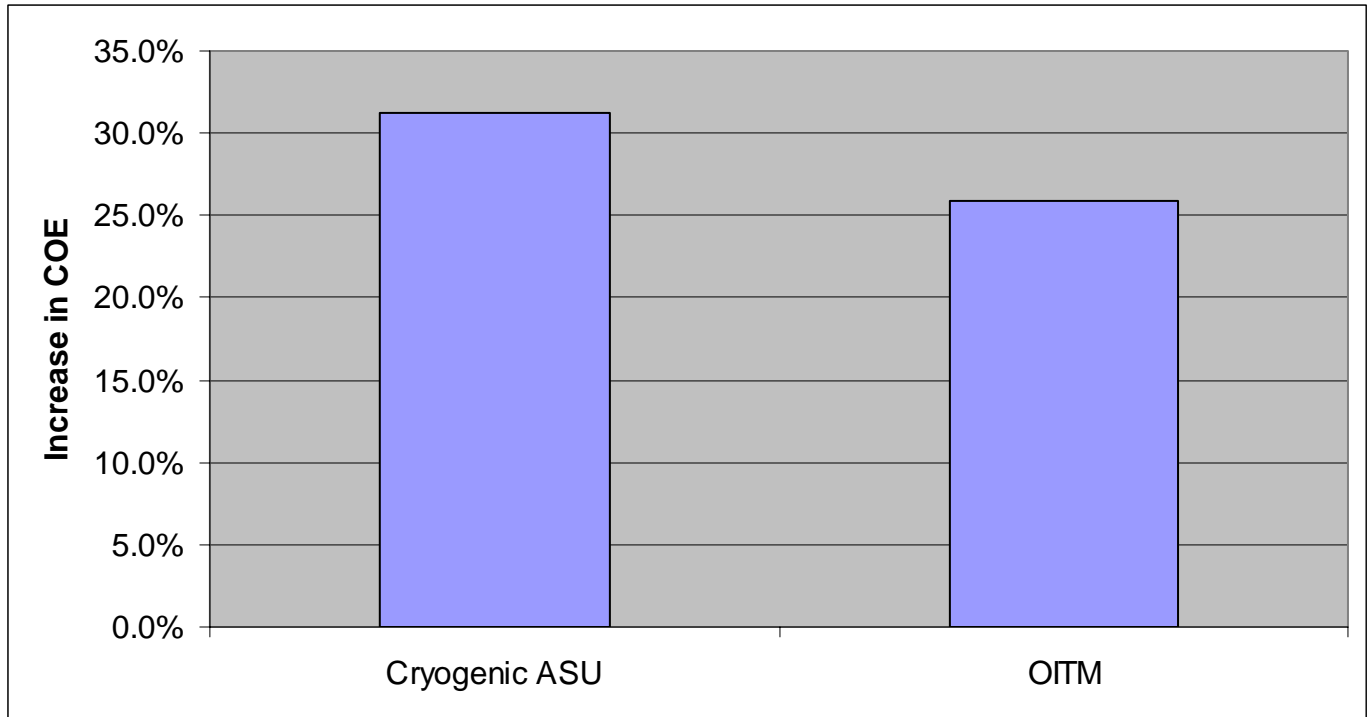


Figure 4.4.2 – COE Breakdown

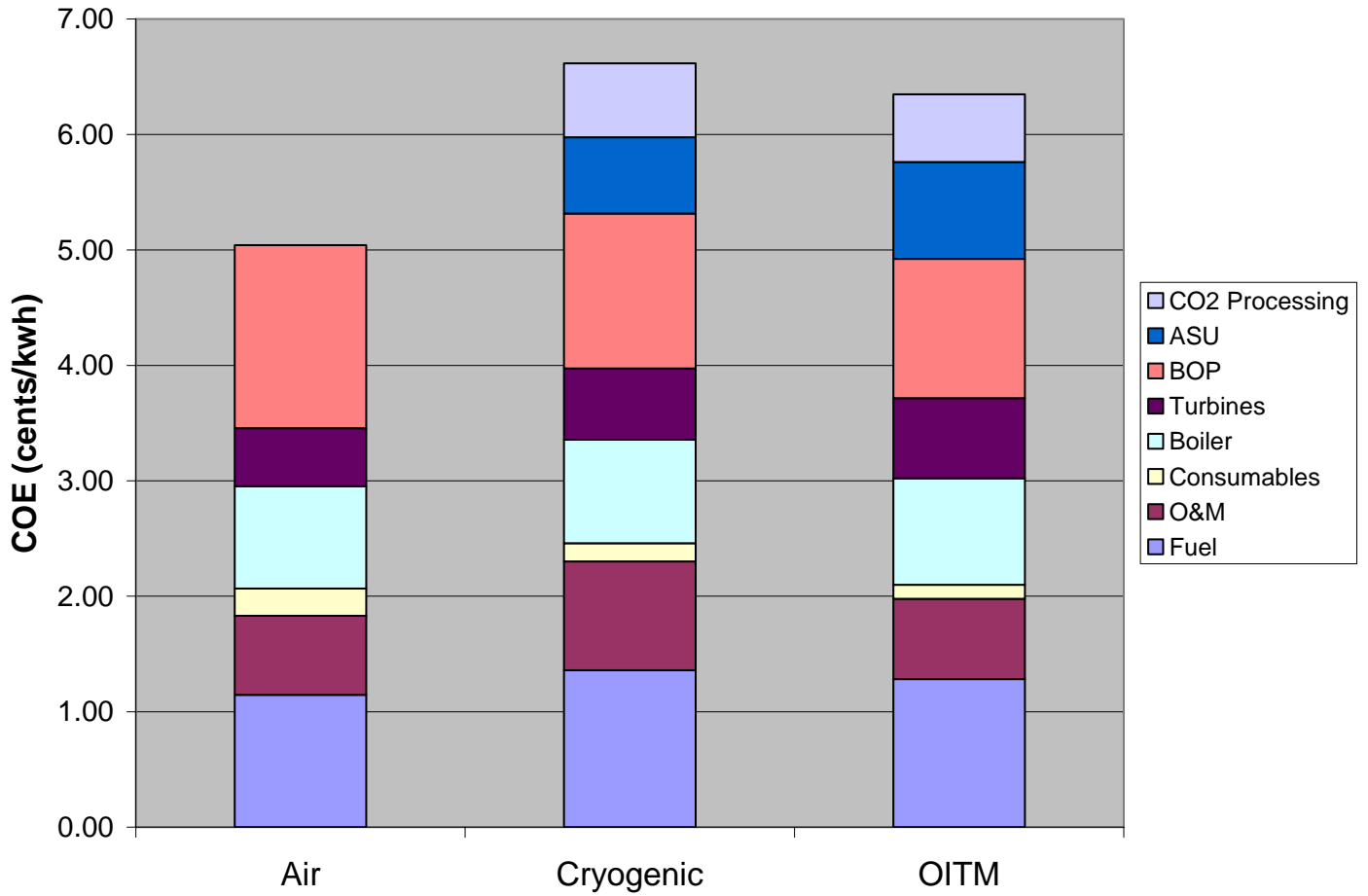


Table 4.4.13 – COE and CO₂ MC with Weld Overlay and 2200 psi Pressure

	Reference Air-Fired Plant	ASU Based Plant	OITM Based Plant
Levelized COE, \$/MWhr			
Base	50.4	66.2	63.5
With tube overlay & 3000 psi pipeline pressure		66.7	63.7
With tube overlay & 2200 psi pipeline pressure		66.5	63.6
CO ₂ Mitigation Cost, \$/tonne			
Base		20.2	16.8
With tube overlay & 3000 psi pipeline pressure		20.8	17.1
With tube overlay & 2200 psi pipeline pressure		20.6	16.8

4.4.9 Comparison with Other Technologies

An economic comparison was performed between the O₂-PC and other competing CO₂ removal technologies. For comparison the following alternate technologies were chosen:

- Air PC: Supercritical PC plant with post-combustion CO₂ mitigation (Ref. [15] case 12).
- NGCC: Natural Gas Combined Cycle with post combustion (Ref. [15] case 14).
- IGCC: Integrated Gasification Combined Cycle with pre-combustion CO₂ mitigation (Ref. [15] case 4).
- SUB O₂PC: Oxygen-fired subcritical PC (Ref. [3]).

The economics of these technologies were compared with the supercritical O₂-PC using both the levelized cost of electricity and the CO₂ mitigation cost as indexes. The CO₂ mitigation cost (MC) shows the cost impact, in dollars per tonne of CO₂ that would otherwise be emitted, of a configuration that allows CO₂ capture relative to the reference plant.

The COE and MC for the Air PC, NGCC, and IGCC were obtained from Ref. 15. Since the economic analysis of Ref. 15 were made for a larger power plant (480-550 MWe net power) they were scaled to a 30% smaller power plant to be consistent with the supercritical O₂-PC analyzed herein. The COE and MC for the subcritical O₂-PC were obtained from Ref. 3 and adjusted from 2004 to 2006 dollars and from a coal cost of \$1.14/MMBtu to \$1.34/MMBtu.

Figure 4.4.3 and Figure 4.4.4 present a comparison of the COE and MC using an 85% capacity factor. Compared to the COE of the supercritical cryogenic O₂-PC, the COE for the other technologies is 52% higher for Air PC, 35% higher for NGCC, 15% higher for IGCC, and 5% higher for the subcritical O₂-PC, and 4% lower for the supercritical O₂-PC with OITM. Compared to the MC of the supercritical cryogenic O₂-PC, the MC for the other technologies is 238% higher for NGCC, 192% higher for Air PC, 25% higher for IGCC, 5% higher for the subcritical O₂-PC, and 17% lower for the supercritical O₂-PC with OITM. Since based on operating experience an 85% capacity factor for IGCC technology appears too optimistic, the COE and MC with a 70% capacity factor is also shown in Figure 4.4.3 and Figure 4.4.4 (COE is increased by 16% and MC by 18%).

Figure 4.4.3 - Comparison of Levelized Cost of Electricity Among Alternative Technologies

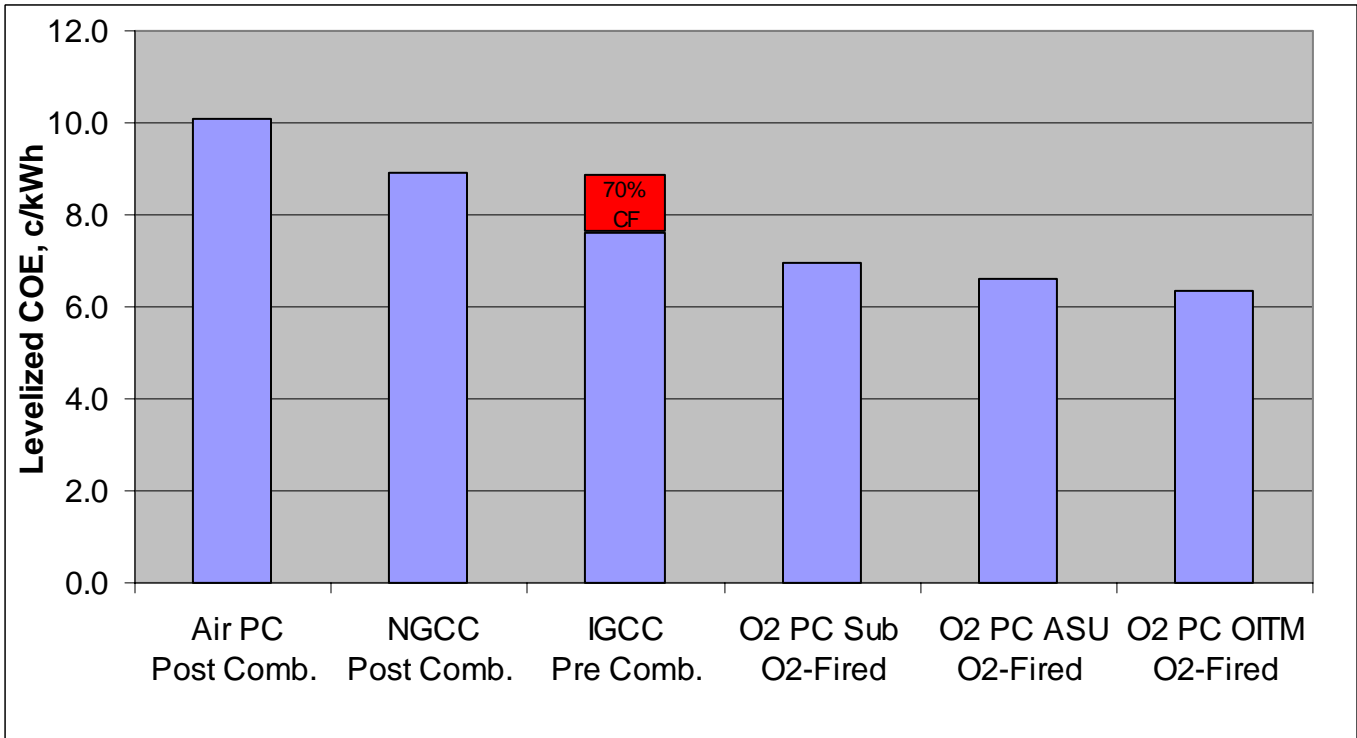
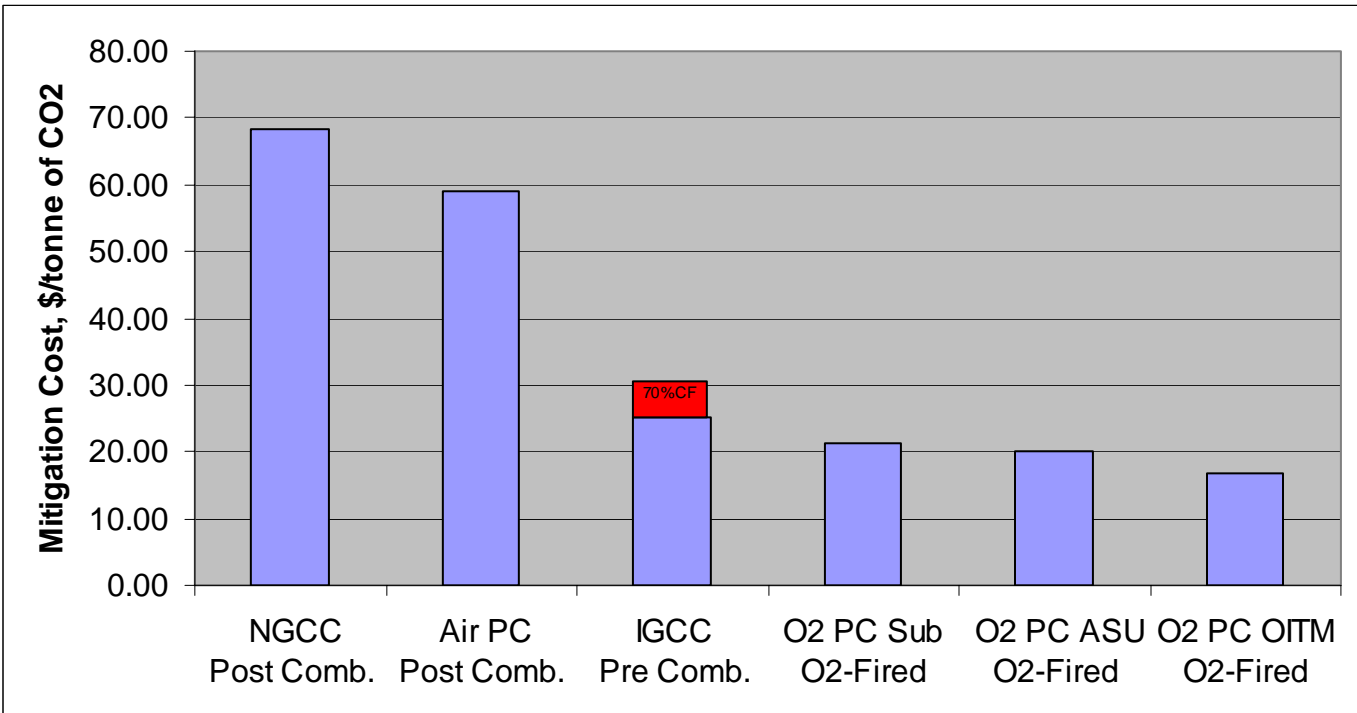


Figure 4.4.4 - Comparison of Mitigation Costs Among Alternative Technologies



5.0 Conclusion

To assure continued U.S. power generation from its abundant domestic coal resources, new coal combustion technologies must be developed to meet future emissions standards, especially CO₂ sequestration. Current conventional coal-fired boiler plants burn coal using 15-20% excess air producing a flue gas, which is only approximately 15% CO₂. Consequently, CO₂ sequestration requires non-condensable gases stripping, which is both expensive and highly power-consumptive. Several different technologies for concentrating the CO₂ by removing the non-condensable gases have been proposed including amine-based absorption and membrane gas absorption. However, these techniques require substantial energy, typically from low-pressure steam.

A new boiler is presented where the combustion air is separated into O₂ and N₂ and the boiler uses the O₂, mixed with recycled flue gas, to combust the coal. The products of combustion are thus only CO₂ and water vapor. The water vapor is readily condensed, yielding a pure CO₂ stream ready for sequestration. The CO₂ effluent is in a liquid form and is piped from the plant to the sequestration site. The combustion facility is thus truly a zero emission stackless plant.

A conceptual design of a CO₂ sequestration-ready oxygen-based 460 MWe supercritical PC boiler plant was developed. The selected O₂-fired design case has a system efficiency of 32.9% compared to the air-fired system efficiency of 39.5%.

The efficiency and cost-effectiveness of carbon sequestration in oxygen-firing boilers can be optimized by specifically tailoring boiler design by appropriate surface location, combustion system design, material selection, furnace layout, and water/steam circuitry. Boiler efficiencies of near 100% can be achieved by recovery of virtually all of the flue gas exhaust sensible heat. Boiler size can be drastically reduced due to higher radiative properties of O₂-combustion versus air-combustion. Furthermore, a wider range of fuels can be burned due to the high oxygen content of the combustion gas and potential for high coal preheat.

A conceptual design of a CO₂ sequestration-ready oxygen-based 460 MWe supercritical PC boiler plant was developed with integration of advanced oxygen separation techniques, such as OITM and CAR. The optimized OITM O₂-fired design case has a CO₂ removal specific power penalty of 42 kWh/klb_{CO2} and a system efficiency of 36.1% compared to the air-fired system efficiency of 39.5%. Considering that CO₂ compression itself consumes 40 kWh/klb_{CO2}, the OITM integration into the O₂-PC is a breakthrough in CO₂ removal. The CAR process efficiency loss and specific power penalty lies approximately midway between the cryogenic ASU and OITM.

The O₂-fired PC CO₂ removal penalty with integration of OITM is nearly a quarter of that from post combustion CO₂ removal technologies, and only a half of IGCC.

OITM faces significant challenges with respect to the manufacture and stability of membranes, and scale up and design of large plants.

A design and analysis of a reference air-fired boiler, an oxygen-fired boiler with cryogenic ASU, and an oxygen-fired boiler with oxygen ion transport membrane were performed. The O₂-PC supercritical boiler incorporates the OTU BENSON vertical technology, which uses low fluid mass flow rates in combination with optimized rifled tubing. The following conclusions are made comparing the air-fired furnace with the oxygen-fired furnace design and performance:

1. The oxygen furnace has only approximately 65% of the surface area and approximately 45% of the volume of the air-fired furnace due to the higher heat flux of the oxygen-fired furnace.
2. Due to the higher O₂ concentration of the oxygen-fired furnace versus the air-fired furnace (40% vs. 21%), the maximum flame temperature of the oxygen-fired furnace is approximately 500°F higher.
3. Maximum wall heat flux in the oxygen-fired furnace is about 2.5 times that of the air-fired furnace (175,000 Btu/hr-ft² vs. 70,000 Btu/hr-ft²) due to the higher flame temperature and higher H₂O and CO₂ concentrations.
4. 100% coal burnout is achieved in the oxygen-fired furnace (compared to 99.6% burnout in the air-fired furnace) due to higher furnace temperature and higher concentration of oxygen. The burnout differential between the oxygen-fired boiler and the air-fired boiler is expected to be significantly greater when harder to burn fuels are fired.
5. The higher heat flux of the oxygen-fired furnace significantly increases the maximum waterwall temperature (from 870°F for the air-fired furnace to 1060°F for the oxygen-fired furnace) requiring the material to be upgraded from T2 to T92.
6. NO_x is reduced by oxygen firing (compared to air-firing) by about a factor of two from 0.38 lb/MMBtu to 0.18 lb/MMBtu.
7. A pressure equalization header is included at an elevation of 80' to ensure stable operation at low loads.
8. The total heat transfer surface required in the HRA is 35% less than the air-fired HRA due to more heat being absorbed in the oxygen-fired furnace and the greater molecular weight of the oxygen-fired flue gas. To minimize the required surface area, the HRA design is in series for the cryogenic ASU O₂-PC and parallel for the OITM O₂-PC.

9. To reduce the corrosion in the O₂-PC, weld overlays with high Nickel and Chromium contents (e.g. alloy 622) are applied to the waterwalls. This reduces the predicted maximum corrosion from 45 mil/yr to 10 mil/yr.
10. The required HRA tube materials and wall thicknesses are nearly the same for the air-fired and oxygen-fired design since the flue gas and water/steam temperature profiles encountered by the heat transfer banks are similar.
11. A tubular convective air heater is included in the OITM O₂-PC to provide the necessary air heating for the membrane separation process. The furnace air heater is an Incoloy MA956 three-pass tubular design situated above the furnace nose.

The levelized cost of electricity of the supercritical pressure, air-fired reference plant was calculated to be \$50.41/MWhr and it operated with an efficiency of 39.5 per cent. The oxygen supply and CO₂ gas processing systems required by the oxygen-based plants significantly increase their plant costs and parasitic power requirements. The cryogenic ASU based plant had a cost of electricity of \$66.17/MWhr and an efficiency of 33.0 per cent.

The oxygen transport membrane of the OITM based plant operates at 200 psia with air heated to 1600°F via tubes placed in the boiler. The high cost of this boiler tubing, together with piping, heat exchangers, and the oxygen transport membrane itself, add considerable costs to the plant. Since the nitrogen exhausting from the membrane is hot and at pressure, it can be used for power recovery via a hot gas expander and HRSG. Although addition of these components further increases plant costs, the added power they provide increases the plant efficiency to 36.1 per cent and enables the OITM based plant to operate with a cost of electricity that is less than that of the ASU based plant e.g. \$63.48/MWhr versus \$66.17/MWhr. As a result the CO₂ mitigation cost of the OITM based plant was calculated to be less than that of the ASU based plant e.g. \$15.66/tonne versus \$17.06/tonne, respectively.

The addition of weld overlay increases the COE approximately 0.75%, but reducing the pipeline pressure from 3000 psia to 2200 psia (specified in Ref. 14) reduces the COE by 0.3%. Thus, the combined effect of these two adjustments on the COE is relatively small (+0.4% for cryogenic O₂-PC and +0.1% for the OITM O₂-PC).

The oxygen supply and the CO₂ gas processing systems have a major impact on the economics and efficiency of oxygen-based plants. Additional R&D aimed at improving these systems, especially OITMs, is necessary to improve both electricity costs and CO₂ mitigation costs.

The O₂-fired PC CO₂ removal penalty is nearly half that of post combustion CO₂ removal technologies and 15% to 30% than that of IGCC pre-combustion

capture. Furthermore, of the CO₂ sequestration-ready technologies, the O₂-fired PC is the simplest, requires the least modification of existing proven designs, and requires no special chemicals for CO₂ separation.

Thus CO₂ sequestration with an oxygen-fired combustion plant can be performed in a proven reliable technology while maintaining a low-cost high-efficiency power plant. As new lower power-consuming air separation techniques, such as membrane separation, become commercially available for large-scale operation in O₂-fired plants, the CO₂ removal power consumption and efficiency reduction will continue to decline.

6.0 References

1. White, J.S., Buchanan, T.L., Schoff, R.L. (Parsons); Stiegel, G. (DOE); Holt, N.A., Booras G. (EPRI); Wolk, R. (WITS), "Evaluation of Innovative Fossil Fuel Power Plants with CO₂ Removal", EPRI Report No. 1000316, December 2000.
2. Wilkinson, M., Boden, John (BP), Panesar, R. (Mitsui Babcock), Allam, R. (Air Products), "CO₂ Capture Via Oxygen Firing: Optimisation of a Retrofit Design Concept for a Refinery Power Station Boiler", First National Conference on Carbon Sequestration, May 15-17, 2001, Washington DC.
3. Seltzer, Andrew and Fan, Zhen, Conceptual Design of Oxygen-Based PC Boiler, DOE # DE-FC26-03NT41736, September 2005.
4. Philip A. Armstrong, E.P. Foster, Dennis A Horazak, Harry T Morehead, VanEric E. Stein, "Ceramic and Coal: ITM Oxygen for IGCC", The 22nd Pittsburgh Coal Conference, Sept.11-15, 2005, Pittsburgh, USA
5. Divyanshu Acharya, Krish R. Krishnamurthy, Michael Leison, Scott MacAdam, Vijay K. Sethi, Marie Anheden, Kristin Jordal, Jinying Yan, "Development of a High Temperature Oxygen Generation Process and Its Application to Oxycombustion Power Plants with Carbon Dioxide Capture", *ibid*
6. A.A. Leontiou, A.K. Ladavos, T.V. Bakas, T.C. Vaimakis, & P.J. Pomonis, "Reverse uptake of oxygen from La_{1-x}Sr_x(Fe³⁺/Fe⁴⁺)O₃ perovskite-type mixed oxides", *Applied Catalysis A: General* 241 (2003) p143-154.
7. "Greenhouse Gas Emissions Control By Oxygen Firing In Circulating Fluidized Bed Boilers: Phase 1 – A Preliminary Systems Evaluation", Alstom Power Inc. Power Plant Laboratories, PPL Report No. PPL-03-CT-09, DOE/NETL Cooperative Agreement No. DE-FC26-01NT41146, May 15, 2003.
8. Philip A. Armstrong, "Method for Predicting Performance of an Ion Transport Membrane Unit-Operation", Air Products and Chemicals, Inc.
9. FW-FIRE, Fossil-fuel Water-walled Furnace Integrated Reaction Emission, Theory and User's Manual, Foster Wheeler Development Corp., 11/30/99.
10. HEATEX Computer Program, "A Program to Determine the Thermal/Hydraulic Performance of Gas-Cooled Heat Exchangers", Revision 24, Foster Wheeler Corporation.

11. EMISS Computer Program, "A Program to Determine Gaseous Emissivity", Foster Wheeler Corporation.
12. STADE2 Computer Program, "Calculation Program for Pressure Drop and Heat Transfer in Tubes", Siemens, Version 4.40.
13. DYNASTAB Computer Program, "Dynamic Stability of the Flow through Evaporator Heating Tubes in Fossil Fired Steam Generators", Siemens, Version 1.1.
14. "Carbon Capture and Sequestration System Analysis Guidelines", DOE/NETL, April 2005.
15. "2006 Cost and Performance Comparison of Fossil Energy Power Plants", DOE/NETL-401/053106, Draft Final May 2006.
16. "Task 1 Topical Report - IGCC Plant Cost Optimization", Gasification Plant Cost and Performance Optimization, DOE/NETL Contract No. DE-AC26-99FT40342, May 2002.

7.0 Bibliography

N/A

8.0 List of Acronyms and Abbreviations

ASU	Air Separation Unit
BOP	Balance of Plant
CAR	Ceramic auto-thermal recovery
CDT	Compressor discharge temperature
CF	Capacity Factor
CFD	Computational fluid dynamics
COE	Cost of Electricity
DNB	Departure from nucleate boiling
E	Emission of CO ₂
EPRI	Electric Power Research Institute
FD	Forced draft
FEGT	Furnace exit gas temperature
FGD	Flue Gas Desulfurization
FW	Foster Wheeler
FW-FIRE	Fossil fuel, Water-walled Furnace Integrated Reaction and Emission Simulation
GT	Gas turbine
HHV	Higher Heating Value
HIPPS	High performance power system
HRA	Heat recovery area
HRSG	Heat Recovery Steam Generator
ID	Induced draft
IGCC	Integrated gasification combined cycle
LCC	Levelized Carrying Charge
LCM	Levelized Consumables
LFC	Levelized Fuel Costs
LFOM	Levelized Fixed O&M
LHV	Lower Heating Value
LMPD	Log mean pressure difference
LMTD	Log mean temperature difference
LOI	Loss on ignition
LP	Low pressure
LVOM	Levelized Variable O&M
MC	Mitigation Cost (CO ₂)
NGCC	Natural gas combined cycle
NOx	Nitrogen Oxides
O&M	Operation and Maintenance
OD	Outside diameter
OFA	Over-fired air
OITM	Oxygen Ion Transport Membrane
OTU	Once-through utility
PC	Pulverized Coal
PFBC	Pressurized fluidized bed combustion
PSA	Pressure swing absorption
RH	Reheater

SCR	Selective Catalytic Reactor
SH	Superheater
SOx	Sulfur Oxides
ST	Steam Turbine
T	Temperature
TCR	Total Capital Requirement
TEG	Triethyleneglycol
TET	Turbine Exit temperature
TPC	Total Plant Cost
TPI	Total Plant Investment
UBC	Unburned carbon loss